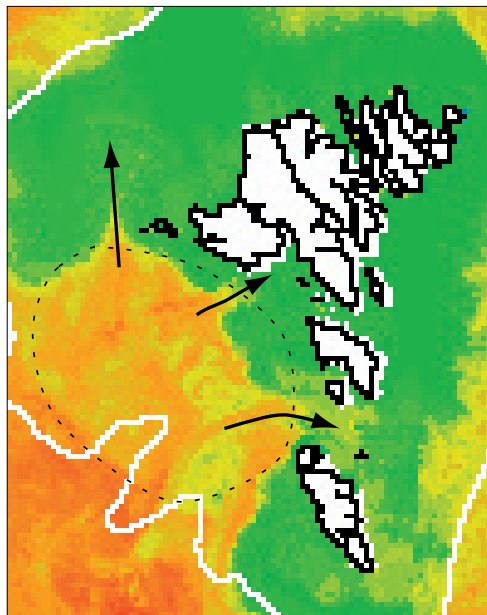


# The Western region

Tórshavn · Mai 2013



**Hjálmar Hátún**  
**Karin Margretha H. Larsen**  
**and Høgni H. Debes**

# Innihald

1	Introduction .....	4
2	Motivation .....	6
2.1	A large-scale perspective.....	6
2.1.1	Sub-decadal oceanic variability ....	6
2.1.2	Sub-decadal open-ocean phytoplankton variability.....	7
2.1.3	Inverse oceanic and shelf variability .....	7
2.2	The Western region .....	8
2.2.1	The spring and summer cruises....	8
2.2.2	Ocean Color.....	9
2.3	Nutrients .....	9
2.3.1	Open ocean nutrient limitation.....	9
2.3.2	Growth and silicate limitation in the Western region .....	9
3	Data material .....	10
3.1	FAMRI routine data .....	10
3.1.1	Standard cruises .....	10
3.1.2	Coastal station Skopun .....	10
3.2	FAMRI new.....	10
3.2.1	Cruise 1012 .....	10
3.2.1.1	SST observations.....	10
3.2.1.2	CTD casts.....	10
3.2.2	Lowered ADCP .....	10
3.2.3	Echo-sounder data.....	11
3.2.4	Moorings .....	11
3.2.4.1	FASA .....	11
3.2.4.2	FASB .....	11
3.2.4.3	FASC.....	11
3.2.4.4	Wave buoy mooring .....	11
3.2.4.5	Short term Aanderaa moorings.....	11
3.2.5	Sections .....	11
3.2.5.1	Towed Termistor Wire .....	11

3.2.5.2 New CTD sections .....	12	at FASB .....	24
3.2.6 Biological and chemical data .....	12	4.2.2 An ADCP at the FASC.....	24
3.2.6.1 Zooplankton data .....	12	4.2.3 Equipping a wave buoy	
3.2.6.2 Primary production data .....	12	with temperature sensors.....	24
3.2.6.3 Nutrient data .....	12	4.3 New sections .....	26
3.2.6.4 A new silicate times series...12		4.3.1 The oceanic tongue:	
3.3 Other .....	12	A ‘cold-cushion’?.....	26
3.3.1 HYCOM model .....	12	4.3.2 Standard sections M, R and V ....	26
3.3.2 Atmospheric reanalysis data .....	12	4.4 Coastal station Skopun .....	26
3.3.3 Satellite Ocean Color data .....	12	4.4.1 Inter-annual chlorophyll concentrations	
3.3.3.1 Standard products .....	12	and air-sea heat exchanges .....	26
3.3.3.2 Very high-resolution		4.4.2 Growth and nutrient dynamics	
products .....	13	at coastal station Skopun .....	32
3.3.3.3 Derived primary		4.4.3 Seasonal phytoplankton	
production fields.....	13	community succession .....	34
3.3.4 Seaglider data .....	13	4.5 Satellite based Ocean Color .....	34
4 Preliminary results .....	13	4.5.1 The widely available	
4.1 Cruise 1012 .....	13	4-km resolution products .....	34
4.1.1 Tidally induced frontal shifts .....	13	4.5.1.1 The characteristic year, 2009 35	
4.1.2 Strong freshwater stratification ...14		4.5.1.2 Out-of-phase relation between	
4.1.3 Highest chlorophyll concentrations		the Western region	
in the fronts .....	14	and the Faroe shelf .....	35
4.1.3.1 Vertical view .....	14	4.5.2 High-resolution satellite maps ... 35	
4.1.3.2 Horizontal view .....	14	4.5.2.1 A high on-shelf production	
4.1.4 A cross-section across		situation in 2009.....	35
the oceanic tongue.....	14	4.5.2.2 Structures of	
4.1.5 Utilizing the ship-mounted		the Western region .....	35
echo-sounder.....	14	4.6 HYCOM .....	37
4.1.6 A virtual mooring at FASB.....	14	4.6.1 A quiescent region .....	37
4.1.6.1 Hydrography .....	17	4.6.2 On-shelf transport	
4.1.6.2 Phytoplankton abundance		from the Western region .....	37
(Fluorescence).....	17	4.7 Other data sources.....	38
4.1.7 Lower fluorescence		4.7.1 Seagliders .....	38
between the islands .....	18	5 Synthesis .....	39
4.1.8 A virtual station		5.1 Pieces of evidence.....	39
near the tidal front .....	18	5.2 A new hypothesis.....	40
4.1.9 Relatively low fluorescence values		5.3 Large-scale and future	
during cruise 1012 .....	18	silicate consideration .....	40
4.1.10 Oxygen measurements .....	21	5.4 Future directions.....	42
4.1.11 Biological data.....	21	5.5 References .....	43
4.1.12 Heat flux.....	21	Appendix.....	45
4.2 New moorings .....	21		
4.2.1 An ADCP at FASB.....	21		
4.2.1.1 Back-scatter intensity .....	21		
4.2.1.2 Back-scatter at FASB			
and primary production at Skopun ..21			
4.2.1.3 Intensity and			
air-sea heat loss.....	23		
4.2.1.4 Linkage to			
bottom temperature at FASB .....	23		
4.2.1.5 Heat loss and			
vertical velocities at FASB.....	23		
4.2.1.6 Average current velocities			

# 1 Introduction

In this report we document the presence of a quiescent region on the western side of the Faroe plateau, which has characteristics that differ from the inner Faroe shelf and from the open ocean waters. The primary production of the Faroe shelf is highly variable from year to year, with large increases happening every 5-8 years. This characteristic sub-decadal variability reverberated in higher trophic levels, zooplankton, prey fish species like sandeel, commercial fish stocks and in the seabird colonies. Understanding the underlying causes of this has been a cardinal research question at the Faroe Marine Research Institute (FAMRI). In the published literature, this variability has been explained by a variable exchange between on-shelf and off-shelf water masses, with a large exchange washing a large fraction of the algae of the shelf and thus reducing the production (Hansen et al., 2005). It has furthermore been observed that good growth conditions occur after cold winters, which adds a link to the atmospheric climate (Hansen et al., 2005). These explanations thus infer that the Faroe shelf primary production is regulated by local, near-shelf processes. The fact that we now observe similar variability over a larger scale in the northeastern Atlantic challenges the generally accepted *exchange hypothesis*. This has resulted in a series of “brain storming” presentations and discussion at FAMRI. From this activity, it has become clear that the Faroe shelf is not homogeneous and that a region on the western side has the highest chlorophyll concentrations, and stands out as the likely most important area to investigate further. This area is hereafter referred to as the *Western region*. This has subsequently been done with e.g. deployments of current meters, adding temperature sensors to a wave buoy mooring, more and high-resolution hydrographic transects through this region (Fig. 1.1). An exploratory cruise (cruise 1012) was also conducted with research vessel Magnus Heinason during a week in late April, 2010, where a broad selection of physical and biological experiments was made. Although this broad selection of new data has given hints to potentially important processes, this information has not been synthesized into a proper new explanation to complement or replace the exchange hypothesis. The question about what is controlling the Faroe shelf primary production is therefore presently hanging in a ‘limbo state’. In this report we collect and present the new data material from the moorings and from

the exploratory cruise. A selection of preliminary results of potential importance, based on the new *in situ* data is presented. The existence of so far not utilized, but promising data is also mentioned, and this report could therefore be used as a *road-map* for future work on this issue. This new data material, necessarily scattered in time or space, is furthermore discussed in the context of spatially and temporally comprehensive data sources, like a high-resolution ocean model, remote sensing data of ocean color and atmospheric re-analysis data. Other relevant data material sampled by FAMRI during a longer time frame, (e.g. the coastal station at Skopun and the standard cruises) are also utilized, and new aspects of these already published data are emphasized. We first present the motivation for investigating the Western region in more detail (section 2), then we give an overview over a wide selection of relevant data sources, both in-house at FAMRI and external (section 3). In section 4, we show a disparate selection of preliminary results, which might become important pieces in the larger puzzle of what is controlling the Faroe shelf primary production. Some of these pieces are synthesized in a new tentative explanation model which involves nutrient limitation in the Western region (section 5). The presented material has not been finalized into scientifically robust results yet and this report is merely intended to be a starting place when doing more research on the Western region.

## Main findings:

- There appears to be an asynchrony between the chlorophyll concentrations on the Faroe shelf and in the surrounding open-ocean.
- The open-ocean surface chlorophyll concentrations appear to be associated with the dynamics of the subpolar gyre.
- The near-shore waters become silicate limited every year.
- When the silicate becomes limiting (below 2-3  $\mu\text{M}$ ), there is a ‘break’ in the shelf (Skopun) chlorophyll concentrations, and the phytoplankton community tend to shift from a dominance of large diatoms to smaller diatoms or flagellates.
- These ‘breaks’ appear to have become more pronounced during the last decade.

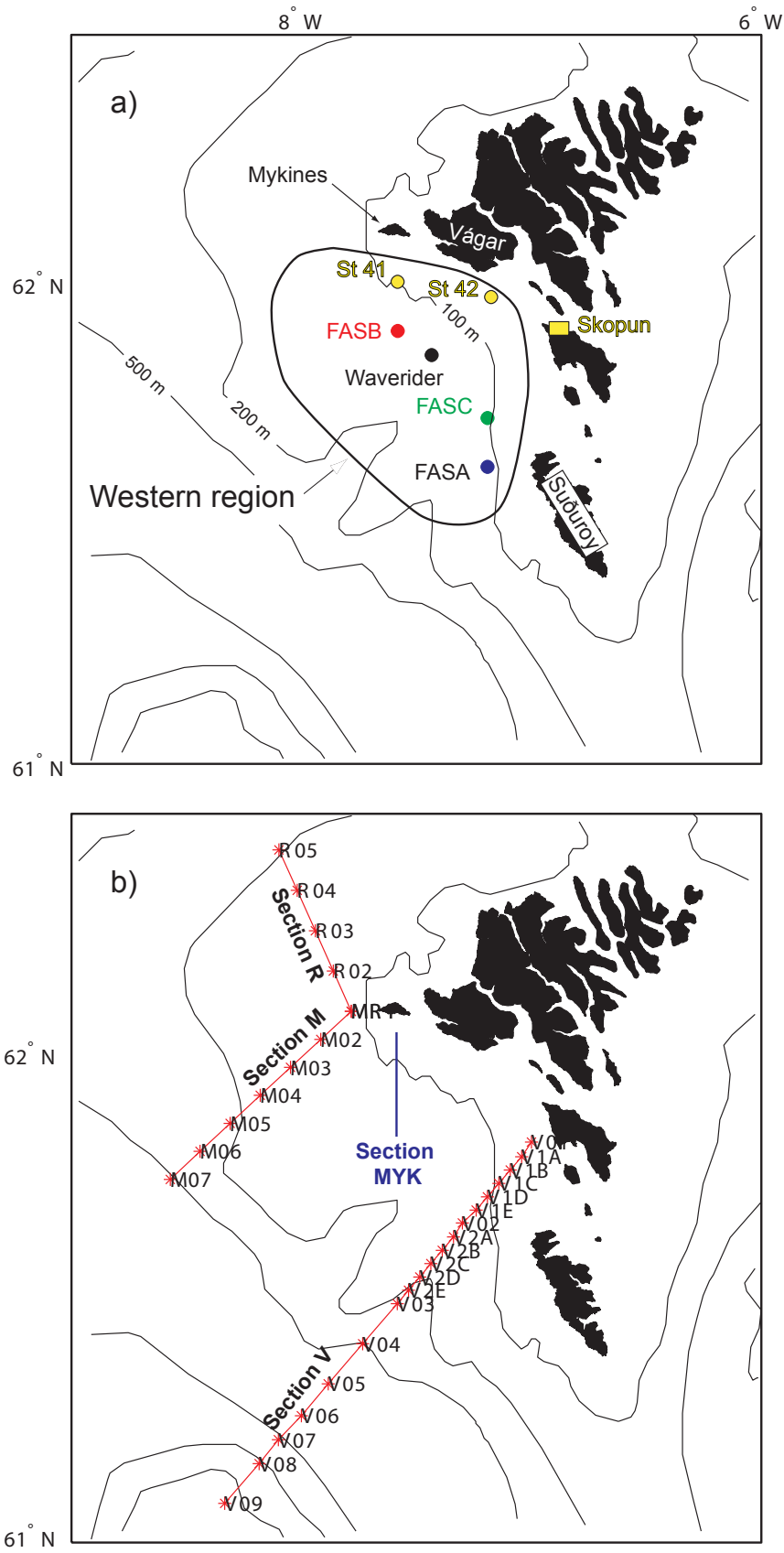
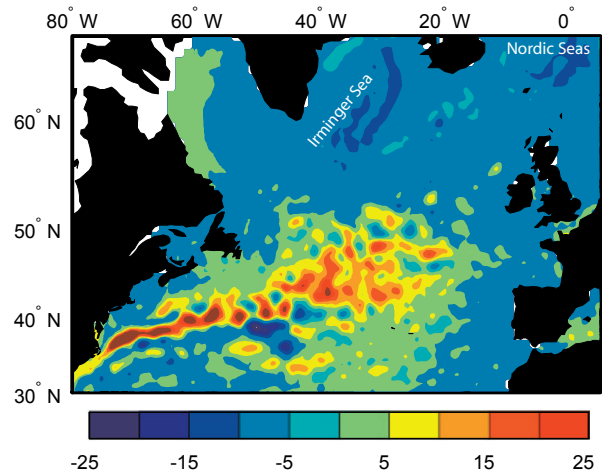


Fig. 1.1 An overview over the monitoring activity of the Western region. a) Moorings, coastal station Skopun and stations 41 and 42, occupied during the standard biological oceanography cruises. b) The new standard hydrographic sections.

- For this Western region, we find that:
  - a) It responds quickly to atmospheric forcing, and can be quickly, and strongly, stratified,
  - b) chlorophyll concentrations can become very high,
  - c) there appears to be an asynchrony between the surface chlorophyll concentrations in this region and the rest of the Faroe shelf,
  - d) the nutrient concentrations in the upper mixed layer become more limiting than in the adjacent shelf and oceanic waters.
- A large on-shelf flux of water comes from the upper-layers in the Western region through three relatively narrow inflows.
- The highest production takes place in the tidal front between the Western region and the inner shelf.
- The Western region is a relatively stagnant pool (low current velocities), which has characteristics of a so-called ‘cold cushion’ during late spring/summer.
- All years with strong on-shelf production are characterized by having days with net heat-loss from the ocean to the atmosphere during the spring bloom. We therefore suggest that net heat-loss is a necessary, but not sufficient, requirement for strong production.
- Near-surface and near-bottom temperature measurements made at a wave buoy mooring show that the stratification within the Western region breaks down quickly when there is net heat-loss to the atmosphere.
- Backscatter observations from an ADCP (intensity) moored within the Western region co-vary with the coastal chlorophyll observations during the growth period in 2010.
- There is a synchrony between nutrient observations in the northeastern Irminger Sea during February, and the primary production index (PPI) from the Faroe shelf (based on observations in June). If this is a causal link, then there is a potential for predicting the health of the Faroe shelf marine ecosystem by half a year.



*Fig. 2.1 The spatial impact of the sub-decadal variability. This has been illustrated by applying Empirical Orthogonal Function (EOF) analysis to annually averaged sea surface height (SSH) fields, after a linear trend has been removed from each data-point. The bluish colors in the spatial pattern (eigenvector) illustrate coherent variability in the Irminger and Norwegian Seas. The associated time series (principal component) is plotted in Fig. 2.2b.*

- The fact that the silicate levels in the North Atlantic and within the Nordic Seas has been declining during the last 20 years is worrisome. Can the decline in sandeel, sea birds and other important components of the ecosystem during the same period be explained by the nutrient levels, and subsequent to large-scale ocean circulation changes?

## 2 Motivation

### 2.1 A large-scale perspective

The state of the subpolar gyre, as represented by the gyre index, was previously revealed by applying Empirical Orthogonal Function (EOF) (Preisendorfer, 1988) analysis to the sea surface height (SSH) over the North Atlantic. The gyre variability is characterized by inter-decadal variability, but is modulated by sub-decadal variability.

#### 2.1.1 Sub-decadal oceanic variability

In order to emphasize the spatial imprint of the sub-decadal variability, the EOF-analysis has been repeated, but after a linear trend has been removed

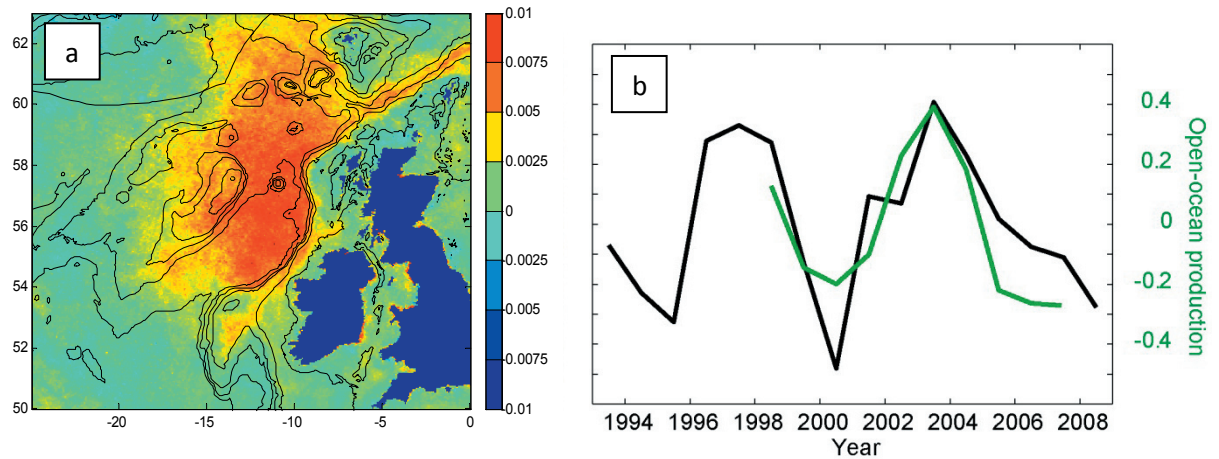


Fig. 2.2 The sub-decadal variability is evident in the surface chlorophyll concentrations. This is shown by applying EOF analysis to annually averaged chl-a data from the SeaWiFS satellite. a) The spatial pattern is shown in and b) the time series (green), plotted against the inverted and de-trended gyre index (black).

from each altimetry data pixel. The resulting spatial pattern illustrates coherent variability from south of Greenland and into the Nordic Seas (Fig. 2.1), with centers of action in the northern Irminger Sea and just northeast of the Faroe Islands (bluish colors). The associated time series (principal component) (Fig. 2.2b), shows that oceanic hydrography adjacent to the south Iceland shelf and the Faroe shelf has exhibited pronounced sub-decadal variability since the early 1990s.

### 2.1.2 Sub-decadal open-ocean phytoplankton variability

A linkage between the marine climate and open ocean phytoplankton has previously been demonstrated on inter-decadal time scales and a so-called phytoplankton color index from the continuous plankton recorder (CPR) survey (Hátún et al., 2009). This linkage is here shown to hold on sub-decadal time scales as well (Fig. 2.2). An EOF analysis of the annually averaged satellite based chlorophyll-a concentrations shows coherent variability in the Rockall-Iceland-Faroe area (Fig. 2.2a), and temporal variability (principal component) that co-fluctuates with the de-trended gyre index (Fig. 2.2b). Periods with low chl-a abundances (e.g. 1999-2001) roughly coincide with a subarctic state (depresses SSH), and thus low depth integrated buoyancy or generally weaker stratification.

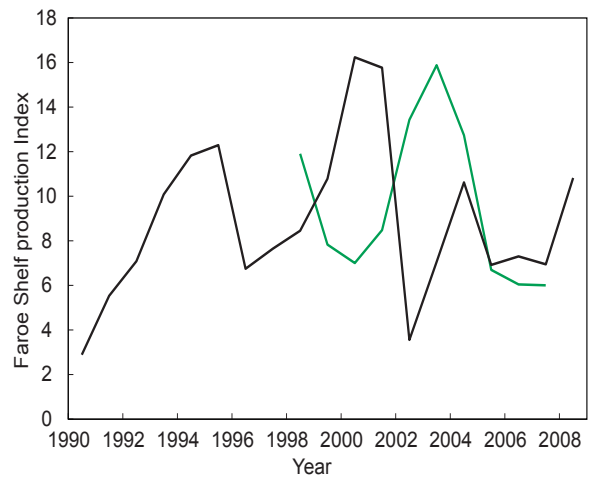


Fig. 2.3 The Faroe shelf primary production index (PPI, black) and the open-ocean chlorophyll time series (from Fig. 2.2b, not to scale)

### 2.1.3 Inverse oceanic and shelf variability

An index for new primary production (the PP-index) on the Faroe Shelf is calculated from the nitrate reduction on-shelf, but is corrected for horizontal nitrate import to the shelf, as described by (Gaard et al., 2003)(Fig. 2.3). This correction assumes constant horizontal exchange rates, which is not realistic, but the correction is, however, relatively small. The PP-index declined sharply from very high values in 2001 to very low values in 2002 (Fig. 2.3). And there appears to be an out-of-phase variability between the oceanic and the Faroe shelf phytoplankton abundances, although more detailed data are needed in order to rigorously confirm this.

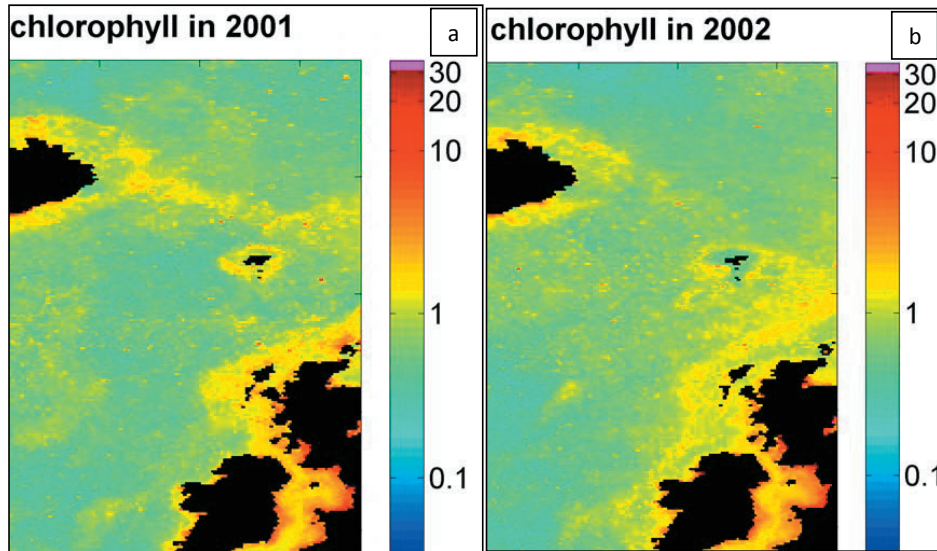
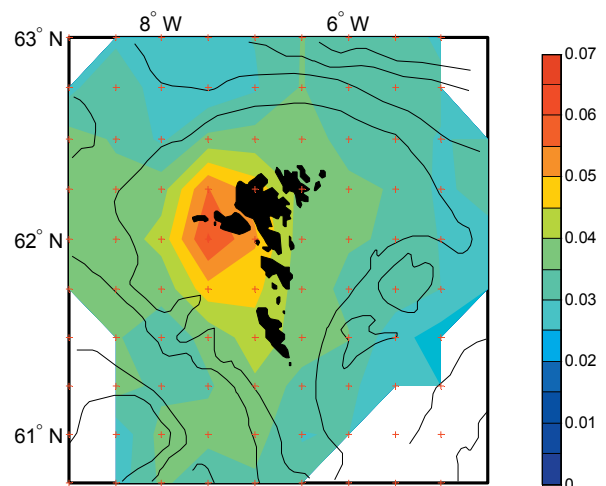


Fig. 2.4 Sharp decline/increase in phytoplankton abundance in shelf/open-ocean water in the northeastern Atlantic from 2001 to 2002. Annual composites of surface chlorophyll concentrations as measured by the SeaWiFS satellite ( $\mu\text{g chl-a l}^{-1}$ , on a log scale).

A conspicuous difference between the satellite based chl-a observations the two extreme years (2001 and 2002) is evident in Fig. 2.4, with high concentrations within the tidal front and low oceanic values in 2001 (Fig. 2.4a) and opposite in 2002 (Fig. 2.4b). This indicates that some synchrony is to be expected between the oceanic and the shelf ecosystem variability. These results indicate that the processes that regulate the Faroe shelf primary production might be basin-scale and not only local to the shelf itself, as hitherto assumed.



## 2.2 The Western region

### 2.2.1 The spring and summer cruises

The chlorophyll (fluorescence) concentrations are largest in the Western part of the Faroe Plateau, and the shelf can therefore not be considered as a homogeneous production region. This is here shown by pooling all fluorescence observations from the annual *biological oceanography* (April) and *O-group survey* (June) cruises (see section 3.1). The fluorescence profiles from each cruise are first depth averaged over the upper 50 m, and then gridded on a regular grid, using an objective mapping routine (Bohme and Send, 2005). This gridding also produces error maps, which enables us to cut out region with too sparse sampling. All the spring and summer cruises, respectively, are subsequently averaged, which gives the spring and summer climatologies shown in Fig. 2.5.

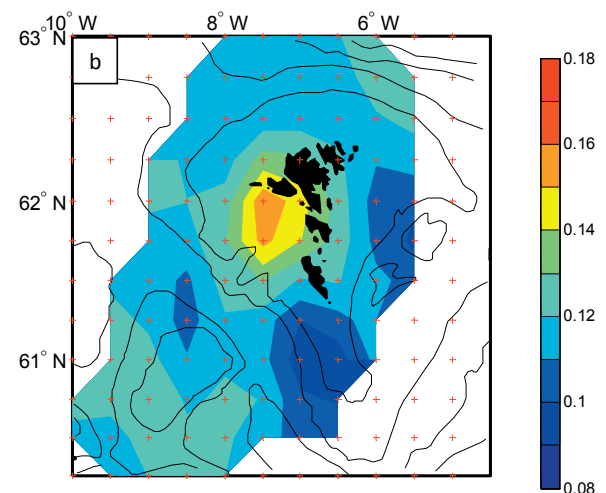


Fig. 2.5 Depth (0-50m) and time averaged fluorescence from the biological oceanography cruise in late April/early May (a, 1994-2008) and from the O-group survey in late June/early July (b, 1990-2008). The red crosses show the grid, on which the station data are gridded onto.

### 2.2.2 Ocean Color

The satellite derived (SeaWiFS) May climatology (1999-2006) of surface chlorophyll concentrations also identified the Western region as a highly productive region (Fig. 2.6). Primary production maps, presented in Zhai et al., (2012), similarly identify the Western region as a ‘hot spot’.

## 2.3 Nutrients

It is well known that silicate, needed by the diatoms to build their calcareous shells, becomes depleted/limiting within upper mixed layer in the subpolar North Atlantic every summer (typically in May)(Henson et al., 2006). When the silicate concentration approaches  $2 \mu\text{M}$ , the diatom community loses in the competition with other phytoplankton species (Egge and Aksnes, 1992), and sink rapidly out of the photic zone.

### 2.3.1 Open ocean nutrient limitation

The observed silicate along the  $20^\circ\text{W}$  WOCE line (<http://www.nodc.noaa.gov/WOCE>) clearly shows that the upper 50 m was severely limited by silicate during the summer of 2003, and must therefore have been depleted in diatoms (Fig. 2.7). Similar silicate limitation takes place every summer.

### 2.3.2 Growth and silicate limitation in the Western region

The chlorophyll concentrations in the upper layers within the Western region are generally higher than both farther on-shelf and farther off-shelf (Fig. 2.8a). This fact is here re-emphasized by pooling all fluorescence observations made along a section across this pool during the *O-group* survey (see below) in June, 1990-2008. This climatological section reveals a clear subsurface maximum within the Western region at around 20 m depths, which is near a pycnocline. The satellite-based identification of the Western region as a ‘hot spot, might therefore be an underestimation.

The associated silicate climatology shows that the upper layers within the Western region on average become silicate depleted/limited in June. Since waters from these upper layers flow onto the Faroe shelf (see section 4.5.2), and since high production is observed in the tidal front interface between the Western region and the shelf (see section 4.1.3), we can expect that the silicate concentrations within the Western region might influence the near/on-shelf primary production.

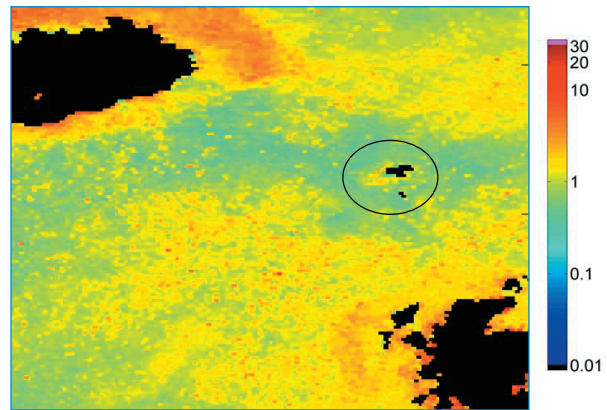


Fig. 2.6 May climatology (1999-2006) of surface chlorophyll concentrations as measured by the SeaWiFS satellite ( $\mu\text{g chl-a l}^{-1}$ , on a log scale). The Faroe Islands are emphasized, with the circle.

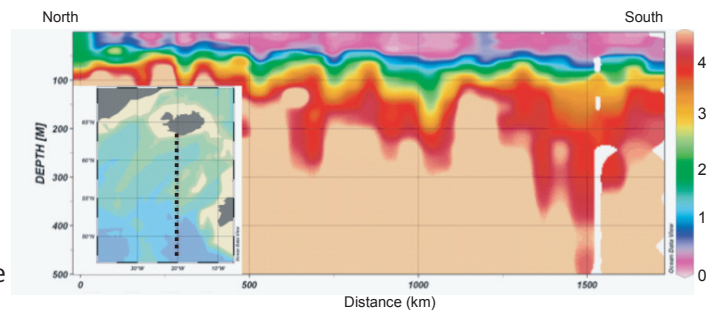


Fig. 2.7 A silicate section (concentration in  $\mu\text{M}$ ) along the  $20^\circ\text{W}$  WOCE line (see inset) in June 2003.

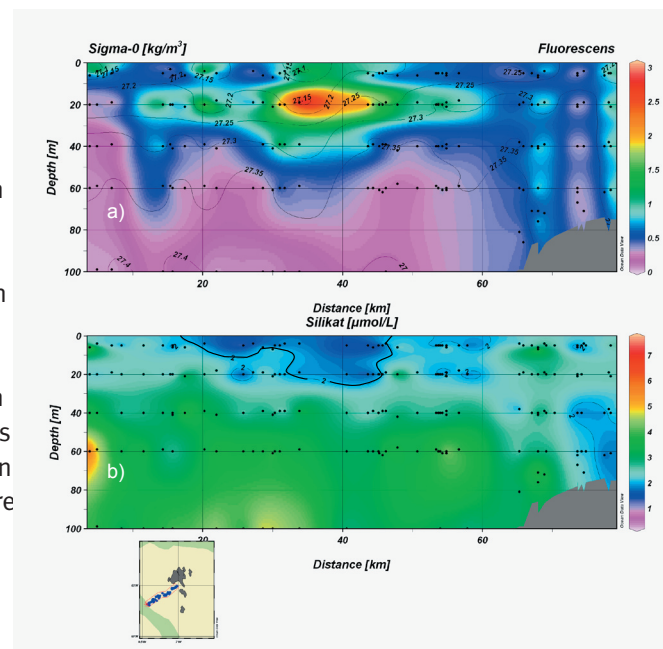


Fig. 2.8 Climatological sections of a) fluorescence and b) silicate ( $\mu\text{M}$ ) across the Western region during late June/early July (all data from the *O-group* surveys, 1990-2008). Distances from the off-shore edge of the section (red cross in the inset map) and towards the islands are shown. Potential density is contoured in a) and the limiting silicate concentration ( $2\mu\text{M}$ ) is contoured b).

## 3 Data material

Inspired by the apparent importance of the Western region, we decided *i)* to utilize the already existing, and relevant, data from this region, *ii)* devote an exploratory cruise with R/V Magnus Heinason to the Western region and *iii)* to intensify the routinely monitoring of this region.

### 3.1 FAMRI routine data

#### 3.1.1 Standard cruises

A standard cruise (*biological oceanography*), targeting the plankton community and relevant environmental parameters on a relatively tight observational net covering the Faroe shelf, has been conducted during late April/ early May since 1994. Another standard cruise (*O-group survey*), targeting juvenile fish, plankton and relevant environmental parameters along sections radiating out from the Islands has been conducted during late June/ early July since the 1970s, and with complete environmental sampling since 1990. Data from these two standard cruises were used for planning purposes, and as a context in which to analysis the more focused new observations within the Western region. Based on these data, a meridional section south from Mykines (intersecting standard stations 41 and 45 from *biological oceanography*) was selected as the focus region. This section will hereafter be termed main section MYK (Fig. 1.1b).

#### 3.1.2 Coastal station Skopun

Water samples from 18 meters depth in well-mixed water at Skopun have been made on a weekly basis during the growth season every year since 1997. The chlorophyll, salinity and nutrient concentrations in these waters are measured in the laboratory. These chlorophyll observations appear to give a good representation of the state of the Faroe shelf ecosystem at any given time. Since 2002, continuous temperature observations are also made at Skopun, using a Starmon temperature recorder and in recent years a Seabird MicroCat has also been deployed at the station. The MicroCat measures temperature and conductivity, but the conductivity observations have been erroneous for some of the deployments. A sampling rate of 5 minutes was used, and this is generally the sampling rate whenever these instruments are used.

### 3.2 FAMRI new

#### 3.2.1 Cruise 1012

The experimental cruise 1012 was an extension of the annual biological oceanography cruise in 2010. A broad selection of data resulted from this week-long exploratory cruise, made during late April in 2010.

##### 3.2.1.1 SST observations

R/V Magnus Heinason is sampling the sea surface temperature (SST) along its track. This is done at the seawater intake (cooling system) using a PT100 sensor, and the sampling rate is 10 seconds. Software was developed, for making real-time plots of the SST on a computer screen in the lab. This was done in order to be able to follow structures in ocean during the cruise, and to arrange the CTD casts accordingly. This approach, which was essential to this type of small-scale study, has to our knowledge not been tried before at FAMRI.

##### 3.2.1.2 CTD casts

236 CTD (Conductivity, Temperature, Depth) profiles were made during the cruise with a Seabird 911+ CTD. Different strategies were explored. *i)* Sections across the tidal front, with closer spacing between the stations near the front (guided by the real-time SST observations), *ii)* A broad net covering the Western region, *iii)* A section across the entire Western region (Mykines to Suðuroy), *iv)* revisiting standard stations which during many years have been visited during the biological hydrography cruises and *v)* two virtual moorings, with regular profiles made at the same location during 6 and 12 hours, respectively. Temperature, salinity and fluorescence measurements were, as usual, made by the CTD. A new oxygen sensor was also bought from Seabird (SBE 43) and added to the CTD for the purpose of cruise 1012. Temperature, salinity and chlorophyll plots for all sections are presented in appendix A.

#### 3.2.2 Lowered ADCP

A lowered Acoustic Doppler Current Profiler (ADCP, Teledyne RDI, Workhorse Sentinel) was rented from the Office of public works (LV – www.landsverk.fo), and attached to the CTD. Data are available and reasonable, but have not been finally processed yet.

Table 3.1 Mooring details

Deployment	Position	Bottom Depth (m)	Valid data period	Instruments
FASA0811	61°37.20N 07°24.10W	157	2008 11 07 – 2009 06 07	ADCP, MicroCat
FASB1002	61°53.95N 07°34.86W	128	2010 02 20 – 2010 09 04	ADCP, MicroCat
FASC1103	61°43.23N 07°11.43W	105	2011 03 10 – 2011 08 23	ADCP, Starmon
VAGA1004	62°00.00N 07°35.00W	106	2010 04 23 – 2010 04 26	2 Aanderaa RCM, 2 Starmon
VAGB1004	61°50.00N 07°34.80W	143	2010 04 21 – 2010 04 26	2 Aanderaa RCM, 2 Starmon
ALDV1103	61°51.00N 07°26.00W	125	2011 03 12 – 2012 04 18	2 Starmon

### 3.2.3 Echo-sounder data

Researchers at FAMRI have noted a clear shift in backscatter across the tidal front, as observed by the echo sounder data onboard the R/V Magnus Heinason (pers. Comm. Jan Arge Jacobsen).

Although large amounts of such data have been collected through the years, these have not yet been utilized. The echo-sounder onboard R/V Magnus Heinason (Simrad EK60, 38, 200 kHz) was operating during the cruise in order to compare structures in the backscatter with hydrographical and/or biological structures.

### 3.2.4 Moorings

Six current and temperature moorings are presented here. Mooring details are listed in Table 3.1 and the mooring locations are all plotted in Fig 1.1a.

#### 3.2.4.1 FASA

A RDI Workhorse Sentinel (ADCP) was deployed in a trawl resistant bottom mount to the west of Suðuroy during winter 2008/09 until summer 2009. This was done in relation to the project *Faroe Shelf Exchange*, and before our awareness of the importance of the Western region. These data have not been utilized in this context yet, but might prove valuable. The ADCP samples horizontal and vertical current velocities, as well as the backscatter intensity divided into 4-m bins through most of the water column. The sampling rate is 20 min. A Seabird MicroCat was added to the ADCP making temperature and salinity observations, with a sampling rate of 5 minutes (Larsen et al., 2009b).

#### 3.2.4.2 FASB

The same ADCP, with same equipment and setting as at FASA, was moored on main section MYK, near the expected position of the tidal front during

the year of the exploratory cruise (cruise1012), 20 February to 4 September, 2010 (Larsen et al., 2011).

#### 3.2.4.3 FASC

The same ADCP, with same equipment and setting as at FASA, except now with a Starmon temperature sensor instead of a MicroCat, was in spring 2011 moored to the northwest of Suðuroy where inflow onto the inner Faroe shelf was expected (see section 4.5.2) (Larsen et al., 2013).

#### 3.2.4.4 Wave buoy mooring

Starmon temperature sensors were attached near the surface (~ 10 m depth) and near the bottom (~ 120 m) on a wave buoy (Waverider) mooring, located within the Western region (Fig. 1.1a). This mooring is operated by LV. Two Starmon sensors are presently (spring 2013) attached to this same mooring, and the idea is to maintain this activity. Additionally, it has been extended to two other Waverider moorings on the Faro shelf.

#### 3.2.4.5 Short term Aanderaa moorings

Two short term moorings equipped with two classical Aanderaa RCM's and two Starmon temperature sensors each, at different depths, were moored along main section MYK during cruise 1012. These are named VAGA1004, and VAGB1004, to the north and south of FASB, respectively (Larsen et al., 2011). The data have not been utilized yet.

### 3.2.5 Sections

#### 3.2.5.1 Towed Termistor Wire

The main section MYK has been occupied four times using a so-called Towed Temperature Wire (TTW). This TTW has four Starmon temperature

sensors attached at roughly 5, 14, 23 and 32 meters depth, and a MicroCat, measuring temperatures, salinity and pressure at roughly 40 m depth. These depths vary with varying towing speeds and current velocities (see Larsen, 2009a). Additionally, the TTW has been used about 20 times approximately along standard section V (between 50 and 220 m bottom depth).

### 3.2.5.2 New CTD sections

The spacing between the hydrographic stations along standard section 'V' has been decreased in the near-shelf (Western) region, and two new standard sections ('M' and 'R') have been added (see Fig. 1.1b). These sections are now (started in 2012) a part of the *standard hydrography* cruises visited in February, May-June and August-September.

## 3.2.6 Biological and chemical data

### 3.2.6.1 Zooplankton data

Zooplankton samples were collected at some of the stations. Most of the zooplankton samples still need to be analyzed, but the 50m and 100m depth replicates over the ADCP are analyzed, and the data are available.

### 3.2.6.2 Primary production data

Primary production measurements using the traditional radio-carbon method were made at selected stations. All samples need to be analyzed before the data is available.

Samples for phytoplankton species analysis were taken at selected stations and different depths. These samples need to be analyzed before the data is available.

### 3.2.6.3 Nutrient data

Samples for nutrient analysis (nitrate and silicate) were collected at selected station, but are since then lost.

### 3.2.6.4 A new silicate times series

A time series of winter silicate concentrations in Faroese open-ocean waters was initiated in February 2011. Samples were made on 5, 50 and 200 m depths on standard hydrographic station V19

(61° 14' N, 9° 43' W), to the north of the Faroe Bank. Station V19 has now been terminated. On 26 March, 2012, samples were made on the same depths, but in the middle of the Faroe Bank Channel (61° 14' N, 7° 51' W). The aim is to find a suitable standard hydrographic station, and continuing this nutrient sampling on future standard hydrographic cruise in February.

## 3.3 Other

### 3.3.1 HYCOM model

In order to investigate the physical processes underlying the characteristic variation in the Faroe shelf primary production, a 3D high-resolution (~1 km) version of HYCOM (Hybrid Coordinate Ocean Model) v2.2.18 (Bleck, 2002) model has been run for the shelf, and the surrounding ocean, by Till Rasmussen at DMI (Rasmussen et al., 2013). These data are available as daily/hourly fields on hard disks at FAMRI.

### 3.3.2 Atmospheric reanalysis data

Atmospheric data of parameters like wind, temperature, and all the parameters needed to calculate the net heat-exchange between the ocean and the atmosphere (in watts per square meter) are downloaded from the National Centers for Environmental Prediction/National Center for Atmospheric Research(NCEP/NCAR) database (Kalnay et al., 1996). These data are available as time series at nine locations around the Faro shelf region, with daily values.

### 3.3.3 Satellite Ocean Color data

Some satellites (SeaWiFS, MODIS-Aqua/Terra, MERIS and others) monitor optical characteristics on the sea surface, from where, amongst other, estimates of the SST, surface chlorophyll concentrations and photosynthetically active radiation (PAR) are being made.

### 3.3.3.1 Standard products

Standard and widely available medium resolution (9-km and 4-km spatial resolution) products have been downloaded from the Ocean Color project data-bank (<http://oceancolor.gsfc.nasa.gov>), and utilized.

### 3.3.3.2 Very high-resolution products

Realizing that the Faroe shelf is not a homogenous compartment, and that understanding the primary production near the tidal front requires spatially more comprehensive data, we have established collaboration with Natural Environment Research Council (NERC) Earth Observation Data Acquisition and Analysis Service (NEODAAS) from whom we get very high resolution (1-km and even 300-m) data. NEODAAS has the capability to automatically receive, archive, process and map global data from multiple polar-orbiting sensors in near-real time, including MERIS, MODIS, SeaWiFS and AVHRR, allowing for very detailed studies. We have also started participation in the CoastColour Project, run by the European Space Agency (ESA) ([www.coastcolour.org](http://www.coastcolour.org)). This project aims at fully exploiting the potential of the MERIS instrument for remote sensing of the coastal zone, and to calibrate/optimize products for selected regions. If we at FAMRI deliver *in situ* data to the CoastColour Project, the Faroe shelf could become one of the selected regions, and we could thus obtain tailored products.

### 3.3.3.3 Derived primary production fields

Collaboration has also been established between FAMRI and the Remote Sensing Group at the Plymouth Marine Laboratory (PML). Based on *in situ* data (sub-surface chlorophyll maximum, P-I curves and more) and satellite data (surface chlorophyll and PAR), they are able to produce fields of primary production, and not just surface chlorophyll. FAMRI has delivered *in situ* data, and a paper on the primary production in the Faroese and Icelandic waters (Zhai et al., 2012) has resulted from this work.

### 3.3.4 Seaglider data

Seagliders are long-range autonomous underwater vehicles which are remotely controlled and collect high-resolution sections of temperature, salinity, dissolved oxygen, fluorescence and optical backscatter as well as depth-averaged horizontal velocity. About 20,000 full-depth (500-1000 m) profiles with 3-6 km horizontal resolution were collected in the Faroe-Iceland region during the period 3 January 2006 to 28 February 2010. The project was owned by the University of Washington, but since FAMRI helped with the deployment work, these data are available here, as well.

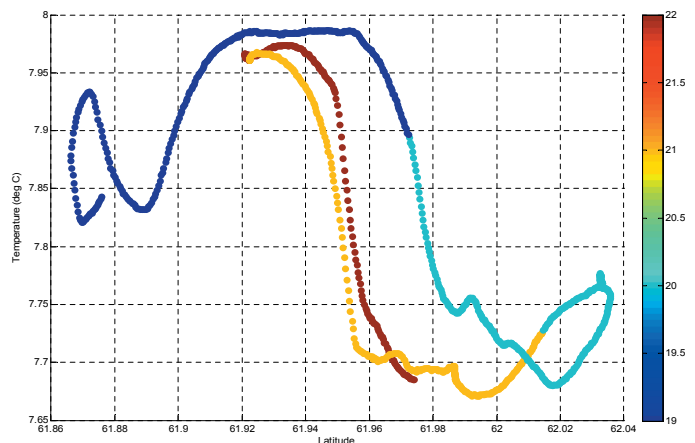


Fig. 4.1 The SST measured along the main section MYK (see Fig. 1.1b). The colorbar shows the hours during the evening of 24 April, 2010.

## 4 Preliminary results

The results are based on varying combination of data sources. The results are mainly structured by those based on data from: the exploratory cruise 1012, new moorings, new hydrographic sections, coastal station Skopun and other, but there is considerable overlap. We have selected some preliminary results here, which should be considered as potentially important pieces in the puzzle of understanding what controls the variable growth on the Faroe shelf. The results do not make up a chronological story.

### 4.1 Cruise 1012

#### 4.1.1 Tidally induced frontal shifts

Utilizing the SST, measured by the research vessel in real-time, proved to be a valuable/necessary tool for conducting the frontal experiments. The SST was monitored on a computer in the lab, and CTD stations were made more frequently where the SST changed rapidly - in the vicinity of fronts. As an example, we crossed the tidal front along main section MYK, several times during the evening of April 24<sup>th</sup>, 2010. The SST observations showed that the front shifted 2-3 km south within a few hours (Fig. 4.1). Such sudden frontal shifts were typical. From this we conclude that the CTD is not an optimal tool for exploring such rapidly shifting fronts. It should, however, be noted that the temperature range of only 0.25°C (Fig. 4.1) is low

for the season – typical values are around 1°C, and might reach 2°C.

#### 4.1.2 Strong freshwater stratification

During the first days of the cruise, small pools with extremely strong freshwater stratification were observed (Fig. 4.2). These were mainly observed offshore of the tidal front, in waters with weak currents. At first, this was considered to be erroneous measurements, but the regularity of these pockets indicates these are probably real. There had been very strong snowfall before the extended cruise 1012, and this is the most likely explanation. Large chlorophyll concentrations (fluorescence) could be observed at the base (10-20 m depth) of the low-saline pools (Fig. 4.2d). These pools eroded away (disappeared) during the cruise. We conclude that strong rain/snowfall can be important for local stratification and biology.

#### 4.1.3 Highest chlorophyll concentrations in the fronts

##### 4.1.3.1 Vertical view

Several detailed sections were made across the tidal front, at different locations (see also the Appendix). Many sections were repeated at longer (1-2 days) and shorter (2-4 hours) intervals. The highest chlorophyll/fluorescence values observed during the cruise were in the vicinity of the tidal front, and often in very concentrated patches (Fig. 4.3d). This example is taken from main section MYK south of Mykines (Fig. 1.1b), where also the highest climatological chlorophyll concentrations are found (see Fig. 2.5).

##### 4.1.3.2 Horizontal view

Lumping all the hydrographic from cruise 1012 together, using the software ODV (Schlitzer 2007), we obtain a larger scale overview of the Western region, although the strong tidally induced shifts are blurring the picture (Fig. 4.4). The tongue of saltier and warmer oceanic water meets the fresher shelf waters in a U-formed tidal front from west of Suðuroy and turning westwards to the south of Vággar. We conclude that a band of elevated fluorescence levels is observed along the average location of the tidal front (Fig. 4.4b).

#### 4.1.4 A cross-section across the oceanic tongue

During the last day of the cruise (26 April), a hydrographic section was made from Mykines to Suðuroy, across the intruding warm and salty oceanic tongue (Fig. 4.5c). A heated, and thus stratified, upper layer was observed over the saline tongue (Fig. 4.5a). Much elevated fluorescence levels were observed in the stratified semi-oceanic pool (Fig. 4.5d). Such relatively high fluorescence values were not observed within the oceanic tongue earlier on the cruise, (see Fig. 4.4b). The air-sea heat exchange shifted on the day before this long section (25 April, see Fig. 4.13), from relatively strong heat loss from the ocean to a net heat input into the ocean. The waters calmed rapidly, and we deduce that the upper layers over the saline oceanic tongue are easily stratified, and that the primary production can quickly build up high fluorescence (chlorophyll) levels there. High fluorescence values were also observed all the way to the seafloor near Suðuroy (Fig. 4.5d), and this was a recurrent feature at this location.

#### 4.1.5 Utilizing the ship-mounted echo-sounder

These data were sub-sampled using the software Echo View (<http://www.echoview.com>), at 1 minute and 10 minutes intervals, to reduce the data volume used in the subsequent analysis steps. Along the Suðuroy-Mykines section (Fig. 4.5c), we find the highest back-scatter values (red colours in Fig. 4.6a) at 30-40 m depths, which is under the highest fluorescence values (Fig. 4.5d). This might be zooplankton, but it is too soon to conclude this, because the echo-sounder has not been tuned for zooplankton detection. We conclude that valuable inter-station information might be obtained by utilizing a tuned, or properly equipped, echo-sounder.

#### 4.1.6 A virtual mooring at FASB

In order to distinguish temporal from spatial variability, a dedicated experiment was conducted over the FASB ADCP mooring on 24 April, 2010 (see Fig. 1.1a and section 4.1.12). Hydrographic profiles were made every half hour over a tidal cycle (12 hours). Together with every CTD cast, zooplankton was sampled using a WP2 net, and water bottles taken for making primary production and nutrient observations. Between every profile, the ship sailed in a 'butterfly formation', while SST was monitored.

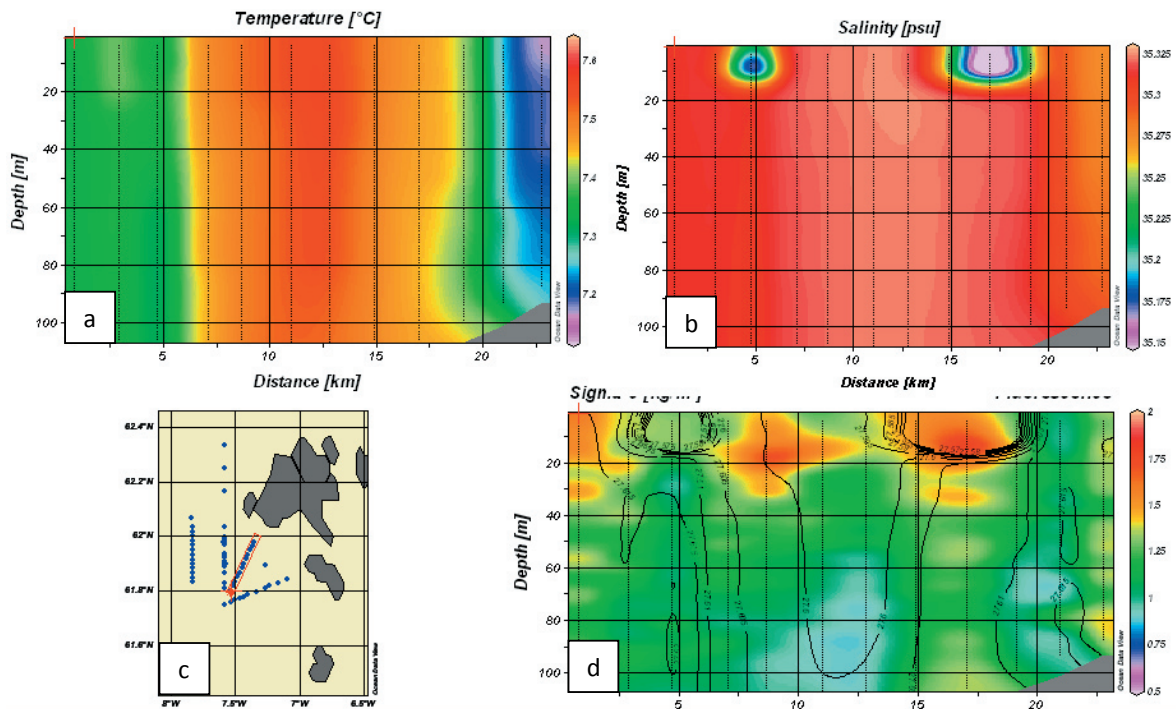


Fig. 4.2 A section where strong freshwater pockets were observed. a) Temperature, b) salinity, c) the location of the section and d) the fluorescence, with potential density overlaid.

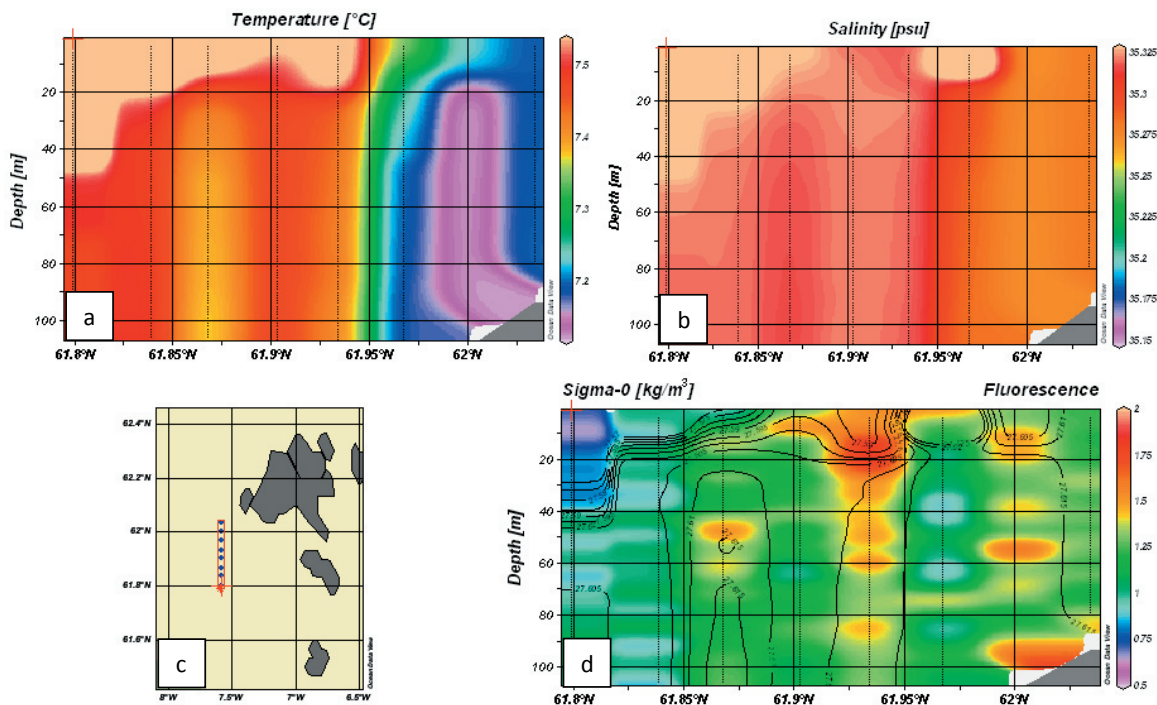


Fig. 4.3 An occupation of main section MYK, when high chlorophyll concentrations are observed in the tidal front (red colors in panel d). a) Temperature, b) salinity, c) the location of the section and d) the fluorescence, with potential density overlaid.

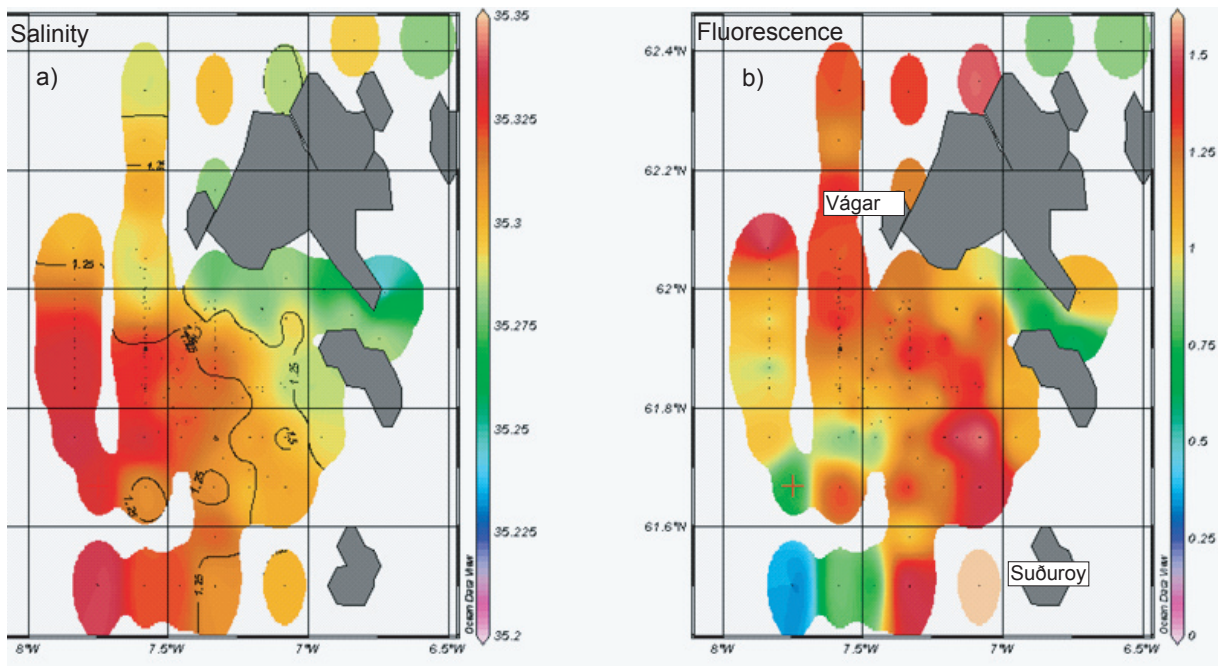


Fig. 4.4 The saline oceanic water meets the fresher shelf water at the tidal front, where increased fluorescence levels are observed. a) The salinity at 25 m depths, with the 1.25 fluorescence isolines overlaid and b) only fluorescence (25 m depths).

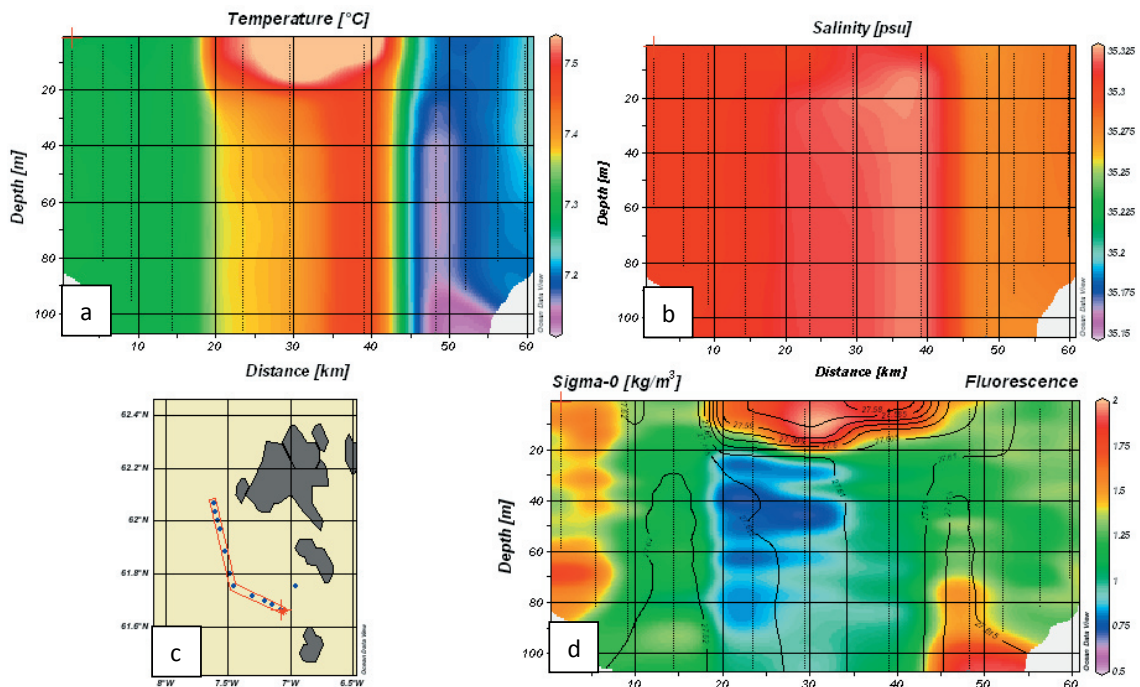


Fig. 4.5 A cross-section from Suðuroy (left) towards Mykines (right). a) Temperature, b) salinity, c) the location of the section and d) the fluorescence, with potential density overlaid.

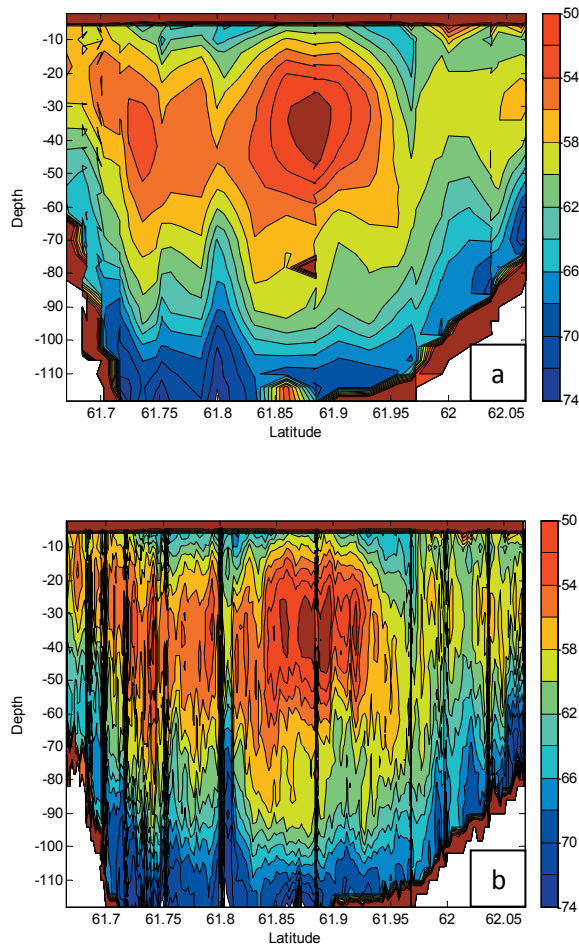


Fig. 4.6 Back-scatter data (dB) from the ship-mounted echo-sounder along the Suðuroy-Mykines section (see Fig. 4.5c). Subsampled (EchoView) at a) 10 minutes and b) 1 minute intervals (Suðuroy to the left and Mykines to the right). The vertical lines result from hydrographic stations taken along the section, when the ship is halted.

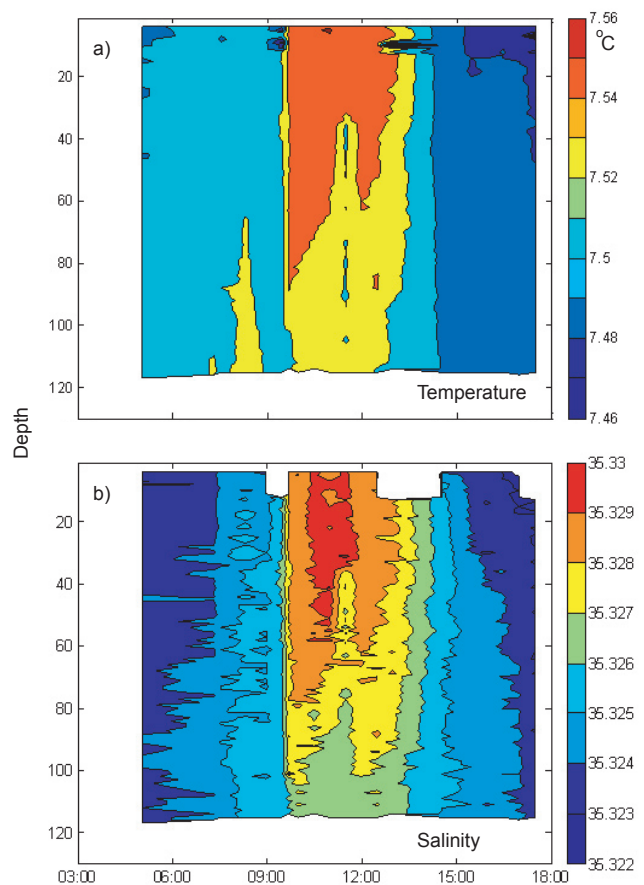


Fig 4.7 Hydrography from a 'virtual mooring' at FASB on 24 April, 2010. Time-depth (Hovmöller) diagrams of a) temperature and b) salinity.

This was done in order to see if any strong front was located in the vicinity of the virtual mooring, and this was not found to be the case.

#### 4.1.6.1 Hydrography

A slight temperature and salinity increase is observed between 0900 and 1400 hours (Fig. 4.7). This is illustrated by aligning all the half-hourly hydrographic casts in time-depth (Hovmöller) diagrams. The relatively sharp onset of this anomaly indicates this is an advective (spatial) feature, and not caused by direct atmospheric forcing (temporal).

#### 4.1.6.2 Phytoplankton abundance (Fluorescence)

The half-hourly fluorescence profiles show low surface values, until around 14.00 (Fig. 4.8). The numerous CTD casts during this cruise showed that low surface fluorescence during the strongest lit hours is a consistent feature in these waters (see also the Seaglider data in Fig. 4.37). There is a slight fluorescence increase after 0900, followed by a much stronger increase after 13.00. We concluded that the strong diurnal cycle in the near-surface layer, likely caused by photo quenching (Frajka-Williams et al., 2009) must be taken into account,

when analyzing the fluorescence data from the FAMRI database. It is not clear whether the large changes in the in-depth fluorescence is a part of a diurnal cycle, or whether it might be related to the advected feature, seen in the hydrography (Fig. 4.7).

#### 4.1.7 Lower fluorescence between the islands

In the coarse composite map shown in Fig. 4.4, it is apparent that the fluorescence values were lower near land during cruise 1012. During 26-27 April, 2010, CTD casts were made on a grid centered on a highly productive tidal front northwest of Suðuroy, followed by a section from the oceanic tongue, through Hestfjørður and towards Tórshavn. This experiment aimed at comparing the front and near-shore production. The composite map of near-surface chlorophyll for the days April 26 and 27 (Fig. 4.9), shows that the lowest fluorescence observed during these days (and in fact the entire cruise), were observed between the islands. These low values were not an artifact by photo quenching near the surface, since the values were consistently low throughout the water column (Appendix). We conclude that the primary production was higher in the vicinity of the tidal front than between the islands, during the period of our cruise.

#### 4.1.8 A virtual station near the tidal front

The region near 62°N and 7°W was very changeable, as the tidal front probably sloshed considerably here. To investigate this frontal variability, we made a virtual mooring at a location to the south of Vágar, at standard station 42 (Fig. 1.1a) that has been revisited almost every year since 1994. CTD casts were made every half hour for 4.5 hours (Fig. 4.10), during the night between April 26 and 27. A pulse with increased temperature, salinity and fluorescence was observed at around 02.00 hours. The anomaly was not strong, but still clearly discernible. Since the observations were made during the night, we should not expect any influence from the diurnal insolation cycle, and the observed changes are therefore due to horizontal advection. The warmest and most saline waters in this region come from the oceanic tongue. We interpret the association between the fluorescence and hydrography as yet another indication of increased production in the near-tidal front waters.

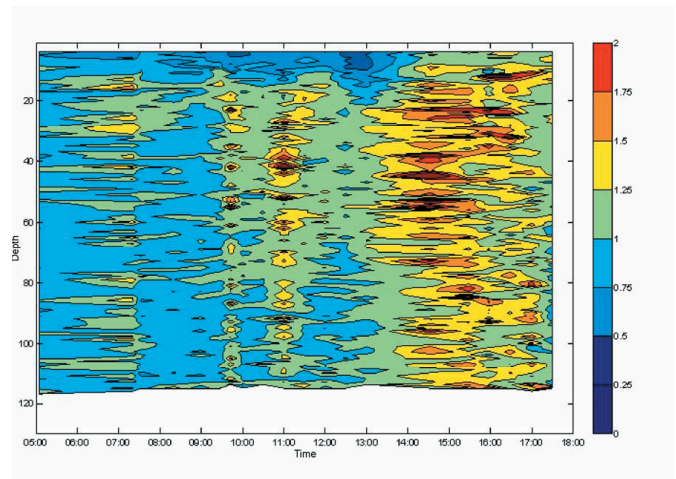


Fig. 4.8 Time-depth (Hovmöller) diagram of the fluorescence at the virtual mooring over the ADCP at station FASB.

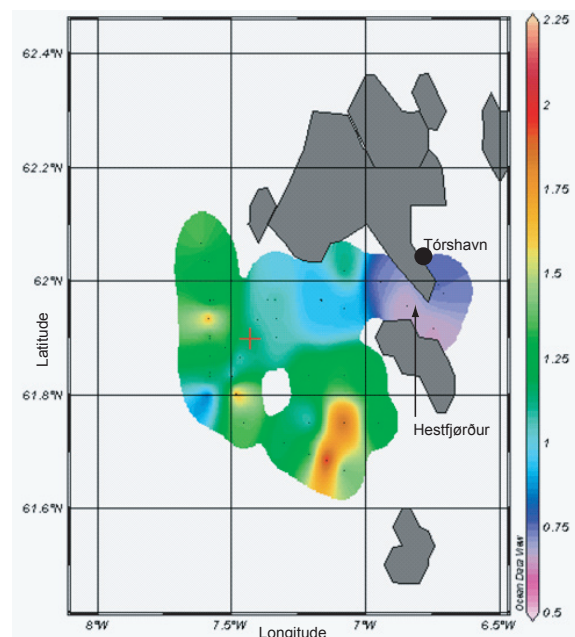


Fig. 4.9 Near-surface fluorescence (15 m depth) from all CTD casts during April 26 and 27, 2010. The stations are shown with small dots.

#### 4.1.9 Relatively low fluorescence values during cruise 1012

Some of the standard biological oceanography stations were revisited several times during cruise 1012, in order to elucidate the shorter term variability at these stations. This information might

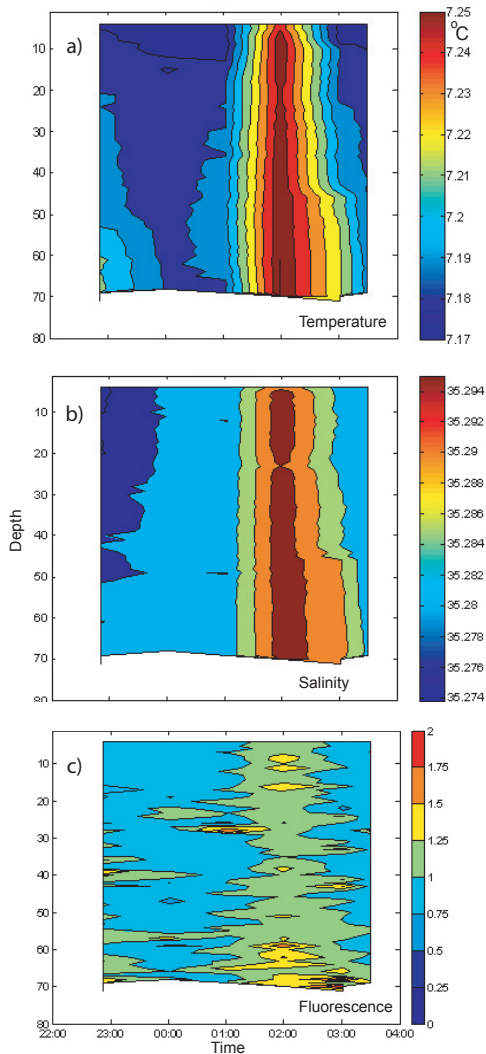


Fig. 4.10. A virtual mooring, made at standard station 42, to the south of Vágar during the night April 26-27, 2010. a) temperature, b) salinity and c) fluorescence.

be valuable when analyzing and interpreting the larger multi-year dataset. Station 41 (Fig. 1.1a) was visited both during the standard *biological oceanography* cruise (Monday, April 19), and subsequently several times on cruise 1012 (Fig. 4.11). This indicates that the phytoplankton concentrations had been larger immediately before the extended leg of the cruise. We speculate that the very strong heat loss to the atmosphere on April 20 (see Fig. 4.13) might have weakened the primary production, due to a general erosion of the stratification throughout the study region.

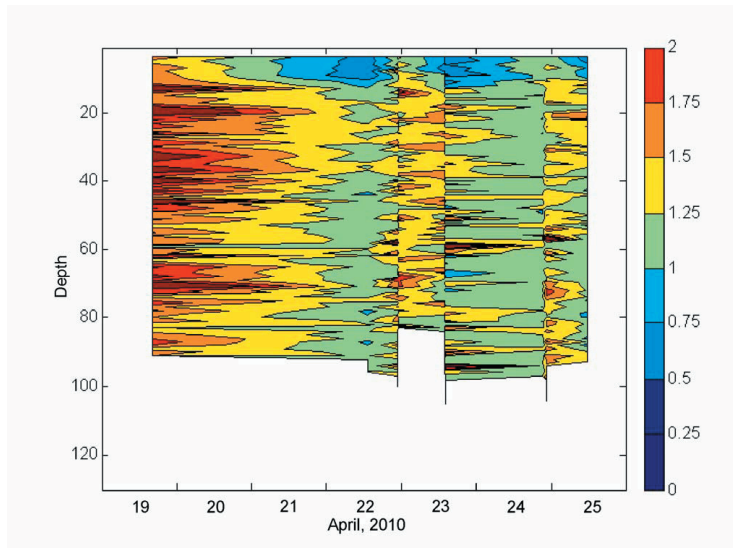


Fig. 4.11 Time-depth (Hovmöller) diagram of the fluorescence at standard station 41, immediately south of Mykines (Fig. 1.1b), before and during the exploratory cruise 1012.

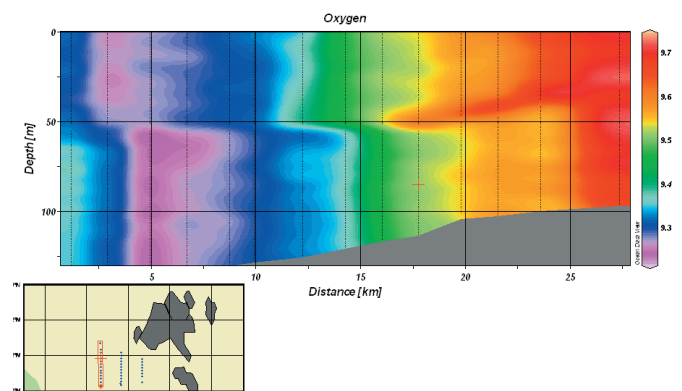


Fig. 4.12 An oxygen section south of Mykines.

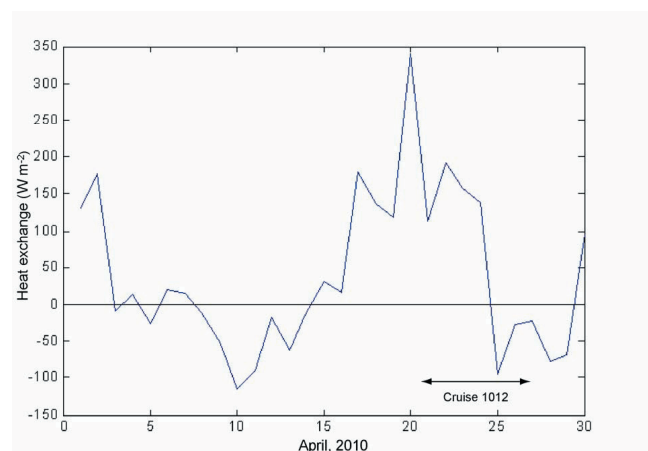


Fig. 4.13 The heat loss from the Western region to the atmosphere (positive from the ocean) during April 2010 (cruise 1012).

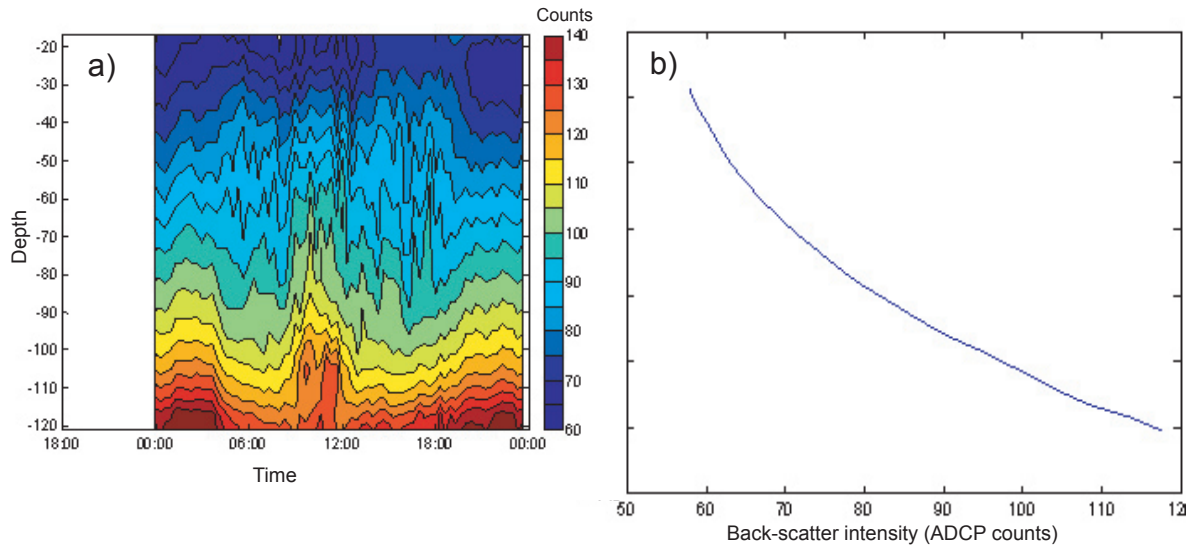


Fig. 4.14 Back-scatter intensity from the bottom mounted ADCP at mooring FASB. a) A time-depth (Hovmöller diagram) of the intensity during April 24 and b) the time-averaged intensity for the full duration of the deployment (20 January-4 September, 2010).

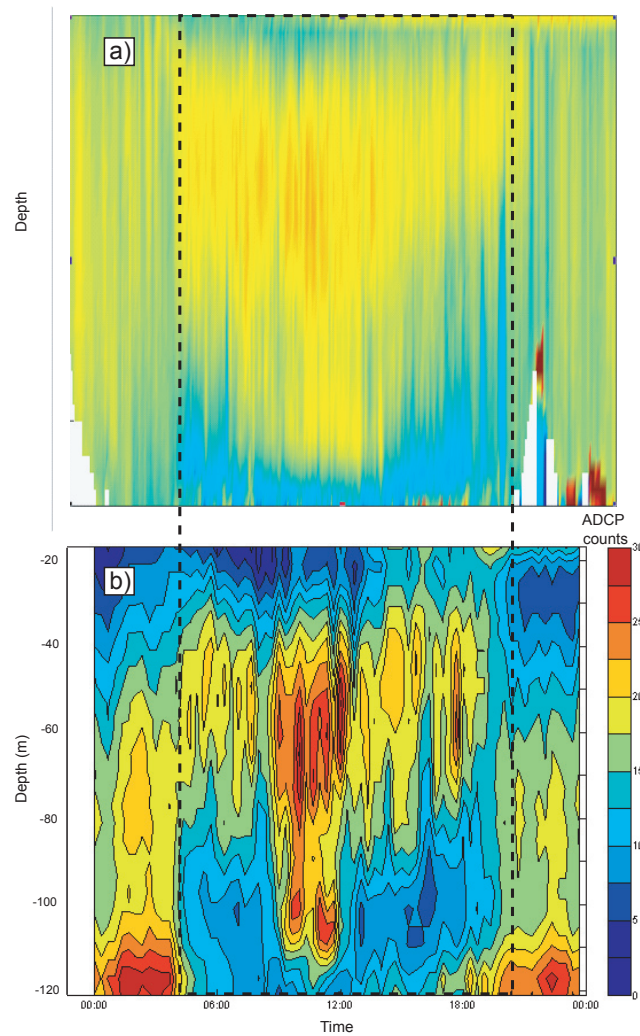


Fig. 4.15 Back-scatter during April 24, 2010. a) output from the ship mounted echo-sounder and b) back-scatter anomaly from the bottom-mounted ADCP, with the time-average profile (Fig. 4.14b) subtracted. The dashed rectangles show the same time window. The depth in a) is approximate.

#### 4.1.10 Oxygen measurements

Inspired by the fact that oxygen have been used as a proxy for the primary production in other locations (Richardson et al., 2000), FAMRI bought a new oxygen sensor from Seabird, and added it to the CTD. Our preliminary analysis of these data did not reveal any clear patterns. Some sections revealed peculiar patterns (Fig. 4.12), but these have not been interpreted as indications of primary production yet. We conclude that no extra information has been obtained from the oxygen observations yet, but analysis of sections later in the year, when the Western region has become firmly stratified, might be informative.

#### 4.1.11 Biological data

Data on nutrients, primary production and zooplankton are available, but not analyzed yet.

#### 4.1.12 Heat flux

The net air-sea heat exchange from the Western region has been extracted for April, 2010 (during cruise 1012) from the NCEP/NCAR reanalysis fields. There was a shift from net heat loss from the ocean, to a net heat input around April 24-25 (Fig. 4.13).

### 4.2 New moorings

#### 4.2.1 An ADCP at FASB

An ADCP was moored near the expected position of the tidal front (based on a long-term analysis of the dataset from the *biological oceanography* cruises) on main section MYK, to measure expected cross-frontal exchanges here.

##### 4.2.1.1 Back-scatter intensity

In addition to current velocities an ADCP also delivers the back-scatter intensity (Fig. 4.14a). The intensity is highest near the instrument (at 125 m depth), and declines up through the water column. This depth-dependent decline in intensity is shown by averaging all pings during the full duration of the deployment (Fig. 4.14b). In order to illustrate the intensity anomaly at every depth bin, the average profile has been subtracted from the observed intensity during April 24, when the 'virtual mooring' was made (Fig. 4.15b). A clear diurnal cycle was observed in the back-scatter pattern at this location and during the days of the cruise (the pattern in Fig. 4.15b is recurrent over several weeks). During

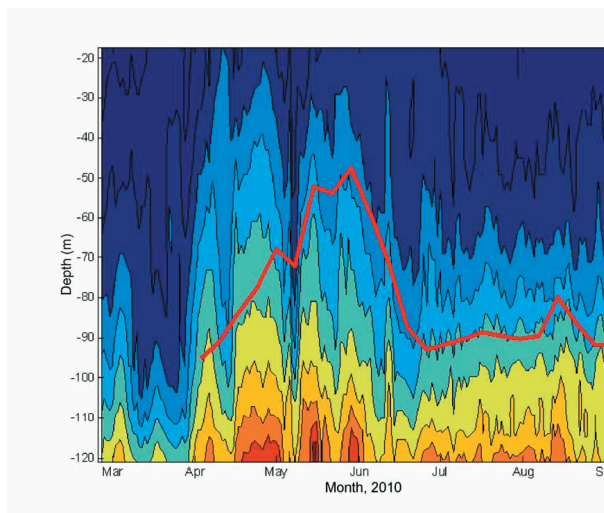


Fig. 4.16 Backscatter intensity (colors) from the bottom mounted ADCP at station FASB, and the chlorophyll concentration at coastal station 'Skopun' (red), not to scale and shifted four days forward in time.

midnight, and the very early hours, there is strong intensity near the seabed. At around 05.00 hours, there is increased intensity in the mid-water column at 40-80 m depths, while the near-bottom and near-surface intensity is much decreased. A strong pulse is observed in the mid-water column between 9.00 and 13.00, which coincides with the observed hydrographic anomaly shown in Fig. 4.7. The near-surface intensity remains low until around 14.00, when there is an increase that lasts until around 20.00. This coincides with the observed near-surface fluorescence shown in Fig. 4.8. A similar pattern is also qualitatively replicated by the ship-mounted echo-sounder data (Fig. 4.15a). We conclude that *i*) the clear diurnal cycle in the intensity is likely related to vertical migration of components of the biosphere (fish and/or zooplankton), *ii*) that the match between the backscatter observed by the ADCP and the echo-sounder lends credibility to both data sources and *iii*) the diurnal cycle in the near-surface fluorescence might be more than just photo quenching (see section 4.6.1.2), since it also appears in the back-scatter.

##### 4.2.1.2 Back-scatter at FASB and primary production at Skopun

The virtual mooring over FASB on April 24, 2010, illustrated that the backscatter from the ADCP likely is a measure of the concentration of biology (species unknown) in the water column (Fig. 4.15). We have also noticed that increased growth near Skopun is observed as increased concentration of

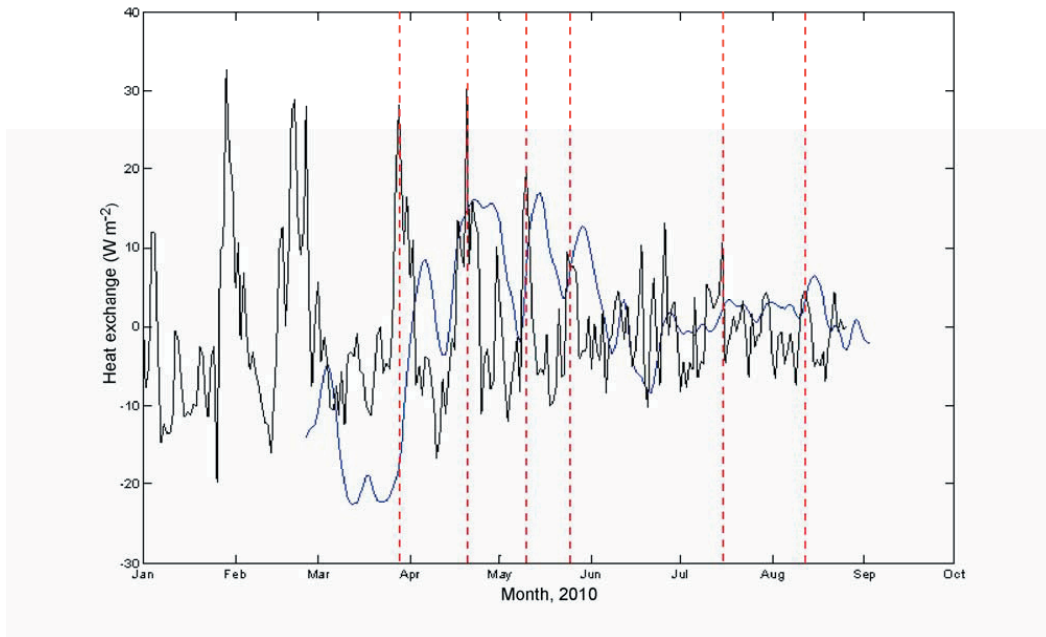


Fig. 4.17 The ADCP backscatter at FASB averaged over the deepest 10 bins (blue, low-passed), and the air-sea heat exchange from the Western region (black). Increased heat loss to the atmosphere is upward. The seasonal cycle has been removed and daily values are shown (which means that the values are relative). The linkage between positive heat loss anomalies and increased backscatter is emphasized with the red dashed lines

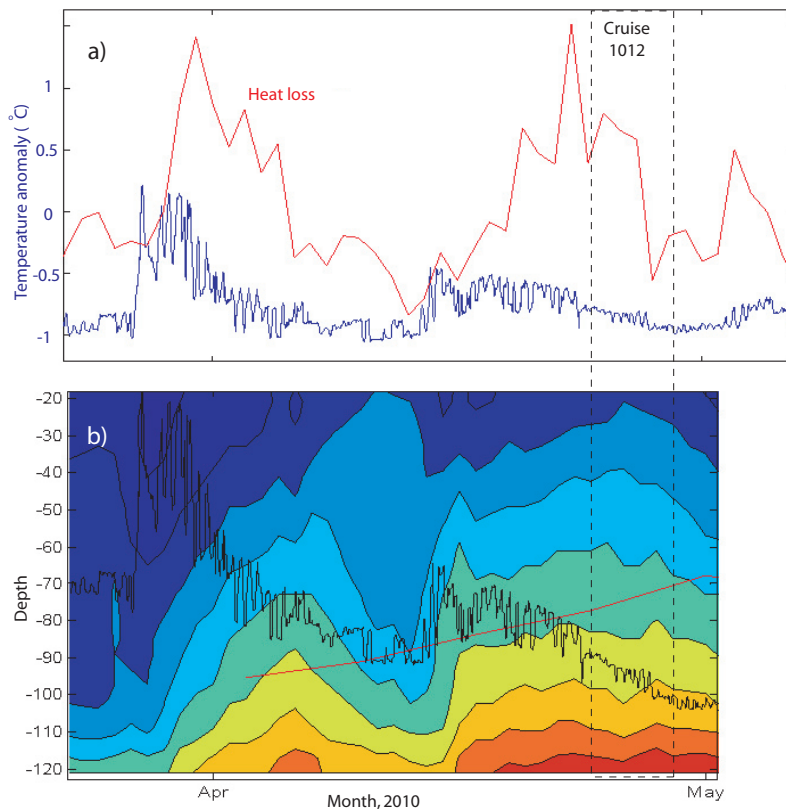


Fig. 4.18 Insight from the bottom temperature at FASB. a) The bottom temperature (blue) and the heat loss anomaly to the atmosphere (red, positive out of the ocean) and b) the backscatter intensity (as in Fig. 4.16), and the bottom temperature (black line) as in a). The dashed rectangle shows the duration of the extended leg of cruise 1012.

backscatter throughout the water column at station FASB, after a four days time-lag (Fig. 4.16, see also Larsen et al., 2011). We conclude that physical/biological processes within the Western region might be linked with the processes that regulate the production observed at Skopun, although we do not know which biological or physical species/parameters the ADCP backscatter represents.

#### 4.2.1.3 Intensity and air-sea heat loss

A time series of the ADCP backscatter is obtained by averaging the deepest 10 bins (~ 40 meters over the seafloor) (Fig. 4.17). The ADCP-derived time series shows that shorter term pulses ride on the main rise between April and June. The ADCP is sampling every 20 minutes, so if the apparent linkage between the ADCP backscatter and the Skopun chlorophyll is real, then the ADCP-derived time series might represent the Skopun chlorophyll variability, (which is only sampled weekly, on a sub-weekly time scale). All pulses of increased backscatter intensity coincide with increased heat loss to the atmosphere. This is shown by comparing the ADCP-derived time series with the heat loss anomalies from the annual cycle (Fig. 4.17). We conclude that the previously hypothesized linkage between heat loss and primary production (Hansen et al., 2005), might hold on a sub-weekly basis.

#### 4.2.1.4 Linkage to bottom temperature at FASB

There was a sudden increase in the bottom temperature at FASB on the order of 0.5-1 °C just prior to the two first increases in backscatter intensity in 2010 (Fig. 4.18b). Positive heat-loss anomalies to the atmosphere occurred after the temperature jumps (Fig. 4.18a), and the bottom temperature declined with marked oscillations riding on top. A tidal analysis of these shorter term temperature fluctuations showed no clear linkage to the main tidal constituents ( $M_2$ ,  $S_2$ ). There was, however, slight association with  $N_2$ . From this we infer that the positive temperature jumps are likely caused by a shoreward shift of the warm and saline oceanic tongue, and thus of the tidal front in this location. The subsequent cooling, and thus increased convection, helps the tidal forces to homogenize the inner region. This region therefore expands and the tidal front is forced off-shore again, as revealed by the declining bottom temperatures at FASB (Fig. 4.18). When the tidal front is located in the vicinity of FASB, the

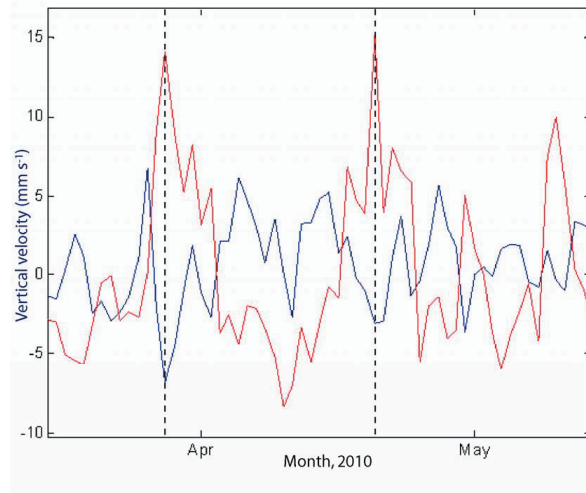


Fig. 4.19 Daily averaged heat loss anomalies to the atmosphere (red, relative values) and vertical current velocities observed at FASB (blue, negative values show sinking).

horizontal fluctuations of this front, probably linked to atmospheric and tidal forcing, are observed as the clear temperature oscillations. The apparent lagged synchrony between the main temperature jumps and the heat loss to the atmosphere is probably coincidental. It is not clear at present how the described processes are linked to the primary production. We merely show that the bottom temperature at FASB may be a valuable supplement for understanding the processes involved.

#### 4.2.1.5 Heat loss and vertical velocities at FASB

The ADCP delivers vertical, as well as horizontal, current velocities. These were compared to the air-sea heat exchange (Fig. 4.19). The first main peak of heat loss to the atmosphere coincides with the largest negative vertical velocities (sinking) observed during the entire deployment (daily average of ~0.7 cm s<sup>-1</sup>), and the second heat loss peak also coincided with sinking. We conclude that the heat losses to the atmosphere likely induce vertical overturning motions, which again will erode potential mixed layers and regulate the fluxes between benthos and the water column, but the potential linkage between heat loss and sinking was not strong.

#### 4.2.1.6 Average current velocities at FASB

The long-term, depth-averaged current velocities, found by averaging all depth bins from all the observations between 20 February and 4 September, 2010, are only  $2.6 \text{ cm s}^{-1}$  (Fig. 4.20). We conclude that the region to the south of the tidal front south of Mykines and Vágar probably is very quiescent.

#### 4.2.2 An ADCP at the FASC

An ADCP was deployed at a location to the northwest of Suðuroy during the summer of 2011 (Larsen et al., 2013), where both simulations and satellite data show on-shelf transport of upper layer waters from the Western region (see section 4.5.2). Progressive Vector Diagrams of the currents, observed within the shallowest bins during these months shows a general north-northeasterly flow, and not the eastward flows as indicated in the simulated and remotely observed maps (see Fig. 4.35). The very shallowest bin (10 m depth) actually diverged from those immediately underneath during June, and started to flow in a more northwesterly direction, as opposed to the expectations. The uncertainty in these measurements is highest in the shallowest bins. It remains to be confirmed whether this divergence is due to measurement error, or if such a sharp transition between 10 and 14 meters depth in this region is real. We conclude that the current observations at FASC do not confirm the apparent on-shelf flow to the northwest of Suðuroy. An ADCP deployment nearer the islands might give a different picture since the expected flows there are expected to be stronger (Fig. 4.34a). Bottom irregularities influence local flows, and might thus limit the conclusions made from point observations.

#### 4.2.3 Equipping a wave buoy with temperature sensors

Temperature sensors were attached near the surface and near the bottom on a Waverider mooring, located within the Western region during 2011 (see Fig. 1.1). The difference between the near-surface and the near-bottom temperatures should give a useful proxy for the stratification within the Western region. Comparing this temperature difference to the coastal chlorophyll concentrations we see that the weak bloom in May, 2011 coincided with increased stratification at the Waverider mooring (Fig. 4.22). There was no association between these parameters later in the year. The buildup of stratification during early May was preceded by

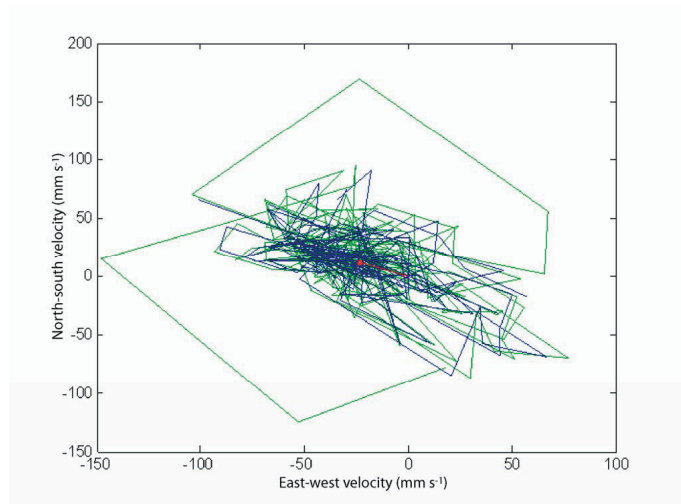


Fig. 4.20 Scatter plot of the depth averaged current velocities (all bins) at mooring FASB. The time-average (over all the full duration of the mooring) is shown with the red dot.

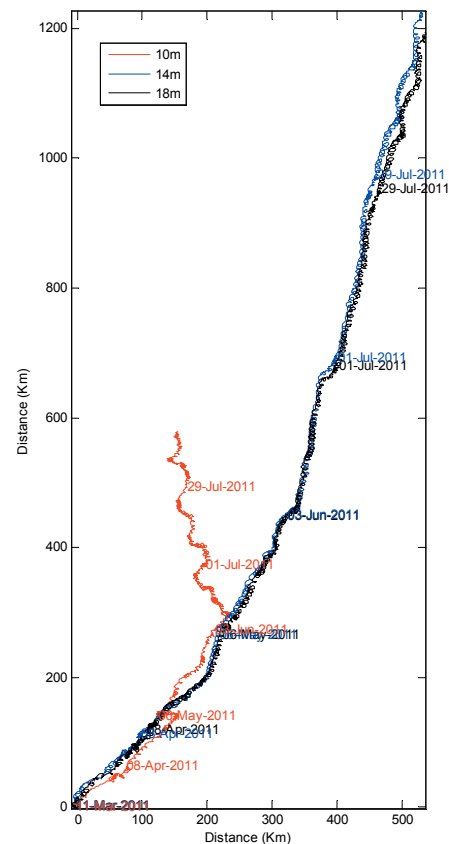


Fig. 4.21 Progressive Vector Diagram (PVD) of the near-surface currents, sampled by an ADCP deployed to the northwest of Suðuroy (FASC, see Fig. 1.1).

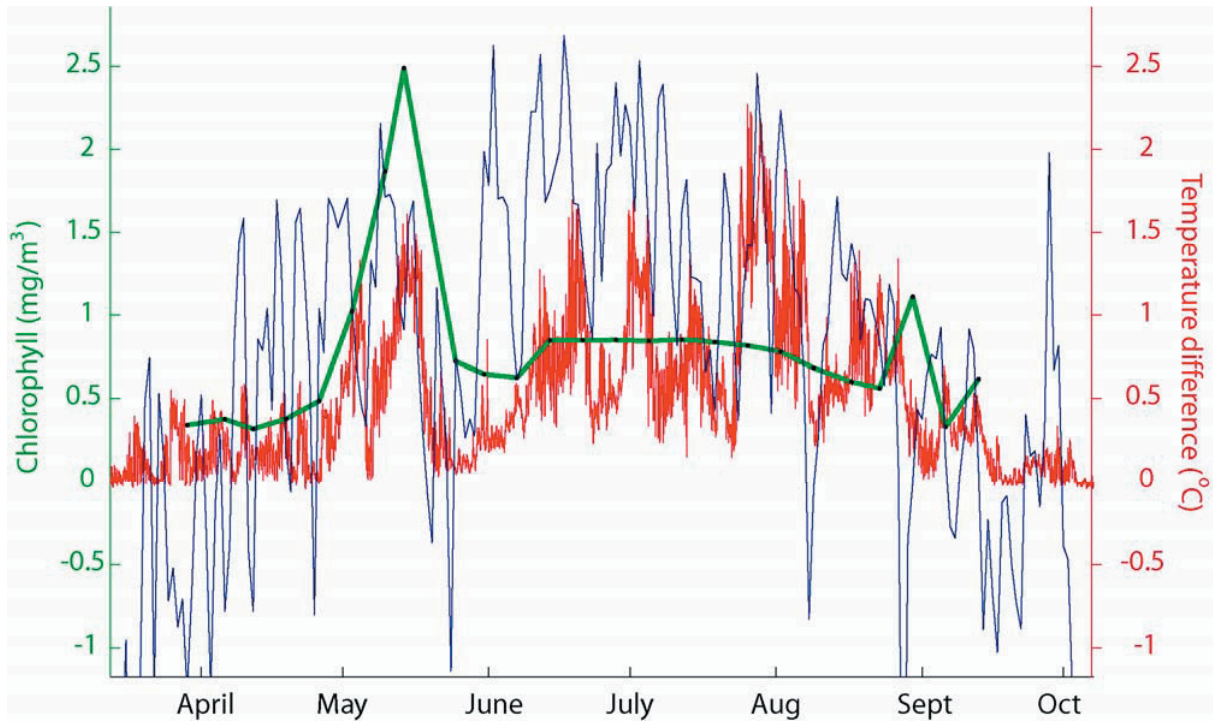


Fig. 4.22 The difference between near-surface and near-bottom temperatures at the Waverider mooring (within the Western region) in 2011 (red), chlorophyll concentrations at coastal station Skopun (green) and the air-sea heat exchange (blue, not to scale, and positive values mean heat input into the ocean).

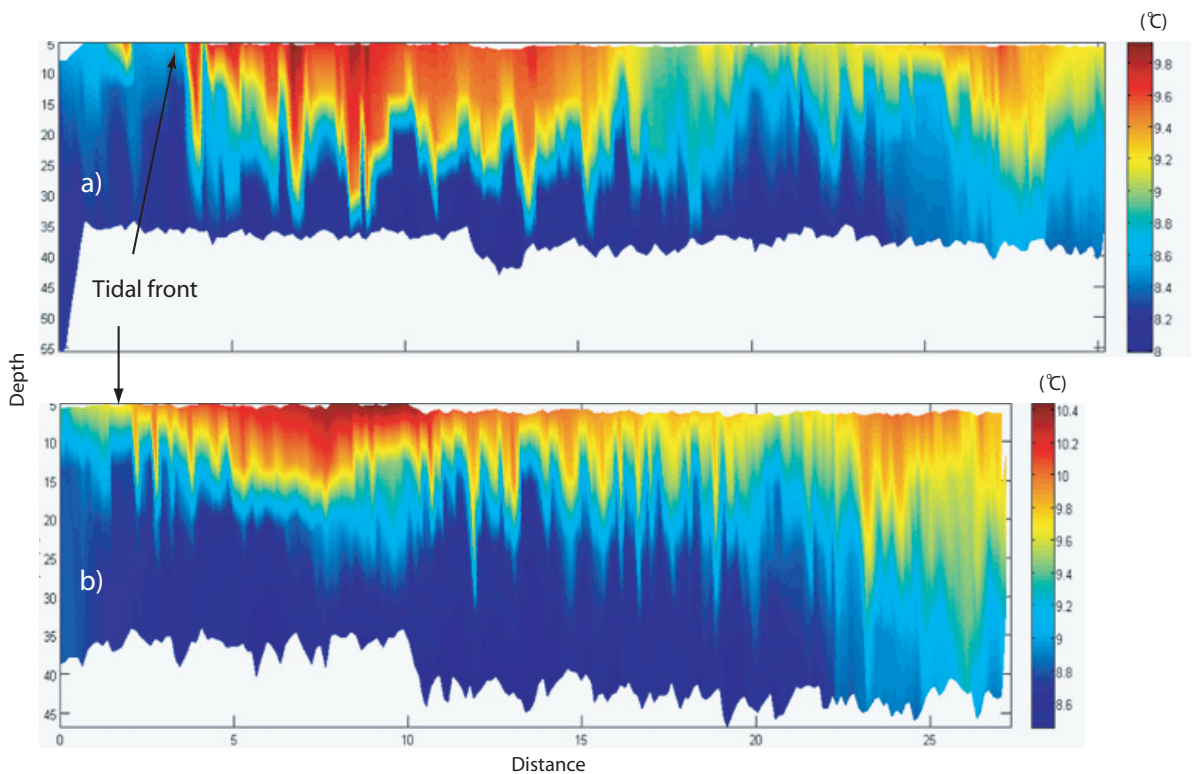


Fig. 4.23 Two temperature sections taken along the main section MYK (see Fig. 1.1b), using the TTW, during a) June 6, 2010 and b) June 23, 2010. Mykines is to the left, and the approximate location of the tidal front is indicated.

relatively large heat fluxes into the ocean and the break-down of the stratification during late May coincided with heat losses to the atmosphere (blue curve). We conclude that the instrumentation of the Waverider mooring is a cheap and convenient way of obtaining valuable data, and this should be continued.

## 4.3 New sections

### 4.3.1 *The oceanic tongue: A 'cold-cushion'?*

The main section MYK, where the highest climatological chlorophyll values are observed (Fig. 2.5), has also been monitored using a Towed Temperature Wire (TTW) (Larsen, 2009). Two occupations of the section during the summer (6 June and 23 June, 2010), following experimental cruise 1012, are shown in Fig. 4.23. The highest upper layer temperatures, and thus stratification, are found immediately to the south of the tidal front, located about 5 km from the section origin, which is near Mykines. The lowest lower-layer temperatures are found under the strongest stratification (~ 40 meter depths) (Fig. 4.24). Our interpretation is that this is a quiescent region, where the heat input from the atmosphere is being arrested within the upper layer, which therefore becomes warmer than its surroundings. Less energy reaches the lower layer, which therefore warms slower than its more mixed surroundings and a so-called 'cold cushion' (Hill et al., 1997) might be formed during the summer.

### 4.3.2 *Standard sections M, R and V*

The new sections M, R and V, with shorter distances between the hydrographic stations than at the long-term hydrographic sections, are intended to resolve the slope-shelf processes. As an example, we show an occupation of section V, made during May 2012 (Fig. 4.25). This section, which has been a part of the regular hydrographic surveys since the late 1980s, shows the presence of stratified Atlantic water in the deep ocean, the underlying cold and fresh Faroe Bank Channel Overflow water and the relatively mixed water on the Faroe Bank and on the Faroe shelf, respectively. But the closer stations on the Faroe shelf also show the presence of the relatively stratified pool within the Western region (Fig. 4.25d) and increased near-surface production (more chlorophyll) at the edges of this region, during these casts (Fig. 4.25e). Whether increased chlorophyll levels actually occur within

this pool, or at its edges, varies in time as shown in other sections in this report (e.g. Fig. 4.31). The addition of oxygen as regularly sampled parameter furthermore reveals the ventilation of the waters near the Faroe shelf (more oxygen), as well as in the overflow waters (Fig. 4.25e). Such important details, which were not properly sampled in the old section, will be regularly monitored in the future at section M, R and V.

## 4.4 Coastal station Skopun

### 4.4.1 *Inter-annual chlorophyll concentrations and air-sea heat exchanges*

The strong inter-annual variability in the primary production on the Faroe shelf, as represented by the PPI (See Fig. 2.3), has previously been linked to the heat loss from the ocean to the atmosphere – cold winters give high production (Hansen et al., 2005).

We here compare the intra-seasonal variability in the chlorophyll concentrations at Skopun during the growth season to daily values of the air-sea heat exchange from the Western region (Fig. 4.26). All bloom periods, during the years with much growth (1999-2001, 2004, 2008-2010), coincided with a short period with net heat loss to the atmosphere. These were also the only periods with net heat loss during the potential growth period (mid-April to mid-September), for each respective year. The characteristic year 2009, with three peaks during the growth period, illustrates the potential linkage to the heat losses particularly clearly (Fig. 4.26). We conclude that a prerequisite for large growth is net heat loss from the ocean sometimes during the potential growth period. Net heat loss does also occur during the other years with less growth, and this shows that heat loss is a necessary, but not sufficient requirement for growth. Another limiting mechanism must thus be at play as well.

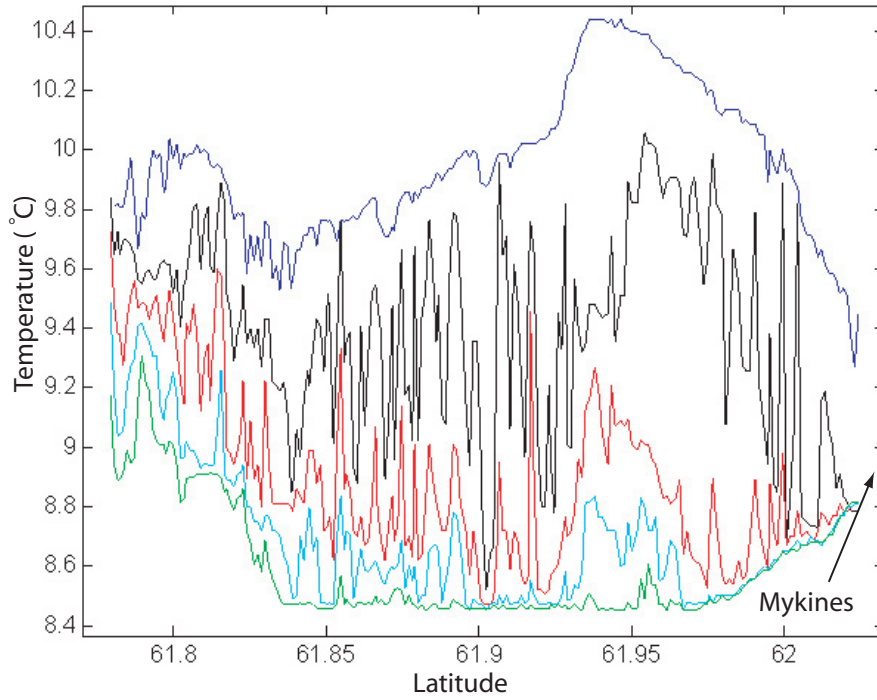


Fig. 4.24 The temperature records from each individual temperature sensors on the TTW, located at roughly 5 m (blue), 14 m (black), 23 m (red), 32 m (light blue) and 40 meters depth (green) are plotted.

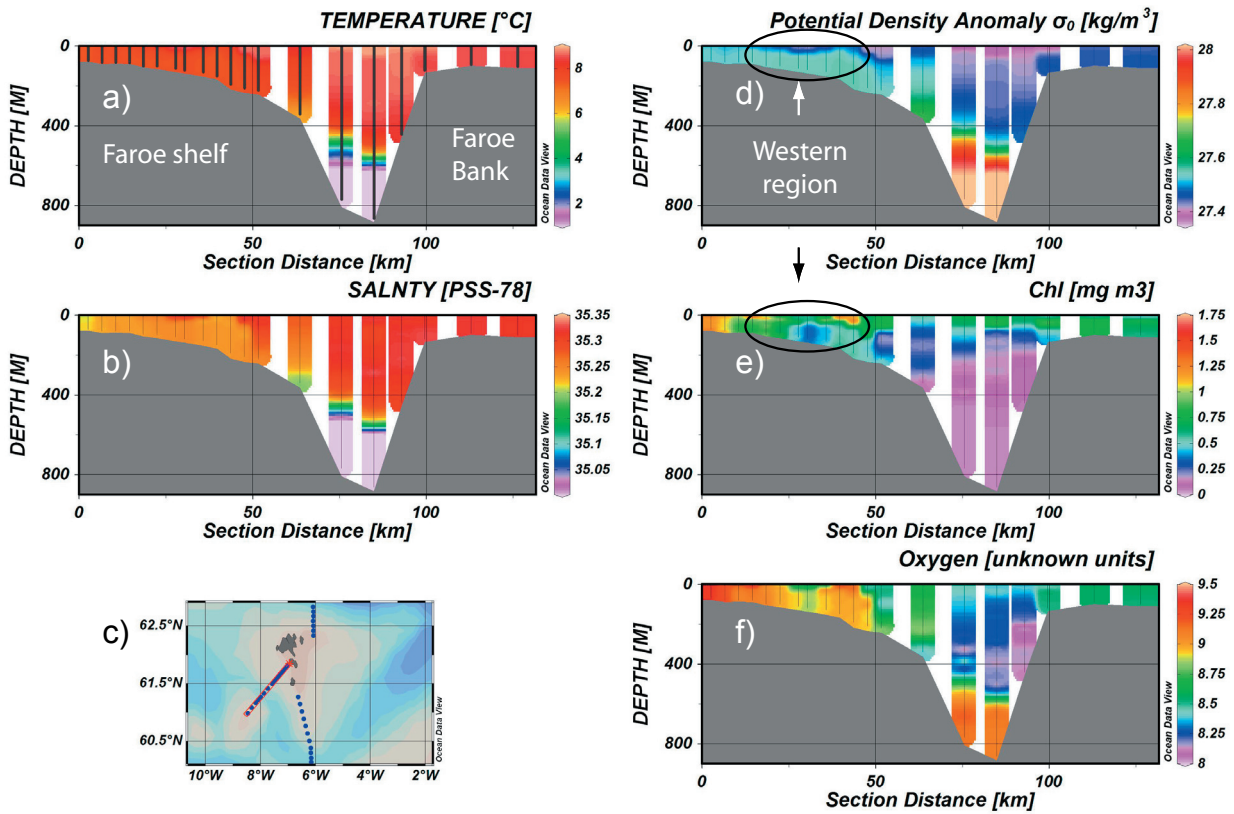
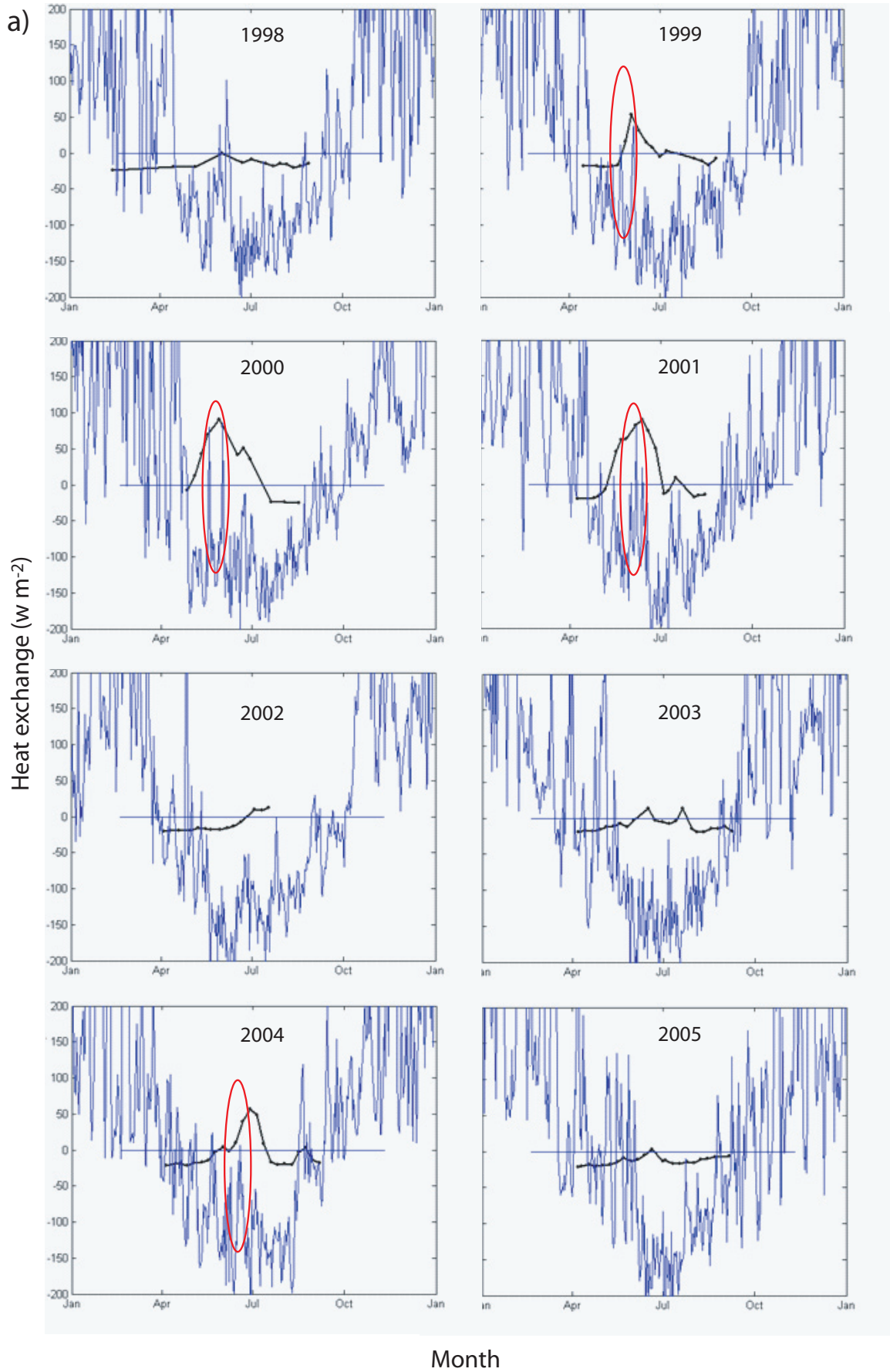


Fig. 4.25 An occupation of the new section V, from the Faroe shelf (left) to the Faroe Bank (right). The positions of the hydrographic stations are emphasized in panel a). Notice the shortened spacing between the stations on the Faroes shelf.



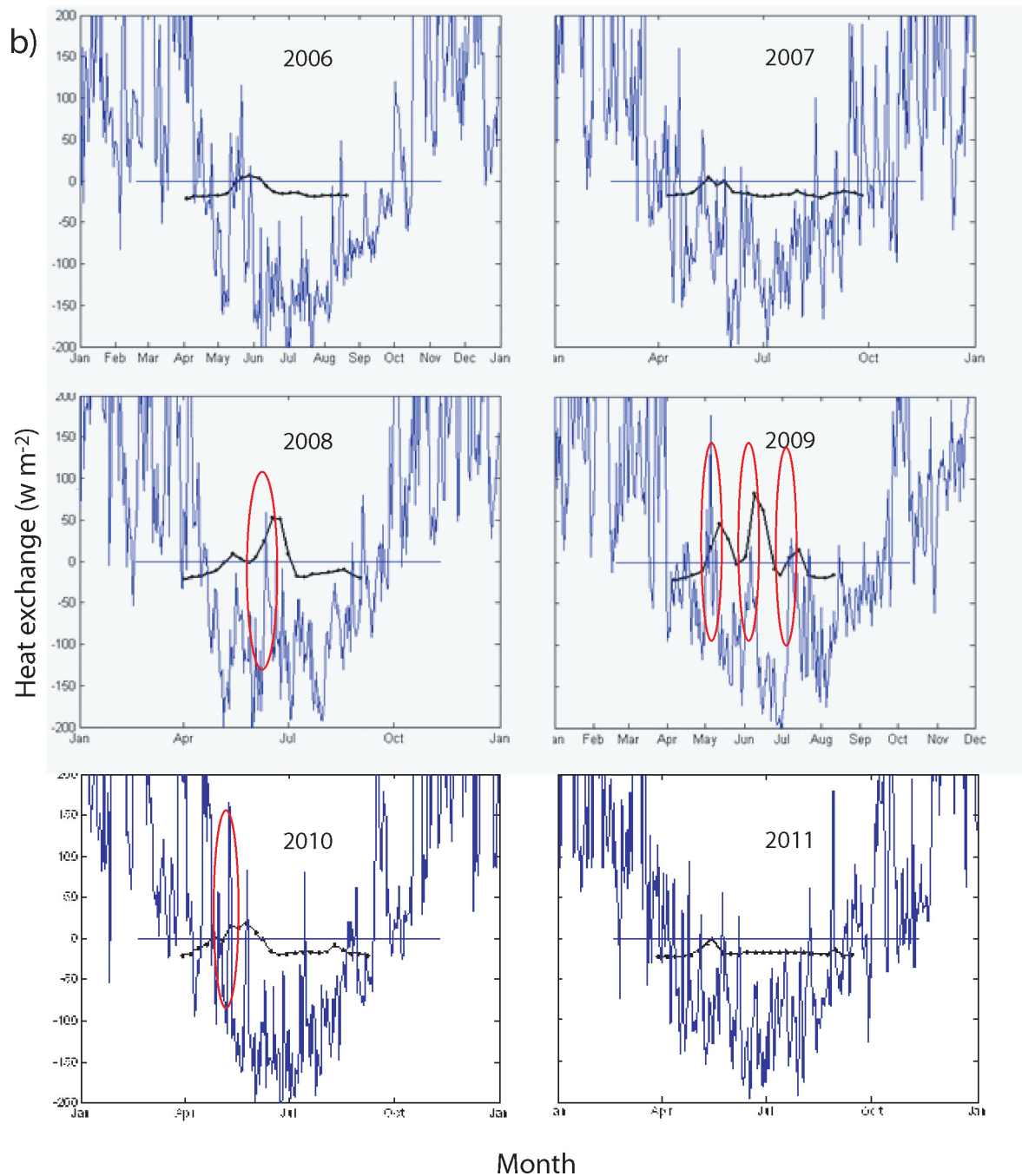


Fig. 4.26 Heat loss from the Western region (blue) and the chlorophyll concentration at coastal station Skopun (black, not to scale). Panel a) shows the years 1998-2005 and panel b) shows the years 2006-2011. Events with heat loss during the years when the concentrations exceeded  $6 \mu\text{g l}^{-1}$  (Rasmussen et al., 2013) are emphasized with the red ovals.

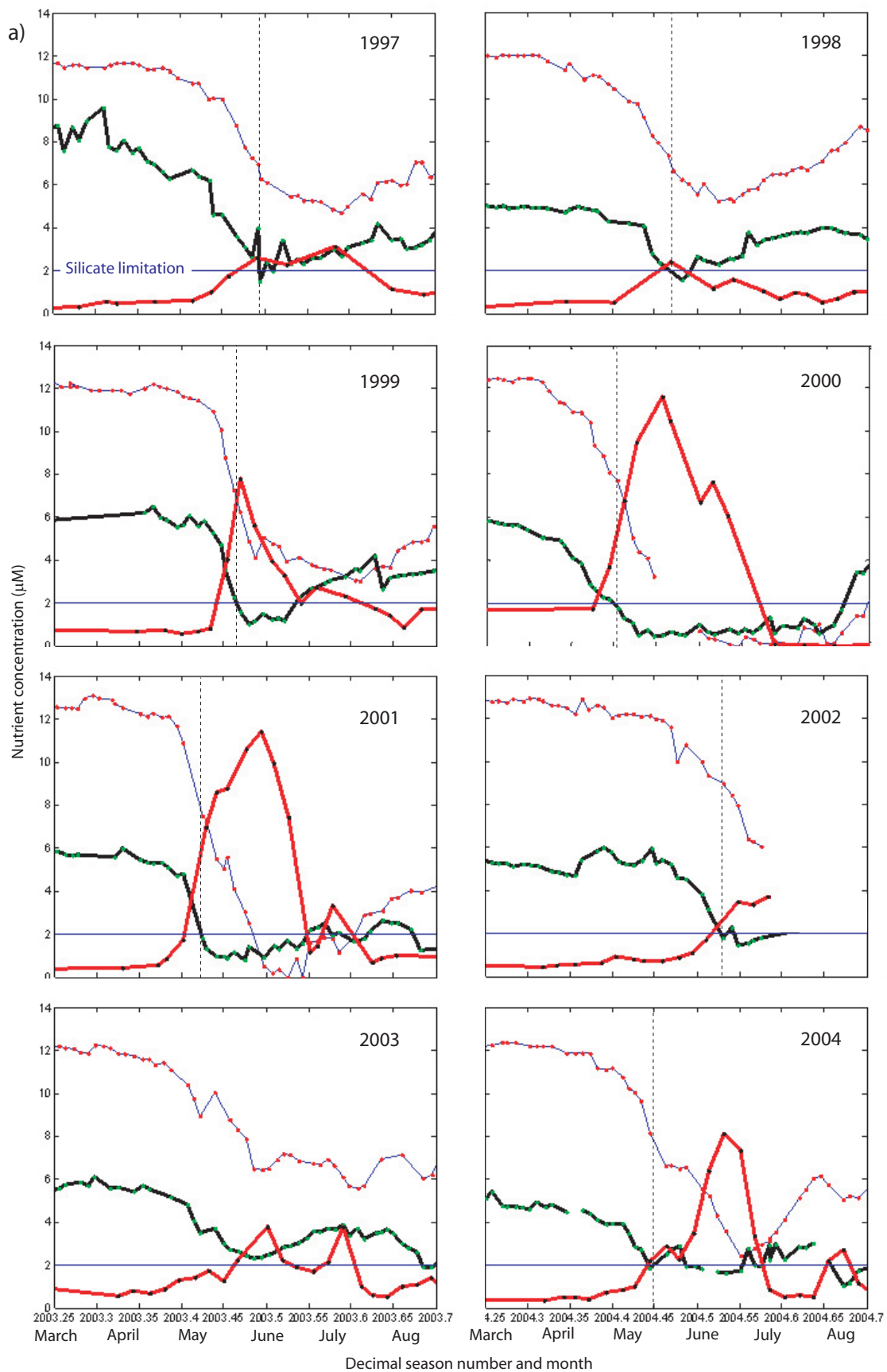
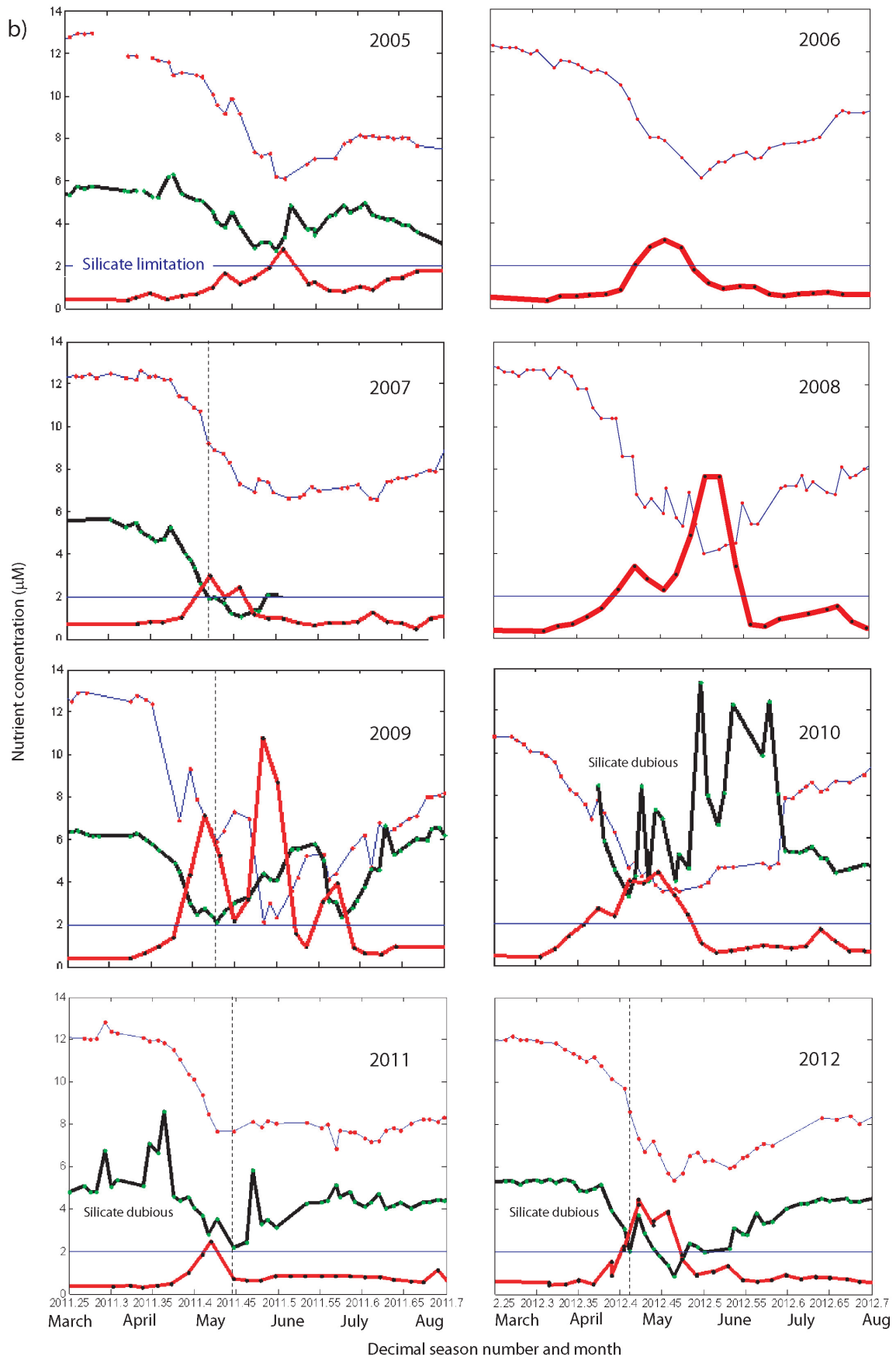


Fig. 4.27 Bloom and nutrient dynamics at coastal station Skopun. The chlorophyll (red), silicate (black) and nitrate (blue) concentrations are plotted for each individual year. The limiting silicate concentration is marked with a blue horizontal line.



#### 4.4.2 Growth and nutrient dynamics at coastal station Skopun

A closer scrutiny of the chlorophyll and nutrient concentration at Skopun supports our proposition of silicate limitation, but the story is more complex than a single nutrient limitation of the growth. We see that the silicate approaches limiting concentrations ( $2\mu\text{M}$ ) every year (Fig. 4.27). The nitrate becomes limiting (concentrations under  $3\mu\text{M}$ ) during the most growth intensive years (1999, 2000, 2001, 2004 and 2009). But growth is not just chlorophyll concentrations, but also a succession of different phytoplankton communities during the season.

The growth in 2009 started in a similar way, as in the very productive years, 2000 and 2001, but there were two marked breaks in the chlorophyll concentration in 2009 (Fig. 4.28). Comparing these contrasting years, in light of the nutrient dynamics, we observe the following:

During the most growth intensive years (2000 and 2001) the chlorophyll concentrations increase, uninterrupted, until a very high peak is reached and the growth becomes nitrate limited (Fig. 4.27a). The silicate values go under limiting concentration, and stay low. We interpret this as a continuing bloom of particularly the fast growing diatoms. Lateral influxes of silicate, and possible re-suspension from the seafloor are thus continually exhausted.

During the characteristic year of 2009, we see that the first peak draws down the silicate, until limiting values are reached (Fig. 4.27b). This first bloom therefore contains a substantial portion of the silicate craving diatoms. After the silicate becomes limiting, the chlorophyll values decrease much, which we interpret as a rapid decrease in the diatom community. A second, and larger, peak follows, but the silicate concentrations continue to rise. This second peak can therefore not be dominated by a diatom community, and the in-fluxed silicate remains in the water column. This peak is terminated when the nitrate becomes limiting. There is a smaller third peak, which strongly draws the silicate down again and subsequently is limited by this nutrient. This must therefore be a second diatom bloom.

The years 2000 and 2001 appear to be exceptional, while a break in the growth curve around the time when the silicate concentration goes below  $2\mu\text{M}$  seems to be the rule (see 1997, 1998, 1999,

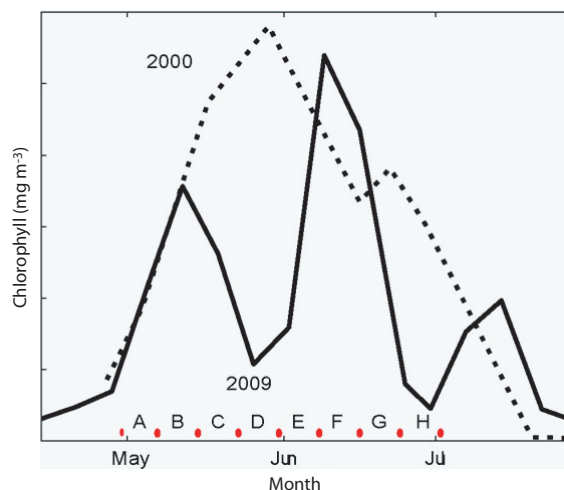


Fig. 4.28 Chlorophyll concentrations at coastal station Skopun in the Faroe Islands for two high-production years - one with a continuous peak (2000, dashed line) and one with three marked decreases during the growth season (2009, full line). The letters at the lower axis refer to the periods covered by the chlorophyll maps shown in Fig. 4.30.

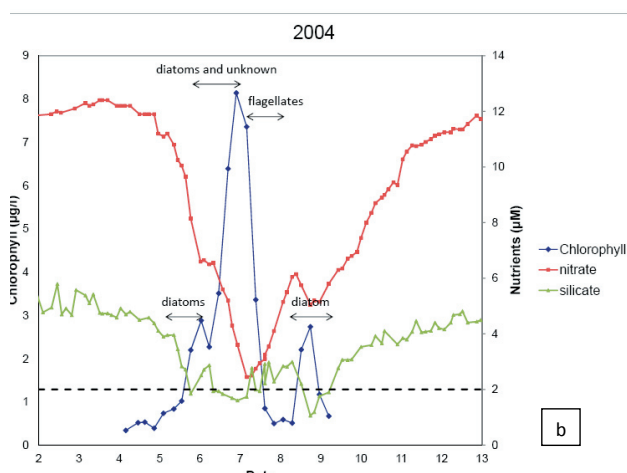
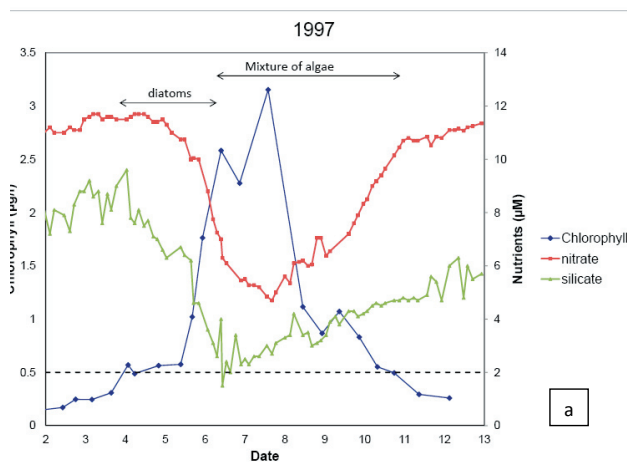


Fig. 4.29 Phytoplankton community shifts in a) 1997 and b) 2004.

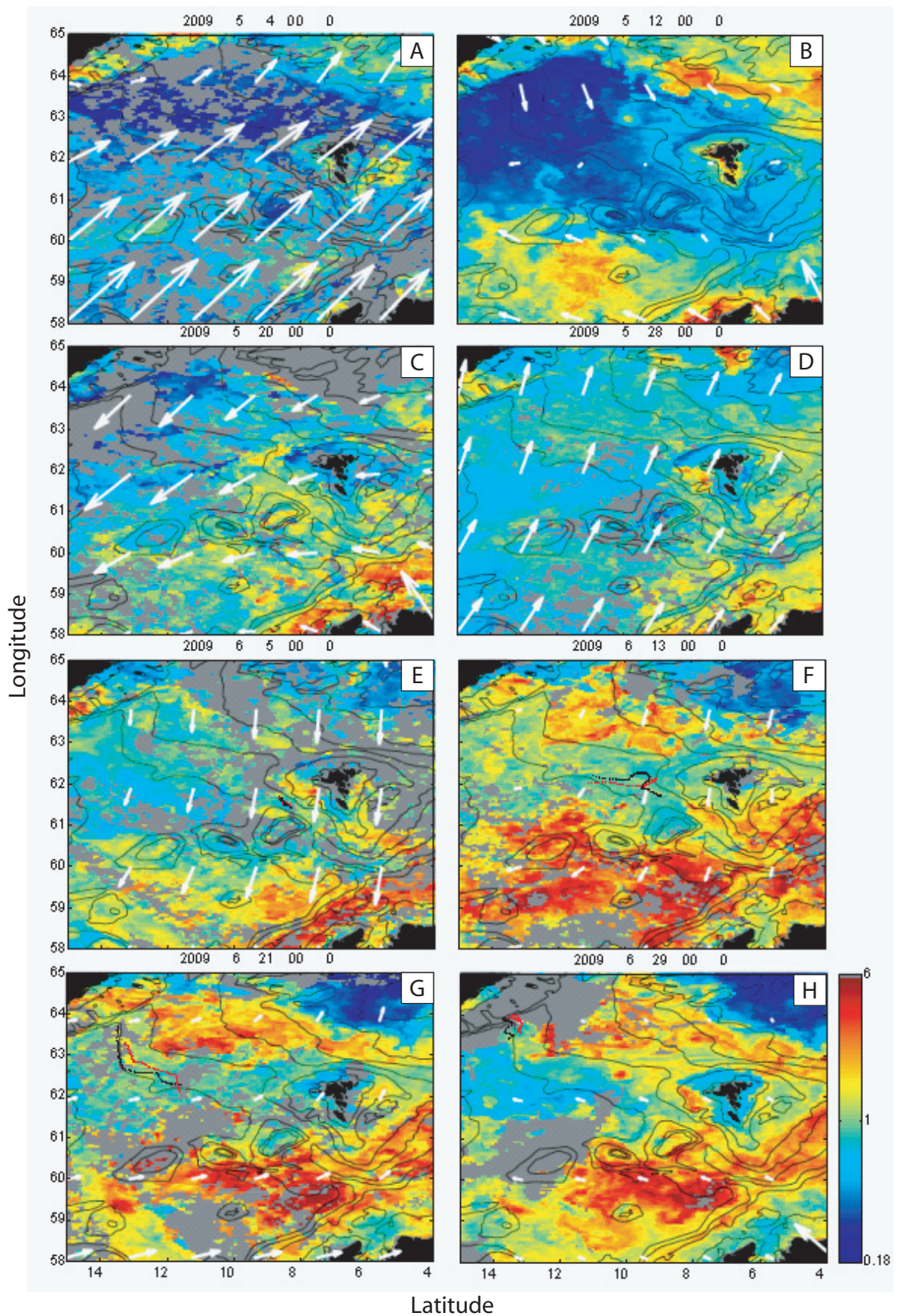


Fig. 4.30 Rapid and inverse variability of surface chlorophyll concentrations on and off the Faroe shelf, as illustrated by eight-day composites from the MODIS-Aqua satellite. The colorbar refers to  $\mu\text{g chl-a l}^{-1}$ . The gray colors show regions with no data during each 8-day period. The white arrows show momentum fluxes (winds) from the NCAR/NCEP, averaged over the 8-day periods covered by the chlorophyll maps. The red and black dots in panels E-H refer to the positions of two Seagliders (see Fig. 4.37). The panel letters are associated with the periods in Fig. 4.28

2004, 2007 and 2009 in Fig. 4.27). The very low production years (2002, 2003 and 2005) are more unclear and silicate data are unfortunately missing during 2006 and 2008. The data during 2010 are clearly of very low quality.

We conclude that silicate limitation typically terminates the first peak of fast growing, and large diatoms. This first silicate induced break in the growth curve during May seems to become an increasingly important process during the recent most years (especially in 2008 and 2009). The highest peaks, either after a declined first diatom bloom or during monotonic growth curve (like in 2000 and 2001), become terminated by nitrate limitation. These statements are based on measurements near land, where the nutrient concentrations are higher than in the upper layer in the open ocean, partly because of re-suspension from the seafloor. This means that the shallow growth near the tidal front farther off-shore might be more severely nutrient limited than illustrated here.

There is a relatively large uncertainty associated with the silicate observations. Potential biases are probably an overestimation of the true concentrations (pers. Comm. Sólva Jacobsen). This strengthens our silicate limitation argument.

#### 4.4.3 Seasonal phytoplankton community succession

After the diatom bloom collapse, when silicate concentrations fall to the threshold level of approximately  $2 \mu\text{M}$ , the phytoplankton community shifts towards an assemblage of one of the following : 1) a mixture of flagellates and small diatoms or 2) dominance of one flagellate species. Although data on this species succession is very limited, we can illustrate main changes happening during the growth period in 1997 and in 2004, respectively. In 1997, the spring bloom was dominated by the three diatom species, *Thalassiosira*, *Chaetoceros* and *Nitzschia* (Fig. 4.29 a). In early June the silicate levels dropped below  $2 \mu\text{M}$  and the diatom community collapsed. The following months the phytoplankton assemblage was a mixture of flagellates and small diatoms. In 2004 the spring mainly consisted of the diatom species *Rhizosolenia styliformis* (large), and *Guinardia delicatula* (average-sized), (Fig. 4.29b). In the beginning of June there must have been a bloom of unknown phytoplankton as the nitrate levels drop down towards  $2 \mu\text{M}$ . This species was

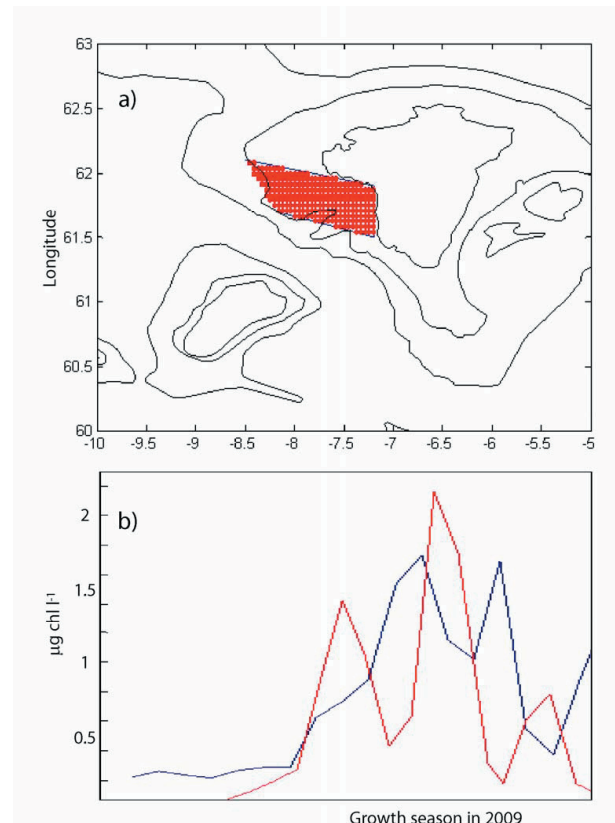


Fig. 4.31 Chlorophyll concentrations in the Western region and on the Faroe shelf during 2009. a) The selected polygon approximately covering region where the satellite data typically show a distinct path of chlorophyll (see e.g. Fig. 4.30d). b) The surface chlorophyll concentrations within the selected polygon as obtained from the satellite data (blue) and the coastal observations at Skopun (red).

however not seen in the microscopic identification. After the bloom collapse in the beginning of July, the phytoplankton community consisted of flagellates mainly *Phaeocystis Pouchetii*. An autumn bloom of a small diatom occurred in late August, 2004.

### 4.5 Satellite based Ocean Color

#### 4.5.1 The widely available 4-km resolution products

Satellite-based ocean color products of relatively coarse spatial resolution (4-km and coarser) are available from several sources.

#### 4.5.1.1 *The characteristic year, 2009*

This characteristic intra-seasonal variability during the growth period in 2009 is here scrutinized using ocean color data (<http://oceancolor.gsfc.nasa.gov>). There appears to be an out-of-phase relation between the surface phytoplankton concentrations in open-ocean and over the Faroe shelf, also on a weekly time-scale (Fig. 4.30). Periods with weak winds appear to be followed by increased open-ocean production and decreased on-shelf production, respectively. This is shown using 8-day composites (4-km resolution) of surface chlorophyll concentrations obtained from the MODIS-Aqua satellite (Fig. 4.30, colors), and 8-day averaged momentum fluxes (white arrows) obtained from daily NCAR/NCEP data.

The first on-shelf bloom starts in early May (period A in Fig. 4.28), during a period with very strong southwesterly winds (compare Figs. 4.28 and 4.30). The following 8-day period (B) is characterized by very low open-ocean and high on-shelf chlorophyll concentrations (Figs. 4.28 and 4.30), but the winds were much weaker during this period. Subsequently (C and D), the open-ocean production increases (more yellowish colors in Figs. 4.30c-d), while the phytoplankton concentrations in-shore of the tidal front decreased (Figs. 4.28 and blue inner region in Figs. 4.30c-d). But the winds picked up again during late May – early June, and a secondary on-shelf phytoplankton peak builds up during the same period (E and F, Figs. 4.30e-f). After the first week in June, the winds weaken again and stay low throughout June (F-H). Very high open-ocean phytoplankton concentrations build up during June (Figs. 4.30f-h), while the concentrations on the Faroe shelf decreased substantially during the latter half of June (Figs. 4.28 and 4.30 g-h). This shows the large-scale imprint of the previously described the rapid (sub-weekly) changes in surface phytoplankton concentrations on the shelf.

#### 4.5.1.2 *Out-of-phase relation between the Western region and the Faroe shelf*

The Western region (outside the front) stands out with particularly high chlorophyll concentrations during the periods when the on-shelf concentrations are at the lowest (see e.g. Fig. 4.30 d and h). In order to elucidate this apparent out-of-phase relation in yet another way, we compare the chlorophyll concentrations observed at coastal station Skopun to a time series of the surface chlorophyll within the Western region (Fig. 4.31b),

obtained by spatially averaging over the polygon shown in Fig. 4.31a. We conclude that too high chlorophyll concentrations (primary production) within the Western region might be detrimental to the growth on the Faroe shelf.

#### 4.5.2 *High-resolution satellite maps*

##### 4.5.2.1 *A high on-shelf production situation in 2009*

In Fig. 4.32 a map of surface chlorophyll from the high-resolution NEODAAS product is shown for May 12, 2009, when the first on-shelf chlorophyll peak was observed at coastal station Skopun (see Fig. 4.28, period B). A comparison of Figs. 4.30b and 4.32 reveals the improvement achieved from using the high-resolution product, before the lower resolution and more readily available 4-km products.

##### 4.5.2.2 *Structures of the Western region*

The archives of NEODAAS have been scanned for periods when there were patches of clear sky (available data) over the Western region during the year 2010, when cruise 1012 was made. Some characteristic patterns can already be observed (Fig. 4.33): *i*) The Western region often stands out with particularly high chlorophyll concentrations *ii*) filaments with high-chl content often stretch from the Western region and onto the Faroe shelf, particularly to the west of Mykines, and to the east of Vágar and *iii*) a low-chl (blue) band often appears immediately within the tidal front from 62°N and northwards to the west of the shelf. But a more careful analysis of these data is needed, before any quantitative statements can be made. We conclude that the high-resolution ocean satellite data give a good qualitative impression of the ongoing processes and a useful context in which to put the available *in situ* data.

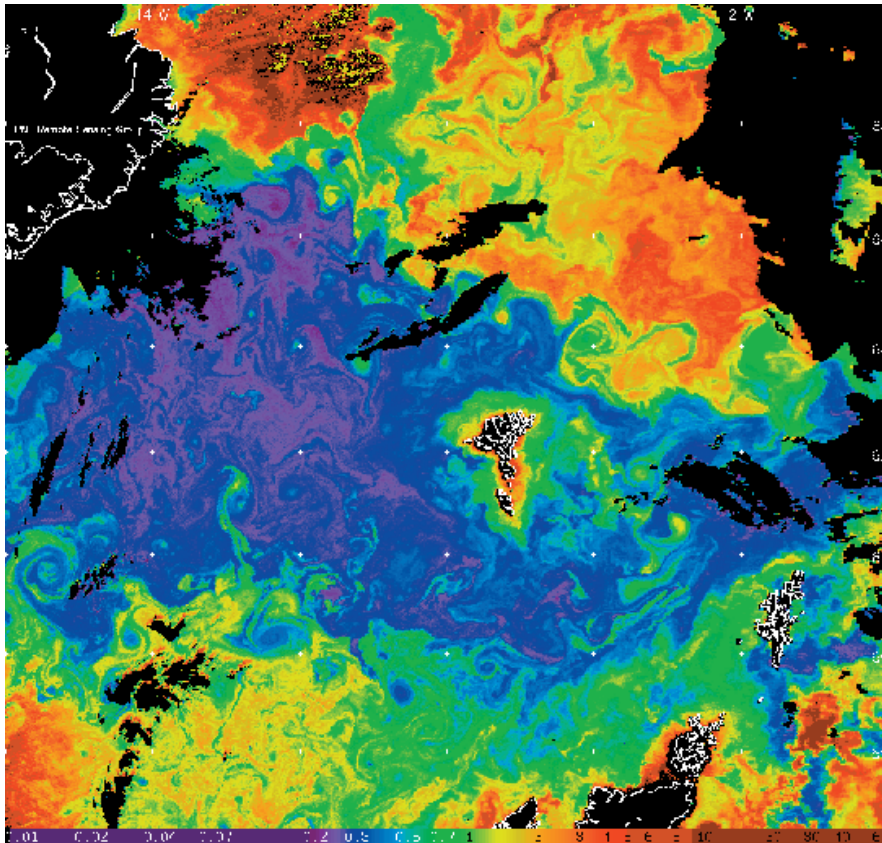


Fig. 4.32 A snap-shot of surface chlorophyll from the high-resolution NEODAAS product on a particularly clear day (12 May, period B in Figs. 4.28 and 4.30) in 2009.

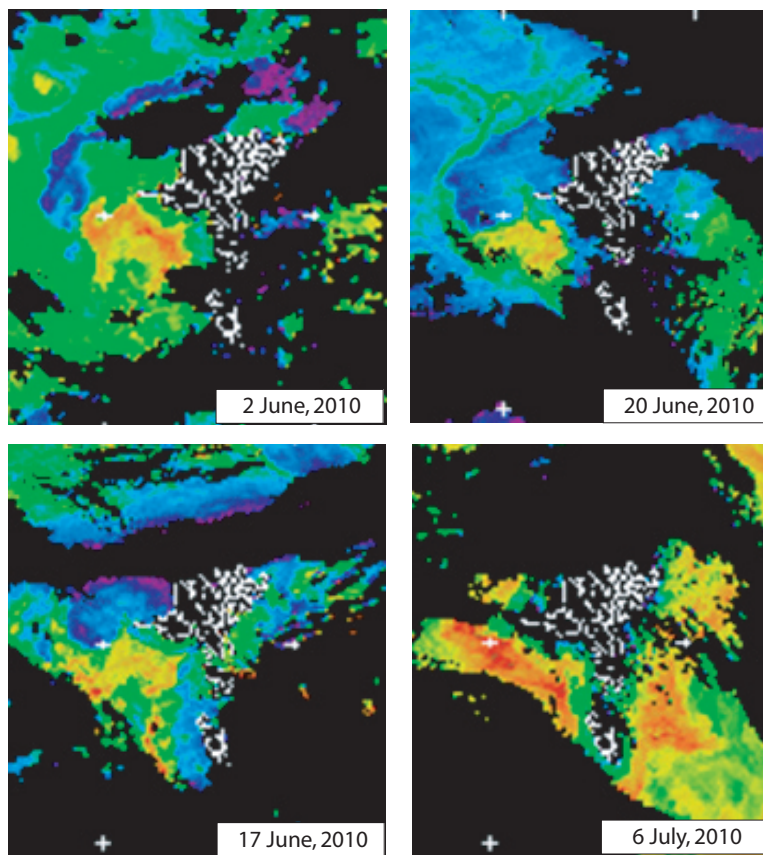


Fig. 4.33 High-resolution (1-km) snap-shots of surface chlorophyll concentrations, during relatively clear days in 2010.

## 4.6 HYCOM

### 4.6.1 A quiescent region

The simulated depth-averaged (barotropic) current velocities show that the Western region is a very quiescent region, with monthly averaged (here exemplified by May, 2000, Fig. 4.34) current velocities below  $5 \text{ cm s}^{-1}$  (bluish colors). This region lies between stronger currents along the slope to the west and the tidal currents near the Faroe Islands. There is a particularly quiescent zonal band across section MYK, between  $61.8^\circ \text{ N}$  and  $62^\circ \text{ N}$ , which is where the TTW indicated the presence of a so-called cold cushion (see section 4.3.1). The simulated currents near mooring FASB this month were below  $2.5 \text{ cm s}^{-1}$ , which is comparable with the observed average currents in this region during the summer of 2010 (see section 4.2.1.6). We conclude that the model support our proposition that the Western region is particularly quiescent, and thus could develop a cold cushion during summer, which dynamically and ecologically could become detached from both the shelf proper and the open-ocean (Hill et al., 1997).

### 4.6.2 On-shelf transport from the Western region

The model shows that the Western region becomes easily stratified, with a well established and shallow mixed layer (Fig. 4.35b), in line with the observations. The model furthermore reveals that we have a strong import of water from the upper mixed layer in the Western region and onto the Faroe shelf. This import takes place between Suðuroy and Vágar, and immediately to the west of Mykines, as here illustrated with the simulated monthly averaged upper layer currents (Fig. 4.35b). The model upper layer is the mixed layer where stratified and the full water column within the tidal front. The simulated dynamics resemble the SST map over the Faroe region (Fig. 4.35a), and thus appears to be realistic. This SST map also clearly shows the presence of these three filaments. Simulated daily averaged fields show that these filaments also are captured by the model. Tongues of well stratified water from the Western region can be drawn onto the shelf (Fig. 4.36). This stratification is probably eroded by the tides within the front, and the imported upper mixed layer waters are thus mixed into the full water column. We conclude that the model confirms the presence of three filaments of on-shelf transport from the Western region, which are apparent in

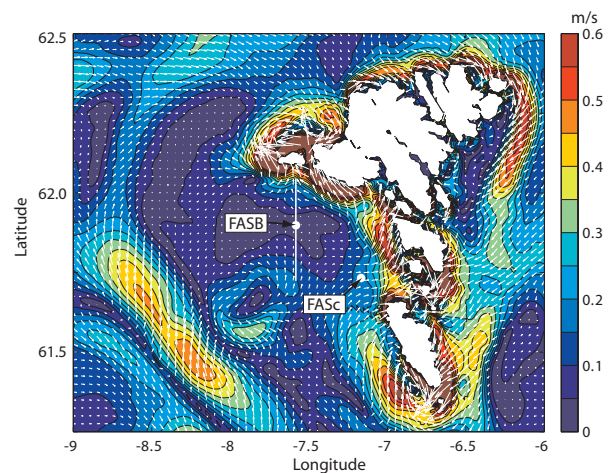


Fig. 4.34 Simulated mixed layer currents for May in 2000.

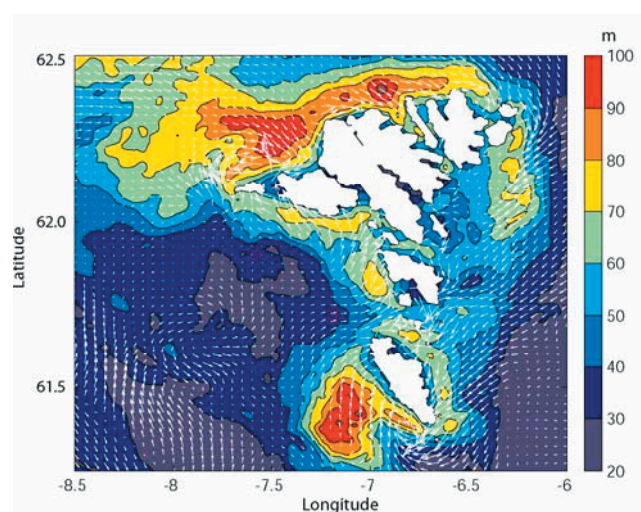
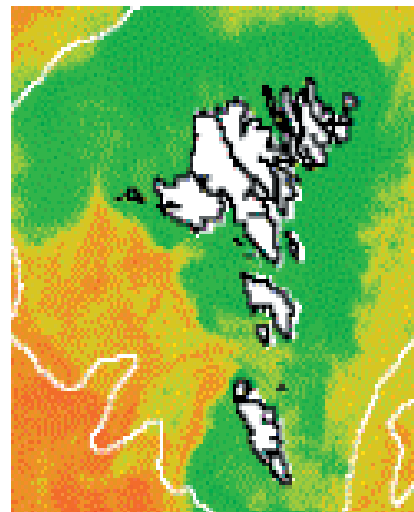


Fig. 4.35 On-shelf transport of upper layer water from the Western region via three flow filaments. a) a frequently used SST map (18 April, 2003) and b) simulated MLD (colors) and upper layer current velocities (arrows) (average over May, 2000).

satellite products. Since the highest chlorophyll concentrations often are observed along the tidal front near these filaments (section 4.1.3), one might assume that the mixed layer processes here and the nutrient content of the imported upper layer water might hold a key for understanding the variable near-shelf primary production.

## 4.7 Other data sources

### 4.7.1 Seagliders

Novel data from the autonomous underwater vehicles, seagliders (Eriksen et al., 2001; Hátún et al., 2007), can extend the discussion around the erratic bloom in 2009 into the deep open-ocean waters. From these data it is evident that the open-ocean water column became strongly stratified, and the phytoplankton concentrations in the upper 50 meters increased rapidly, during the period June 13-16 (Fig. 4.37), concurrently with the latter sharp drop in the on-shelf concentrations (period E-G in Fig. 4.28, see also Figs. 4.30e and g). The seagliders were deployed in the Faroe Bank Channel on June 3 (Fig. 4.30e) and were heading for Iceland along similar paths during June (Figs. 4.30e-h). Since the seagliders are moving slowly through the water, it can be challenging to determine whether the variability observed by these vehicles is caused by spatial or temporal changes. But the data are obtained by two independent seagliders situated several tens of kilometers apart, and which move through relatively homogeneous waters with no clear oceanic structures (e.g. eddies, fronts), as deduced from the fairly homogeneous surface chlorophyll concentrations (Fig. 4.30f). It should therefore be safe to assume that the rapid and roughly concurrent changes observed (Fig. 4.37) are not due to spatial in-homogeneities, but rather due to temporal variability with a wide spatial imprint. From this we deduce that the open-ocean water column immediately southwest/upstream of the Faroe Plateau (Faroe Bank Channel), changed from being weakly stratified down to 100-150 meters in early June to becoming strongly stratified at about 50 meters depths on around June 13 (Fig. 4.37b). This was followed by a phytoplankton maximum in the mixed layer after about a week (~ June 20) and a drop in the on-shelf phytoplankton concentration. We conclude that the seagliders support the previous statements about an asynchrony between the growth in on-Faroe shelf and open-ocean waters. This link is here extended to the in-depth chlorophyll concentrations and the mixed layer dynamics.

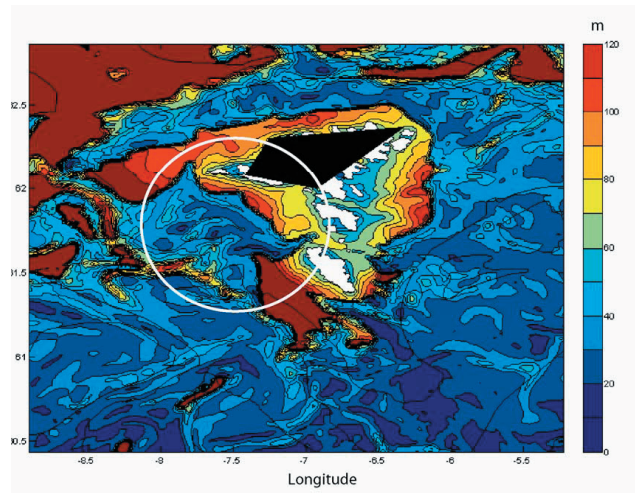


Fig. 4.36 Simulated mixed-layer depths on May 5, 2000, using HYCOM. The inflowing filaments of stratification from the Western region and onto the shelf are emphasized within the white circle.

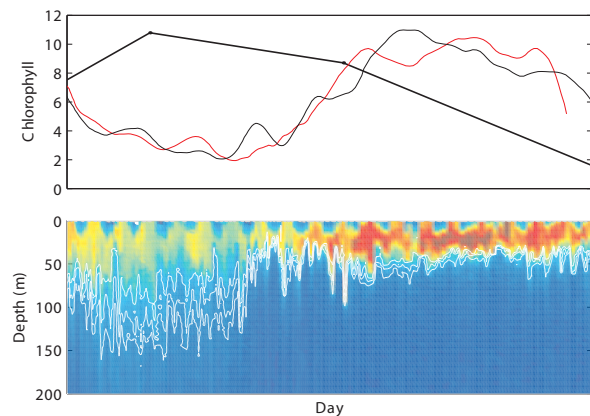


Fig. 4.37 Rapid open-ocean stratification and bloom and on-Faroe shelf decline in chlorophyll concentrations during the period 5-25 June, 2009. Upper panel: Chlorophyll concentrations on the Faroe shelf (black line – as in Fig. 4.28), and in the open-ocean (averaged over the upper 50 meters) as measured by two Seagliders to the west of the Faroe Islands (blue and red)(positions shown in Figs. 4.30 E-H). The lower panel shows vertical distribution of chlorophyll concentrations and the stratification (three isopycnals shown with white lines) as measured by one of the Seagliders. Note the diurnal near-surface variability.

## 5 Synthesis

We will here synthesize the presented pieces of evidence and based on this, put forth a new hypothesis involving silicate limitation, which could supplement the generally accepted *exchange hypothesis* and its link to the Faro shelf primary production. After this, we will give some large-scale considerations and suggestions for future work on this issue.

### 5.1 Pieces of evidence

We have shown that there appears to be an asynchrony between the surface chlorophyll concentrations in the open-ocean waters between the Faroe Islands and the European continental shelf and the Faro shelf primary production (Figs. 2.3 and 2.4). Increased open-ocean chlorophyll is associated with a smaller on-shelf production, and vice versa. The open-ocean chlorophyll abundance appears also to be associated with large-scale ocean dynamics, as represented by the so-called gyre index - a weak subpolar gyre results in increased chlorophyll, and vice versa (Fig. 2.2). Seaglider data show that increased surface chlorophyll concentrations are associated with a shallowing of the upper mixed layers during summer (Fig. 4.37). We furthermore illustrate, what is well known (Henson et al., 2006), that this upper mixed layer in the North Atlantic becomes severely silicate limited during summer (Fig. 2.7). The stratification of the upper layer, and the depletion of the silicate, typically happens in May (Henson et al., 2006).

The near-shore waters around the Faroe Islands become silicate limiting (approach 2  $\mu\text{M}$ ) every year (Fig. 4.27). When this happens, there is a break in the growth curve, as represented by the chlorophyll concentrations at coastal station Skopun. This break is a consistent feature every year, except during the very productive years, 2000 and 2001. It is evident that it is linked to a break-down of a phytoplankton community dominated by large and productive diatoms, to either smaller diatoms or to a more flagellate dominated community (Debes et al., 2008; Djurhuus and Jørgensen, 2011; Gaard, 2000) (see Fig. 4.29). These breaks appear to be important for what is referred to as the net production on the shelf, which again is associated with the cumulated chlorophyll concentrations on the shelf through the production season (Eliassen, 2013). The severity of

these ‘breaks’ during May appear to have increased during the recent most years.

Satellite data show a region of typically much increased surface chlorophyll concentrations immediately west of the Faroe shelf (Figs. 2.6 and 4.30). Climatological maps of the *in situ* (upper 50 m) chlorophyll verify that the concentrations are highest in this Western region. The in-depth concentrations are highest near the tidal front between the Western region and the inner shelf region in late April/early May (Fig. 2.5a), while they are highest in a subsurface layer within the Western region during late June/early July (Figs. 2.5b and 2.8a). The upper layer within Western region becomes more silicate limited than the adjacent open-ocean region (the Faroe Bank Channel) and the inner shelf region (Fig. 2.8b).

According to output from a high-resolution ocean model, there should be a strong on-shelf transport of water from the upper layer in the Western region. This simulated in-flux, furthermore, occurs in three filaments, one west of Mykines, one between Vágur and Koltur, and one to the north of Suðuroy (Figs. 4.35b). Although high-resolution images from satellites also clearly suggest the presence of three such filaments (Figs. 4.33 and 4.35a), we have not been able to verify this with current measurements yet (Fig. 4.21).

During late April/early May, when the bloom on the shelf typically begins, the highest chlorophyll concentrations are often observed along the tidal front (Figs. 4.3 and 4.4), and these can be substantially higher than between the islands (Fig. 4.9). This high production, which probably occurs in the stratified region where lighter water from the Western region overlays the denser water inside the tidal front, can be much localized (Fig. 4.3), and thus difficult to identify with conventional CTD-based cruises. There are, however, periods when the production is highest near the Islands (Fig. 4.32)

The simulations clearly identify the Western region as a pool of relatively stagnant water (Fig. 4.34). The low simulated current velocities within this region are supported by *in situ* current measurements (Fig. 4.20). Temperature sections, obtained by dragging a termistor wire through this quiescent region reveals characteristics of a so-called ‘cold cushion’ (Fig. 4.23) – a region that become strongly stratified during summer, where the upper layer receives most of the atmospheric heat input and warms,

while the lower layer stays colder. Such a region will become somewhat separated from adjacent waters, both physically and biologically (Hill et al., 1997). Just one day after net heat input into the ocean during the extended cruise 1012 (Fig. 4.13), this Western regions became strongly temperature stratified and the chlorophyll levels rapidly increased (Fig. 4.5). Both the clear demarcation and the flickering nature of this Western region are revealed by the satellite images (Figs. 4.30 and 4.33). And there are indications of an asynchrony between the surface chlorophyll concentrations in this Western region, and the region within the tidal front on a weekly time-scale (Figs. 4.30 and 4.31).

The oceans around the Faroes start to receive heat (daily averages) during April (Fig. 4.26). But there are days with neat heat loss from the ocean during every rapid and significant growth period during the last 15 years (Fig. 4.26). This indicates that heat loss is a necessary, although not sufficient requirement for good on-shelf growth. Heat loss deteriorates the stratification within the Western region (Fig. 4.22), although the effect wind stress must be added in order to get the full picture. The link between growth and heat loss is considered to be robust, although the causal link is not thoroughly understood yet.

As a curiosity, we see that there is a close relation between the backscatter observed by the ADCP at FASB (quiescent region) and the air-sea heat exchange – increased heat loss leads to increased backscatter through the deeper parts of the water column (Fig. 4.17). This backscatter also co-varied with the coastal chlorophyll concentrations at Skopun (Fig. 4.16). There is a clear diurnal variation in the backscatter signal, with an increased near-bottom signal during the night and a mid-level signal during the sunlit hours (Fig. 4.15), indicating one of the following: it must be due to diurnal vertical migration of biota (zooplankton or small fish) or due to re-suspension during the nocturnal convection.

## 5.2 A new hypothesis

We suggest that the strongest primary production during the early growth phase occurs in the tidal front, and especially between the Western region and the inner Faroe shelf. A necessity for obtaining high production is that a phytoplankton community with large and efficient diatoms remains intact in this region. This again requires that a steady supply of silicate is transported to this region. If

the silicate concentrations become limiting for a too long period and this large diatom community breaks down, then the growth has shifted into the next, and less efficient, phase. This will be growth of smaller organisms that contribute to re-cycling of organic material, more than feeding the higher trophic levels of the ecosystem. We suggest that the on-shelf flux of water from the Western region is an important, although variable, source of silicate for this production. To obtain high silicate fluxes requires both high silicate concentrations in the inflowing water and a high transport. This means that high exchange, and not low exchange as previously suggested (Hansen et al., 2005), would be beneficial for growth. The general pre-bloom silicate concentrations in the North Atlantic, regulated by the severity of winter atmospheric forcing (e.g. heat loss), convective activity and large-scale ocean dynamics, will again control the overall silicate concentrations in the Western region. Shorter term atmospheric forcing will regulate the degree to which the Western region becomes stratified and thus silicate limited in the upper layer. Days with net heat-loss will mix and replenish this layer with new nutrients. This means that the atmosphere regulates the frontal primary production both through the winter pre-conditioning and through the timing and intensity of mixing event during the growth phase itself.

## 5.3 Large-scale and future silicate consideration

The waters that flow past the Faroe Islands come partly from the North Atlantic Current, waters that are admixed with water from the subpolar gyre, and partly from the eastern region near the Bay of Biscay. The climatological silicate fields at 50 m depths show that the source water near the subpolar gyre are rich in silicate while the eastern waters are very poor in silicate (Fig. 5.1). As the subpolar gyre has declined (Häkkinen and Rhines, 2004), more eastern water have reached the Nordic Seas, and the salinities in Atlantic water have increased (Hátún et al., 2005) while winter silicate concentrations have declined (Rey, 2012).

Since the Faroe plateau is situated near fronts, and in an ocean with shifting currents, and variable winter convection, we cannot assume that the pre-bloom (winter) nutrient concentrations is constant. If important aspects of the Faroe shelf primary production are regulated by the nitrate and silicate concentrations as suggested here, one

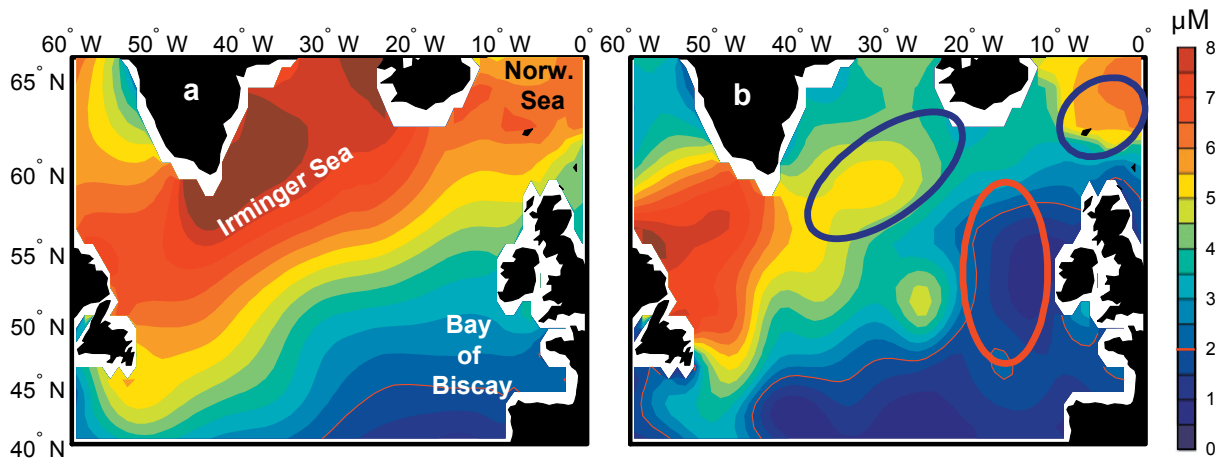


Figure 5.1 Climatological silicate fields at 50 m depths for a) January and b) June. The high-silicate region in the Irminger and Norwegian Seas and the low-silicate waters from the Bay of Biscay region, respectively, are illustrated with the blue and red ellipses. The critical  $2 \mu\text{M}$  isoline is shown in red. The data are obtained from the World Ocean Atlas (WOA, <http://www.nodc.noaa.gov>)

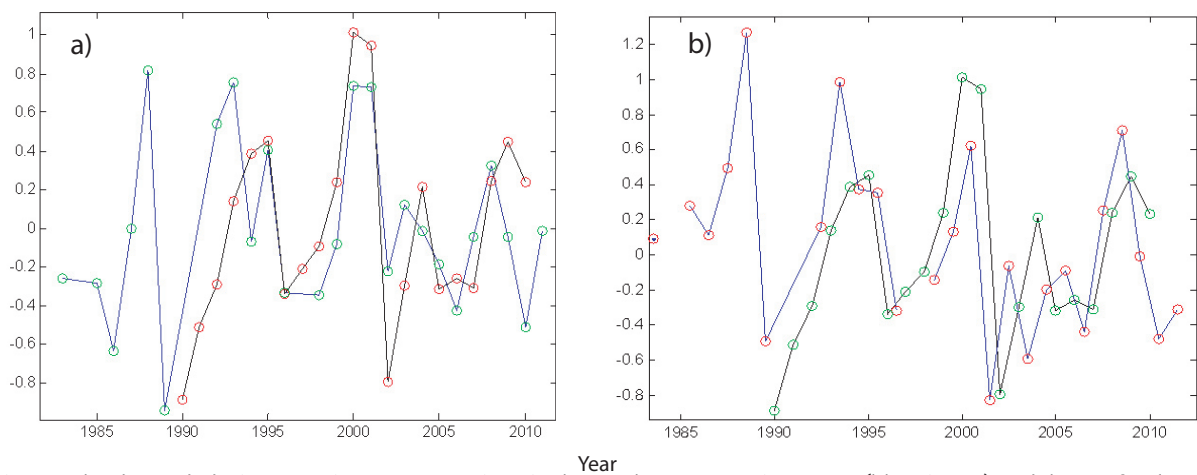


Fig. 5.2 The detrended winter nutrient concentrations in the northeastern Irminger Sea (blue, in  $\mu\text{M}$ ) and the PPI for the Faroe shelf production (black, not to scale). a) Silicate and b) nitrate.

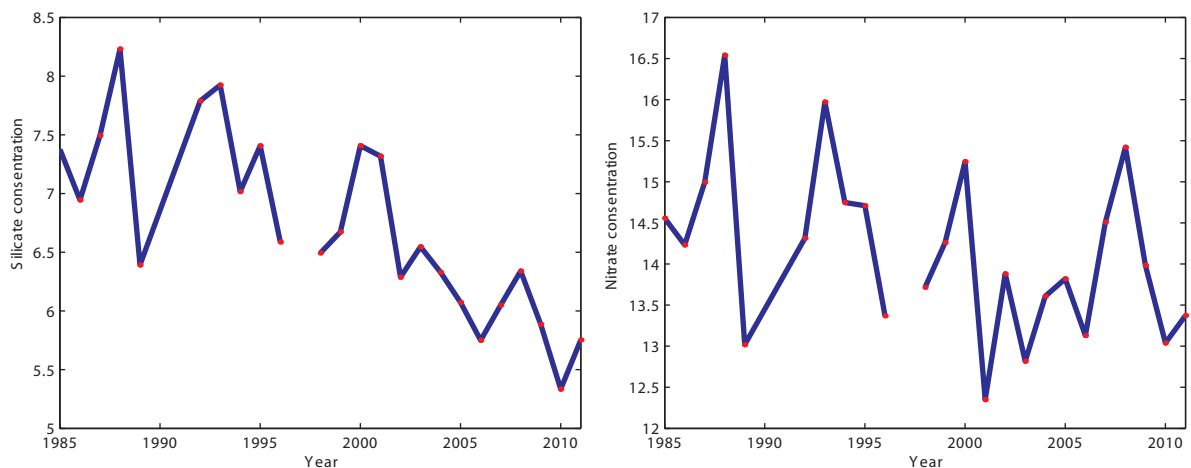


Fig. 5.3. The real winter nutrient concentrations in the northeastern Irminger Sea (in  $\mu\text{M}$ ). a) Silicate and b) nitrate.

could assume that higher nutrient concentrations throughout the deeply convected open-ocean water column should be beneficial for the on-shelf production. We do not have open-ocean time series near the Faroes, but silicate observations have been made by the Marine Research Institute (Reykjavik) along the Faxaflói section, within the northeastern Irminger Sea since the mid-1980s. The silicate observations from Faxaflói (station 9) during winter (February-March) have been compared to the PPI from the Faroe shelf (Fig. 5.2). The nutrient data have been de-trended (linear trend removed) and shifted by half a year, to match the PPI series. There appears to be some synchrony between years with high nutrient concentrations in the Irminger Sea and peaks in the PPI. If there is causality here, then it might be possible to predict the growth on the Faroe shelf, by about half a year. Such a potential causality will involve a combination of silicate and nitrate limitation.

There is, naturally, a long stretch from the winter nutrient concentrations in the Irminger Sea to the production on the Faroe shelf. The first assumption to be made is that the winter nutrient concentrations around the Faroe shelf resemble those in the Irminger Sea. Processes that could cause synchronous (within the year) variability in these two locations would be *i*) that an expanded subpolar gyre would export nutrient rich subpolar water to both locations at approximately the same time (time-lag of about a year might, however, be expected) and *ii*) similar atmospheric forcing causes similar convection activity, and thus nutrient enrichment from the deep water masses, at both locations.

The nitrate concentration shows a stronger sub-decadal variability, while the silicate concentration has a stronger trend (Fig. 5.3). This trend is not reflected in the PPI, which might indicate that it is not simply the pre-bloom silicate concentrations that regulate the on-shelf production. Yet again, the exceptionally high production in 2000 and 2001 is better reflected in the silicate anomalies, than in the nitrate anomalies. These results are just tentative – more to be regarded as an interesting observation. And again, this involves the nutrients that are used to calculate the PPI and which appear to impact the Faroe shelf. It would therefore be difficult to argue that the observed covariability is purely coincidental. The decline in silicate south of Iceland is strong (from around 7.5  $\mu\text{M}$  to around 5.5  $\mu\text{M}$  in a bit over 20 years), and a parallel silicate

decline has been observed along the Norwegian slope (from around 5.5  $\mu\text{M}$  to 4.5  $\mu\text{M}$  during the same period, (Rey, 2012)). If this trend continues, it is clear that this will reorganize the phytoplankton community structure in the North Atlantic. And the impact may be especially important on the shelves, where diatoms typically dominate.

## 5.4 Future directions

- The new high-resolution hydrographic sections (V,M and R) should be continued.
- The bottom-mounted ADCP should be deployed in strategic locations, preferably where it can complement other observational activity, like one of the standard hydrographic stations, the stratification observations at the Waverider mooring or other.
- Temperature sensors should be mounted to all Waverider moorings around the Faroe shelf.
- The time series of open ocean winter silicate concentrations should be continued.
- Better sampling of the phytoplankton community structure is important. The seasonal succession of different communities is probably crucial for the functioning of the entire shelf ecosystem.
- Better usage of acoustics might prove very useful. The signals from the existing acoustic samplers, like the ADCP and the ship mounted echo-sounder should be better validated against in situ biological and physical observations. This would enable us to better utilize large volumes of already collected data. These instruments might also be better tuned for biological observations, or new specialized acoustic instruments could be bought.
- The apparent linkage between coastal station Skopun and the quiescent Western region should be further investigated. Because of the short distances involved, this might even be achieved using a small boat and handheld small CTD.

- The high-resolution HYCOM model has not nearly been fully utilized yet. This dataset should be further investigated.
- Advance frontal studies are needed, but complicated. The CTD is not well suited for such work, which would require instruments like a Seasoar or a similar towed vehicle.
- The utilization of the SST sampled by the ship is a good help while doing near-front work

## 5.5 References

Bleck, R., 2002. An oceanic general circulation model framed in hybrid isopycnic-Cartesian coordinates. *Ocean Modelling* 4, 55-88.

Bohme, L., Send, U., 2005. Objective analyses of hydrographic data for referencing profiling float salinities in highly variable environments. *Deep-Sea Research Part II-Topical Studies in Oceanography* 52, 651-664.

Debes, H., Gaard, E., Hansen, B., 2008. Primary production on the Faroe shelf: Temporal variability and environmental influences. *Journal of Marine Systems* 74, 686-697.

Djurhuus, A. and Jørgensen, J., 2011. Seasonal variation in the bacterial community of the Faroes Shelf in relation to physical and biological parameters. PhD Thesis, University of the Faroe Islands.

EGGE, J. K., AKSNES, D. L., 1992. Silicate As Regulating Nutrient in Phytoplankton Competition. *Marine Ecology-Progress Series* 83, 281-289.

Eliassen, K., 2013. *Ammodytes spp.*, as a link between climate and higher trophic levels on the Faroe shelf. PhD Thesis, Aarhus University.

Eriksen, C. C., Osse, T. J., Light, R. D., Wen, T., Lehman, T. W., Sabin, P. L., Ballard, J. W., Chiodi, A. M., 2001. Seaglider: A long-range autonomous underwater vehicle for oceanographic research. *IEEE Journal of Oceanic Engineering* 26, 424-436.

Frajka-Williams, E., Rhines, P. B., Eriksen, C. C., 2009. Physical controls and mesoscale variability in the

Labrador Sea spring phytoplankton bloom observed by Seaglider. *Deep-Sea Research I* 56, 2144-2161.

Gaard, E., 2000. *The plankton community structure on the Faroe Shelf.* PhD Thesis, University of Tromsø.

Gaard, E., Hansen, B., Heinesen, S., 2003. Phytoplankton variability on the Faroe Shelf. *ICES Journal of Marine Science* 55, 688-696.

Häkkinen, S., Rhines, P. B., 2004. Decline of subpolar North Atlantic circulation during the 1990s. *Science* 304, 555-559.

Hansen, B., Eliassen, S. K., Gaard, E., Larsen, K. M. H., 2005. Climatic effects on plankton and productivity on the Faroe Shelf. *ICES Journal of Marine Science* 62, 1224-1232.

Hátún, H., Eriksen, C. C., Rhines, P. B., 2007. Buoyant eddies entering the Labrador Sea observed with gliders and altimetry. *Journal of Physical Oceanography* 37, 2838-2854.

Hátún, H., Payne, M., Beaugrand, G., Reid, P. C., Sandø, A. B., Drange, H., Hansen, B., Jacobsen, J. A., Bloch, D., 2009. Large bio-geographical shifts in the north-eastern Atlantic Ocean: From the subpolar gyre, via plankton, to blue whiting and pilot whales. *Progress in Oceanography* 80, 149-162.

Hátún, H., Sandø, A. B., Drange, H., Hansen, B., Valdimarsson, H., 2005. Influence of the Atlantic subpolar gyre on the thermohaline circulation. *Science* 309, 1841-1844.

Henson, S. A., Sanders, R., Holeton, C., Allen, J. T., 2006. Timing of nutrient depletion, diatom dominance and a lower-boundary estimate of export production for Irminger Basin, North Atlantic. *Marine Ecology-Progress Series* 313, 73-84.

Hill, A. E., Brown, J., Fernand, L., 1997. The summer gyre in the western Irish Sea: Shelf sea paradigms and management implications. *Estuarine Coastal and Shelf Science* 44, 83-95.

Kalnay, E., Kanamitsu, M., Kistler, R., Collins, W., Deaven, D., Gandin, L., Iredell, M., Saha, S., White, G., Woollen, J., Zhu, Y., Chelliah, M., Ebisuzaki, W., Higgins, W., Janowiak, J., Mo, K. C., Ropelewski, C., Wang, J., Leetmaa, A., Reynolds, R., Jenne, R., Joseph, D., 1996. The NCEP/NCAR 40-year reanalysis project. *Bulletin of the American Meteorological Society* 77, 437-471.

Larsen, K.M.H., 2009a. *Circulation and exchange of water masses on the Faroe Shelf and the impact on the Shelf ecosystem*. PhD Thesis, University of Bergen.

Larsen K. M. H., Hansen, B., Kristiansen, R., and Mortensen, E. 2009b. *Current measurements on the Faroe Shelf 2008-2009*. Havstovan NR.: 09-04, Technical Report.

Larsen K. M. H., Hátún, H., and Debes, H. 2011. *Current measurements on the Faroe Shelf 2010*. Havstovan NR.: 11-01, Technical Report.

Larsen K. M. H., Hansen, B., Hátún, H., and Kristiansen, R. 2013. *Current measurements on the Faroe Shelf 2011*. Havstovan NR.: 13-01, Technical Report.

Preisendorfer, R., 1988: *Principal Component Analysis in Meteorology and Oceanography*. Elsevier Science Publishing Company Inc., Amsterdam, pp. 425.

Rasmussen, T. A. S., Olsen, S. M., Hansen, B., Hátún, H., Larsen, K. M. H., 2013. *Modeling of the Faroe shelf water exchange and variability*. Ocean Modelling, Submitted.

Rey, F., 2012. *Declining silicate concentrations in the Norwegian and Barents Seas*. ICES Journal of Marine Science, 69: 208-2012

Richardson, K., Visser, A. W., Pedersen, F. B., 2000. *Subsurface phytoplankton blooms fuel pelagic production in the North Sea*. Journal of Plankton Research 22, 1663-1671.

Schlitzer, R. 2007. *Ocean Data View*. <http://odv.awi.de>.

Zhai, L., Gudmundsson, K., Miller, P., Peng, W. J., Gudfinnsson, H., Debes, H., Hatun, H., White, G. N., Walls, R. H., Sathyendranath, S., Platt, T., 2012. *Phytoplankton phenology and production around Iceland and Faroes*. Continental Shelf Research 37, 15-25.

# Appendix

The individual hydrographic sections, occupied during the extended leg of cruise 1012 (late April, 2010) are presented here.

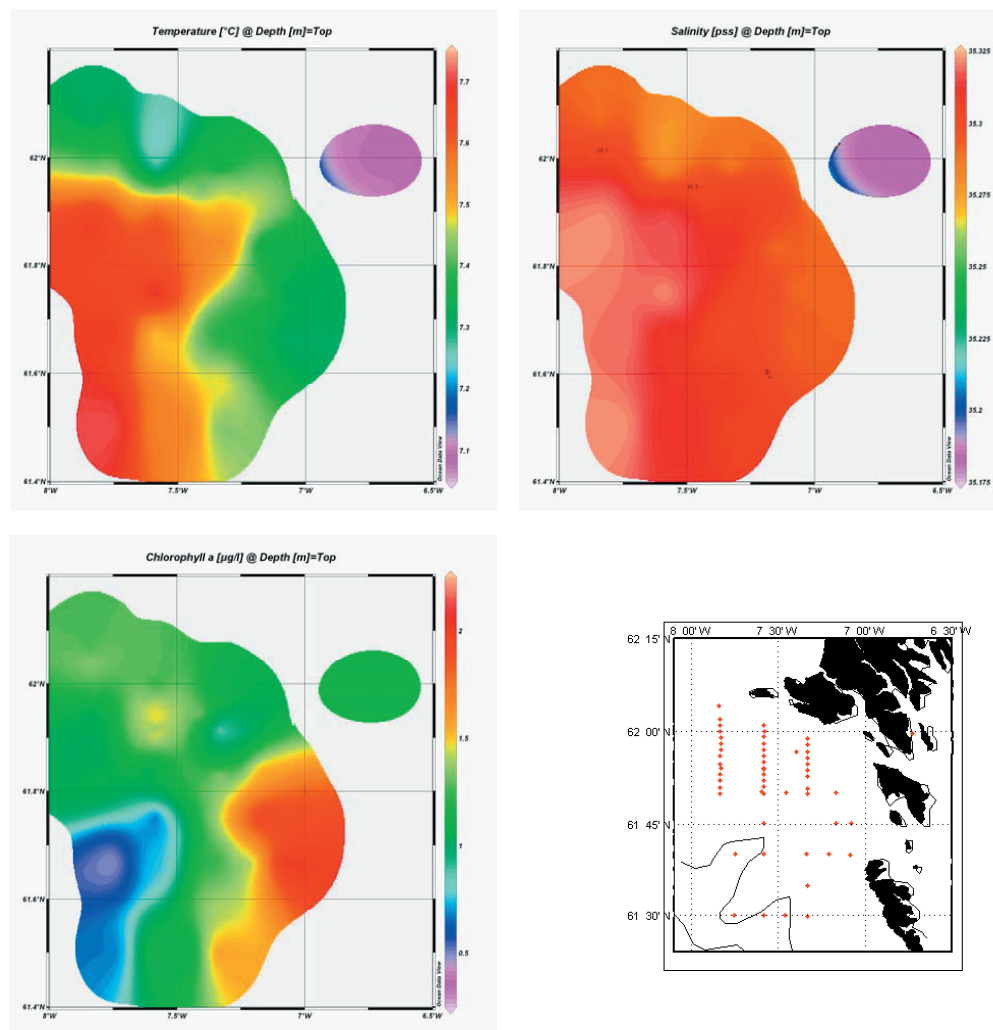


Figure A1. Surface plot for station 73 – 132 (21. – 23. April). Upper left: temperature; Upper right: Salinity; Lower left: Chlorophyll a; Lower right: Station map.

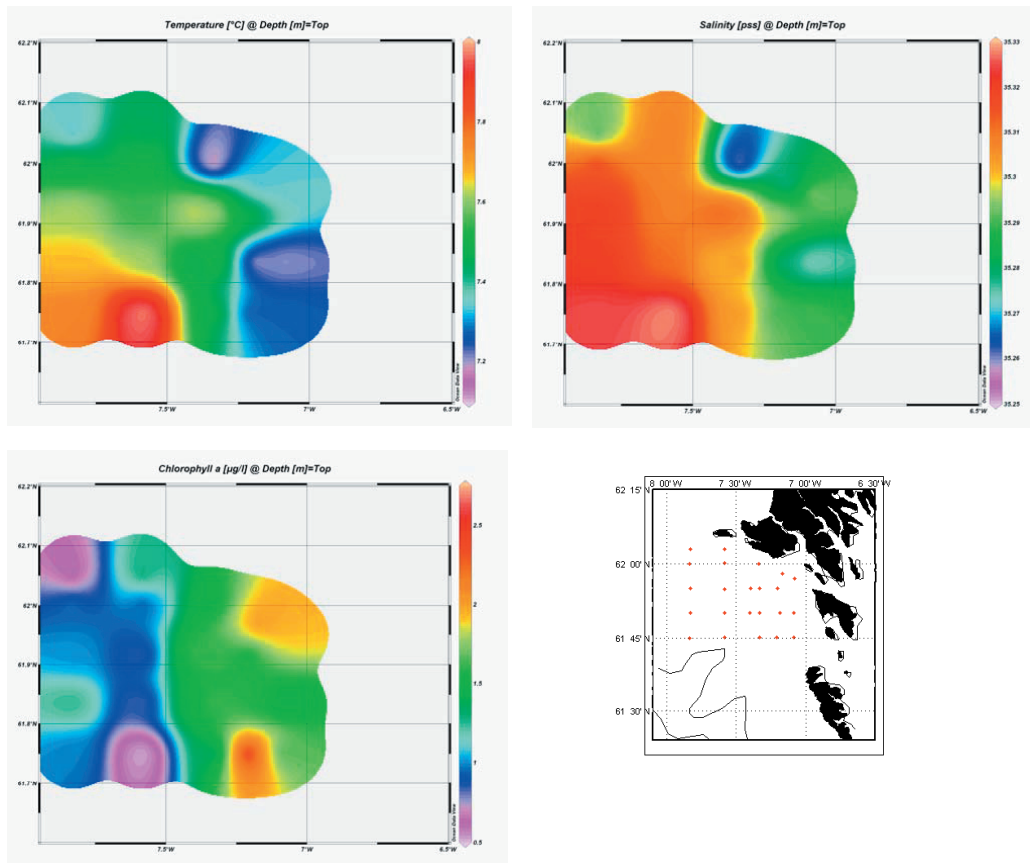


Figure A2. Surface plot for station 199 – 222 (25. April). Upper left: temperature; Upper right: Salinity; Lower left: Chlorophyll a; Lower right: Station map.

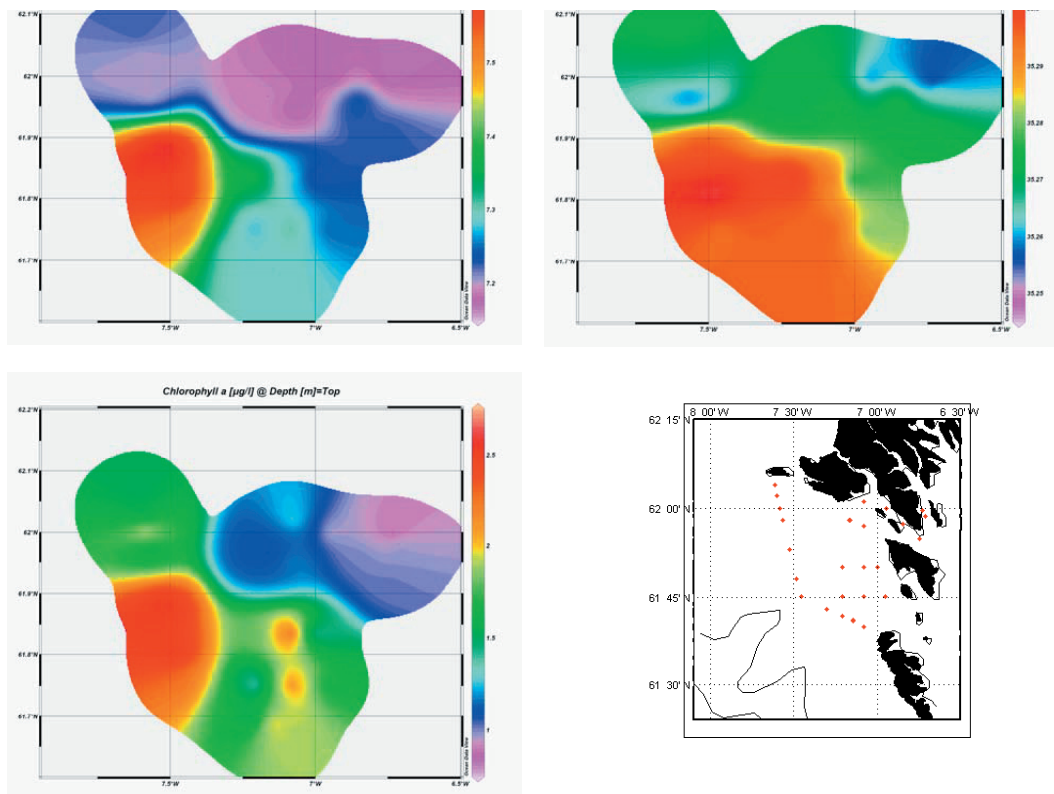


Figure A3. Surface plot for station 255 – 285 (26. – 27. April). Upper left: temperature; Upper right: Salinity; Lower left: Chlorophyll a; Lower right: Station map.

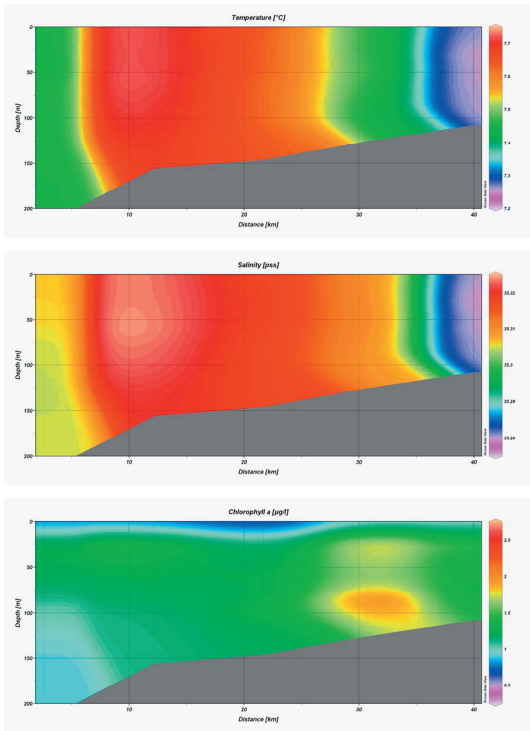


Figure A13. Section (1) plot for station 93 – 97 (22. April, am). Upper panel: temperature; Middle panel: Salinity; Lower panel: Chlorophyll a; Left: Station map.

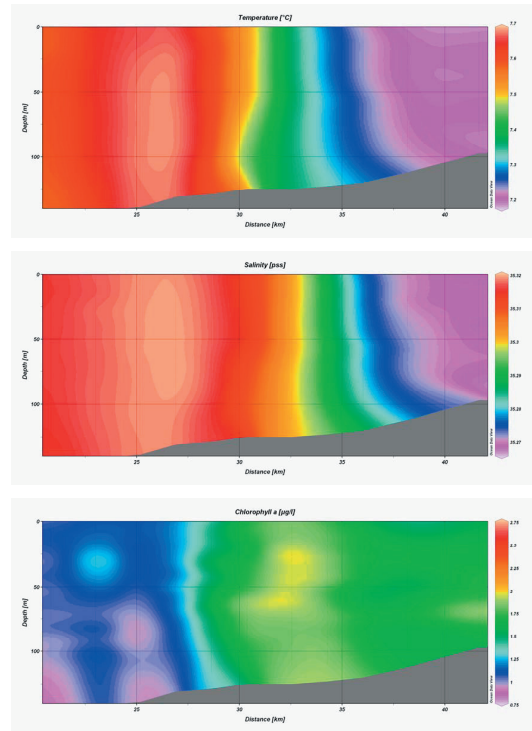


Figure A6. Section (3) plot for station 108 – 118 (22. April, pm). Upper panel: temperature; Middle panel: Salinity; Lower panel: Chlorophyll a; Left: Station map.

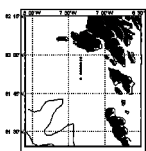
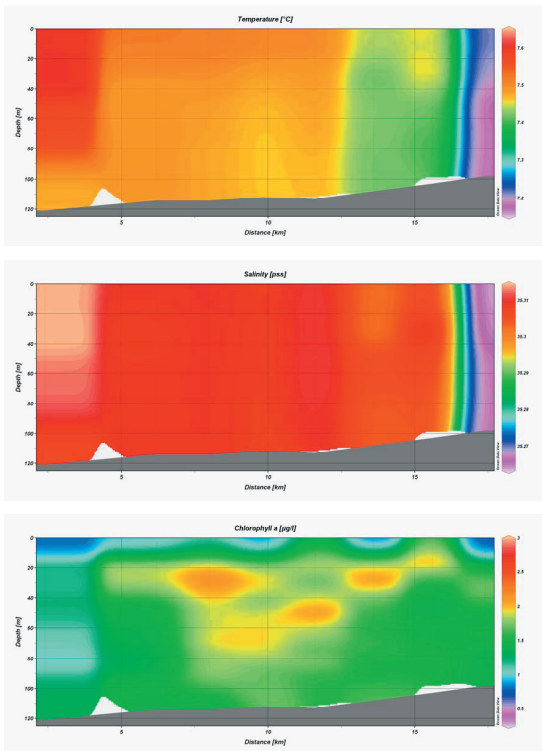


Figure A5. Section (2) plot for station 98 – 105 (22. April, pm). Upper panel: temperature; Middle panel: Salinity; Lower panel: Chlorophyll a; Left: Station map.

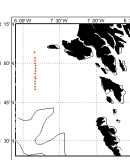
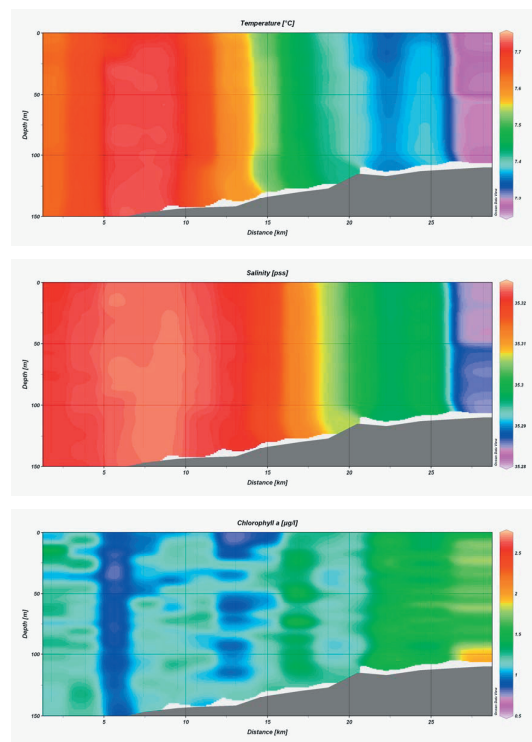


Figure A7. Section (4) plot for station 119 – 132 (23. April, am). Upper panel: temperature; Middle panel: Salinity; Lower panel: Chlorophyll a; Left: Station map.

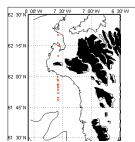
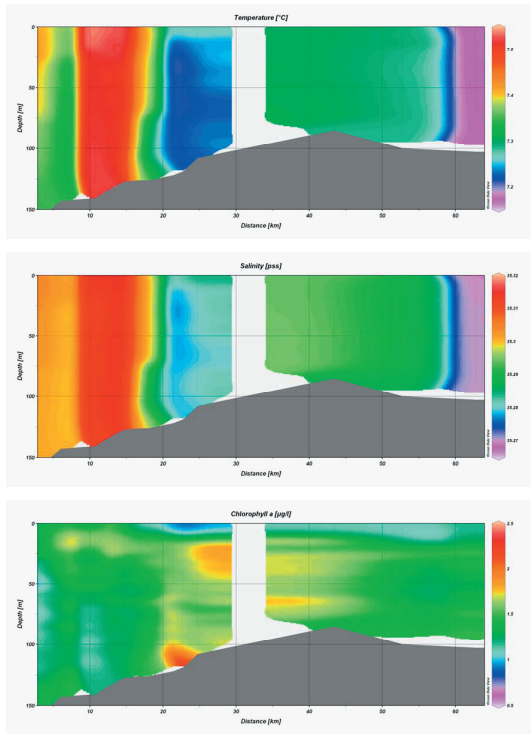


Figure A8. Section (5) plot for station 136 – 149 (23. April, am - pm). Upper panel: temperature; Middle panel: Salinity; Lower panel: Chlorofyll a; Left: Station map.

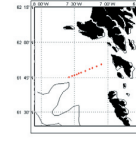
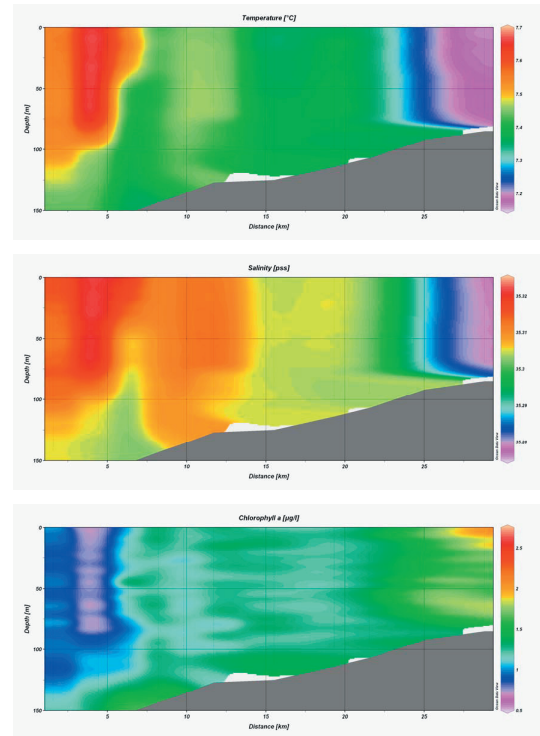


Figure A10. Section (7) plot for station 163 – 173 (24. April, am). Upper panel: temperature; Middle panel: Salinity; Lower panel: Chlorophyll a; Left: Station map.

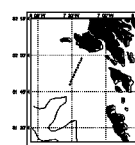
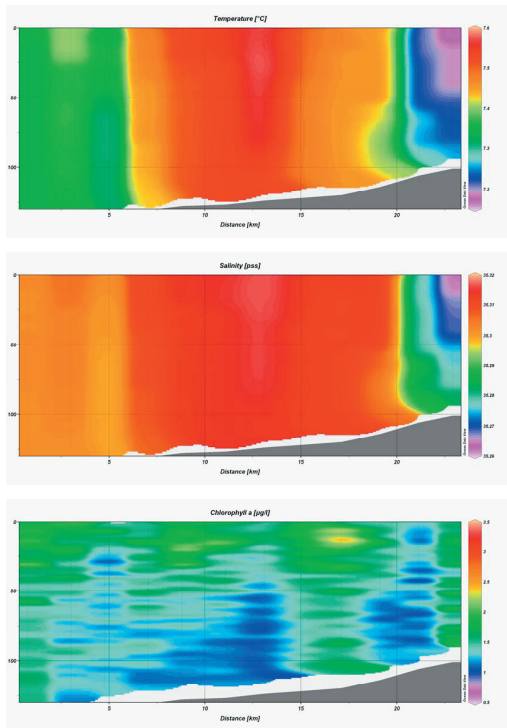


Figure A9. Section (6) plot for station 150 – 161 (23. April, pm). Upper panel: temperature; Middle panel: Salinity; Lower panel: Chlorofyll a; Left: Station map.

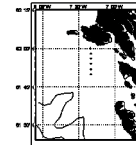
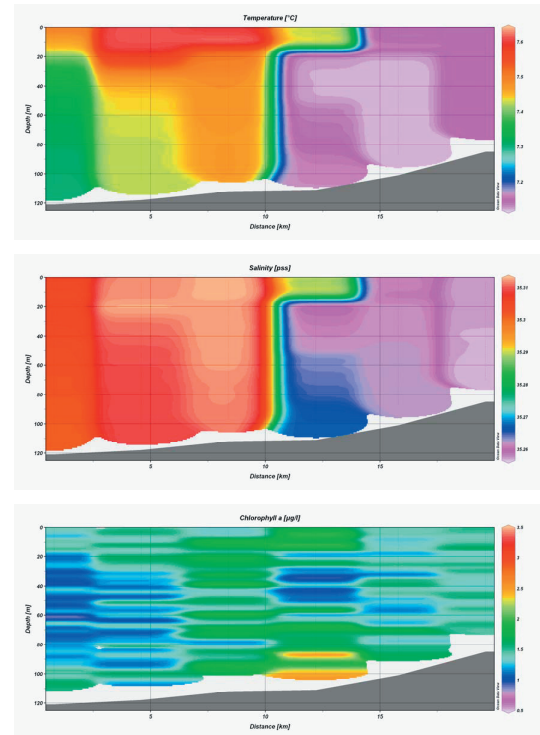


Figure A11. Section (8) plot for station 222 – 227 (25. April, pm). Upper panel: temperature; Middle panel: Salinity; Lower panel: Chlorophyll a; Left: Station map.

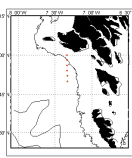
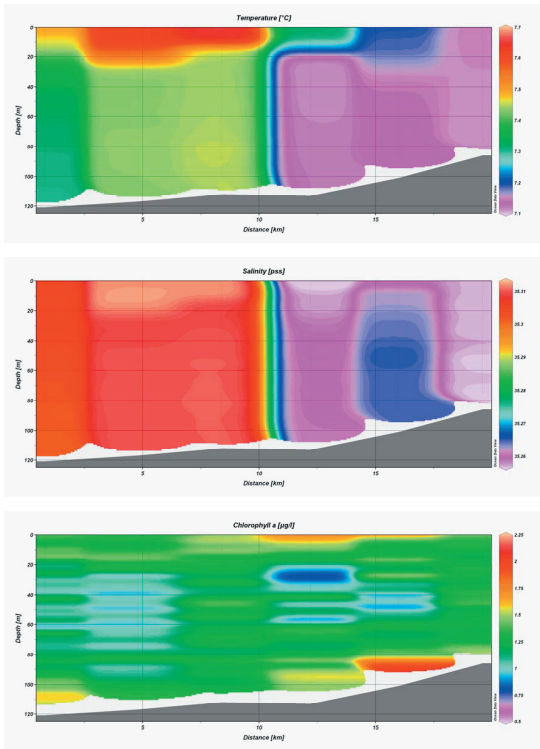


Figure A12. Section (9) plot for station 227 – 232 (25.-26. April, pm). Upper panel: temperature; Middle panel: Salinity; Lower panel: Chlorophyll a; Left: Station map.

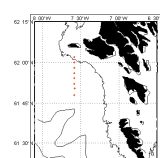
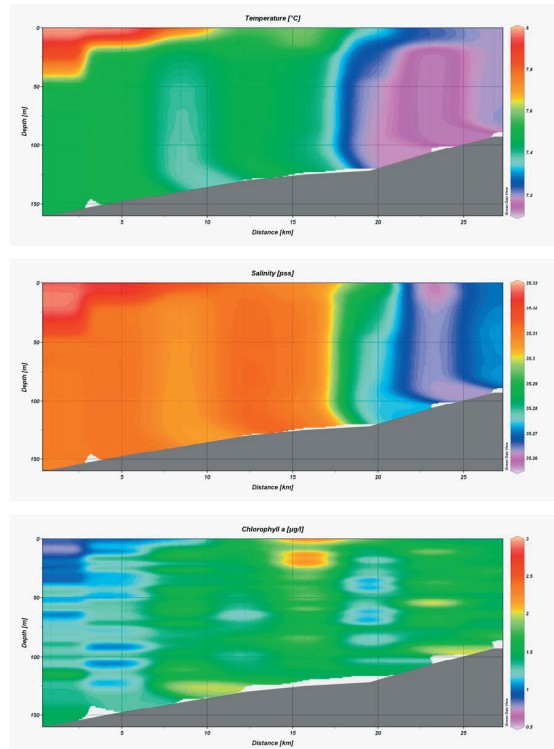


Figure A14. Section (11) plot for station 239 – 246 (26. April, am). Upper panel: temperature; Middle panel: Salinity; Lower panel: Chlorophyll a; Left: Station map.

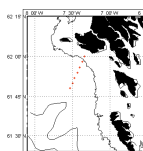
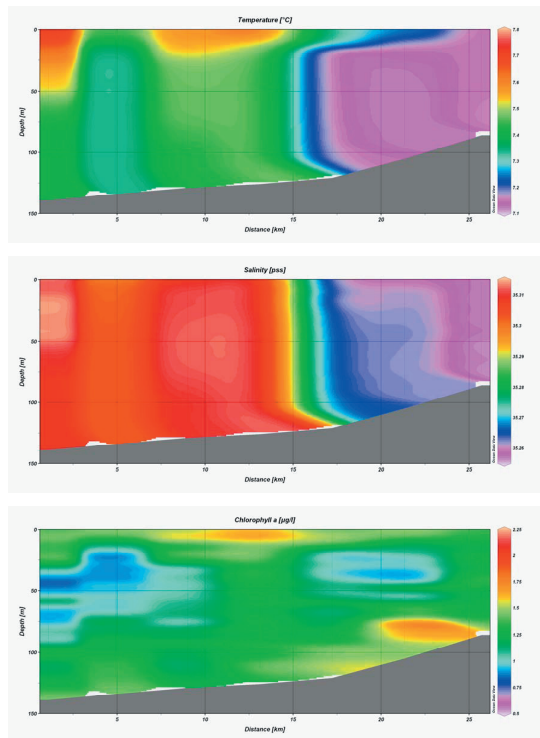


Figure A13. Section (10) plot for station 232 – 238 (26. April, am). Upper panel: temperature; Middle panel: Salinity; Lower panel: Chlorophyll a; Left: Station map.

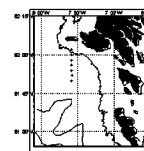
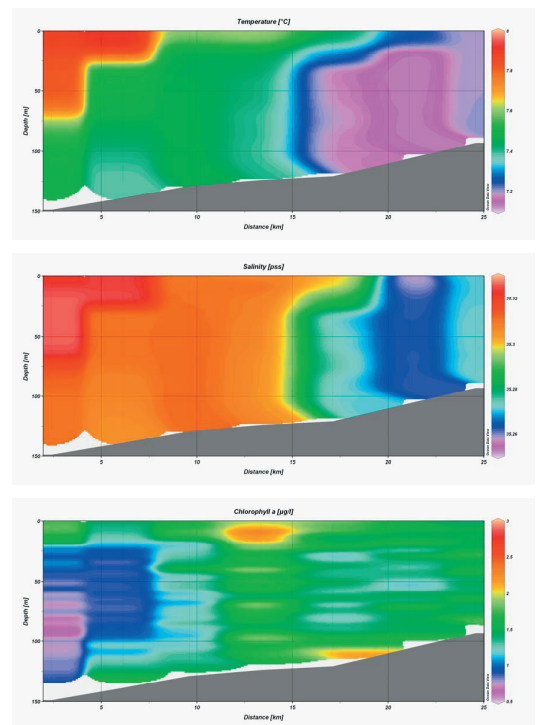


Figure A15. Section (12) plot for station 246 – 253 (26. April, am). Upper panel: temperature; Middle panel: Salinity; Lower panel: Chlorophyll a; Left: Station map.

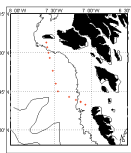
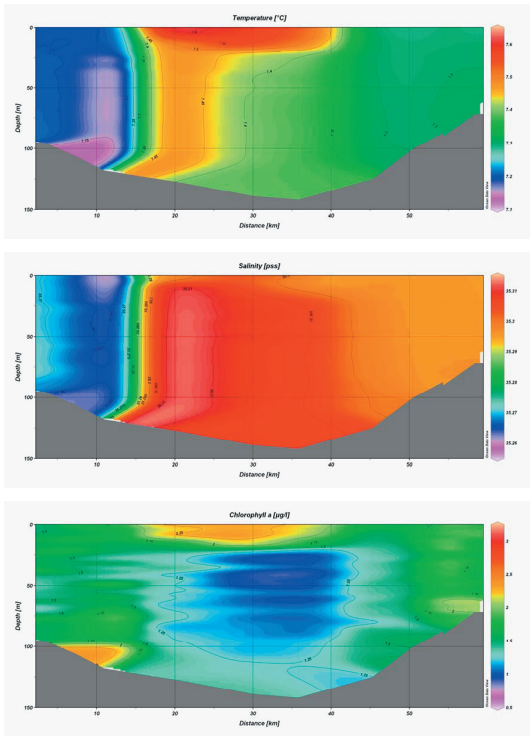


Figure A16. Section (13) plot for station 255 – 266 (26. April, pm).  
Upper panel: temperature; Middle panel: Salinity; Lower panel: Chlorophyll a; Left: Station map.

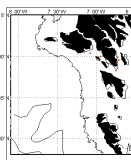
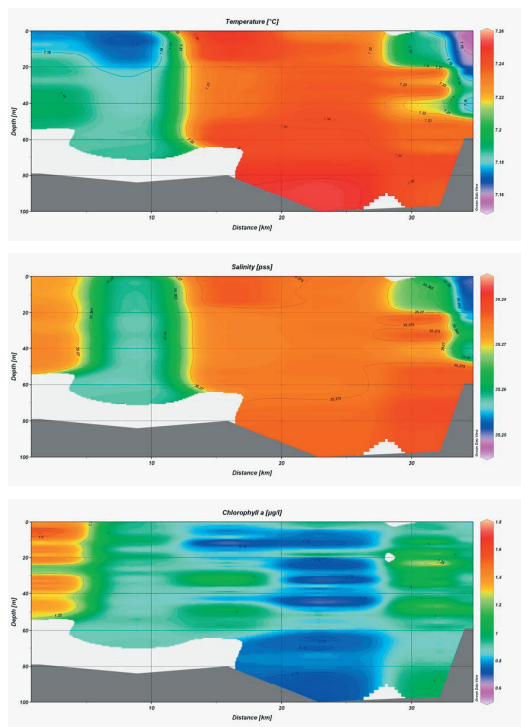


Figure A17. Section (14) plot for station 280 – 285 (267 April, am).  
Upper panel: temperature; Middle panel: Salinity; Lower panel: Chlorophyll a; Left: Station map.





P.O. Box 3051 · Nóatún 1  
FO-110 Tórshavn  
Faroe Islands

Tel +298 35 39 00  
hav@hav.fo  
www.hav.fo